Predictions for the Search for Anomalous Couplings of Gauge Bosons and Leptons in e^+e^--scattering

D I S S E R T A T I O N

zur Erlangung des akademischen Grades
doctor rerum naturalium
(Dr. rer. nat.)
im Fach Physik

eingereicht an der
Mathematisch-Naturwissenschaftlichen Fakultät I
der Humboldt-Universität zu Berlin

von

Herrn Dipl.-Phys. Jochen Biebel
geboren am 04.09.1966 in Groß-Gerau

Präsident der Humboldt-Universität zu Berlin:
Prof. Dr. J. Mlynek

Dekan der Mathematisch-Naturwissenschaftlichen Fakultät I:
Prof. Dr. B. Ronacher

Gutachter:
1. Prof. Dr. Thomas Hebbeker
2. Prof. Dr. Fred Jegerlehner
3. Prof. Dr. Dieter Lüst

Tag der mündlichen Prüfung: 30. April 2001

Abstract

Predictions are made for the effects of anomalous couplings in the processes of W-pair and ZZ production. Analytical expressions for the differential cross-sections are derived in both cases and numerical results are presented. The analytical results for W-pair production were implemented into the Fortran program `GENTLE`, while the ZZ production results are available in the stand-alone program `ZAC`. The numerical results are compared with the Standard Model predictions. For W-pair production radiative corrections are considered by using the structure function approach for the description of initial state radiation.

Effects of an anomalous magnetic moment a_τ of the τ lepton to the final state radiation in the process of τ-pair production at LEP1 are examined. This process allows to determine experimental limits for the anomalous magnetic moment of the τ. As a result we find that contributions linear in a_τ, which were believed to be small, cannot be neglegted at the present limits.

Keywords:
W-pair production, ZZ production, anomalous couplings, anomalous magnetic moment of the τ-lepton

Zusammenfassung

Die Auswirkungen von anomalen Kopplungen bei den Prozessen der W-Paar- und der ZZ-Erzeugung werden untersucht. Analytische Ausdrücke für die differentiellen Wirkungsquerschnitte werden für beide Prozesse abgeleitet und numerische Ergebnisse werden präsentiert. Die analytischen Ergebnisse zur W-Paarerzeugung wurden in das Fortranprogramm `GENTLE` eingebaut, während die Ergebnisse zur ZZ-Erzeugung in einem separaten Program `ZAC` zur Verfügung stehen. Die numerischen Resultate werden mit den Vorhersagen des Standard Modells verglichen. Bei der W-Paarerzeugung sind Strahlungskorrekturen durch den Strukturfunktionszugang im Rahmen der Anfangszustandsabstrahlung berücksichtig worden.

Die Auswirkungen eines anomalen magnetischen Momentes a_τ des τ-Leptons auf die Endzustandsabstrahlung im Prozess der τ-Paarproduktion bei LEP1 wurden untersucht. Dieser Prozess erlaubt die Bestimmung des experimentellen Limits für das anomale magnetische Moment a_τ. Als ein Ergebnis erhalten wir, dass Beiträge, die linear in a_τ sind und als klein angesehen wurden, bei den heutigen Limits nicht mehr vernachlässigt werden können.

Schlagwörter:
W-Paar-Erzeugung, ZZ-Erzeugung, anomale Kopplungen, anomales magnetisches Moment des τ-Leptons

Contents

1 Introduction **1**
- 1.1 Motivation . . . 1
- 1.2 Structure . . . 3

2 Standard Model of Electroweak Interactions and Beyond **5**
- 2.1 Towards a Standard Model – Historical Overview . . . 5
- 2.2 The Particle Content of the Standard Model . . . 7
  - 2.2.1 Fermions . . . 8
  - 2.2.2 Gauge Fields . . . 9
  - 2.2.3 Higgs sector . . . 10
  - 2.2.4 Gauge Fixing and Ghosts . . . 13
- 2.3 Theories beyond the Standard Model . . . 14
- 2.4 Anomalous Triple Gauge Boson Couplings . . . 16
  - 2.4.1 Linear Realization . . . 18
  - 2.4.2 Nonlinear Realization . . . 18

3 The Anomalous Magnetic Moment of the τ Lepton **20**
- 3.1 Analytical Predictions . . . 22
- 3.2 Numerical Results . . . 25

4 W Pair Production **30**
- 4.1 The Signal Cross-Section . . . 31
- 4.2 A Classification: Background Contributions of the `CC11` Class . . . 33
  - 4.2.1 The Background-s-channel Interference . . . 34
  - 4.2.2 The Background-t-channel Interference . . . 35
  - 4.2.3 The Pure Background Contribution . . . 36
- 4.3 Anomalous Couplings in W Pair Production . . . 39
  - 4.3.1 The `CC03` Process with Anomalous Couplings . . . 41
  - 4.3.2 The `CC11` Process with Anomalous Couplings . . . 43
- 4.4 Radiative Corrections – Initial State Radiation . . . 44
  - 4.4.1 Structure Function Approach . . . 45
  - 4.4.2 Lorentz Boost . . . 46
- 4.5 Numerical Results . . . 48
  - 4.5.1 Standard Model Contributions . . . 48
  - 4.5.2 Anomalous Couplings . . . 51

5 Anomalous Couplings in ZZ Production **56**
5.1 The Differential Cross-Section for ZZ Production . . . 57
5.2 Numerical Results . . . 61

6 Conclusions **66**

A Feynman Rules **68**
A.1 External Particles . . . 68
A.2 Propagators . . . 69
A.3 Vertices . . . 70

B Phase Space and Momenta **73**
B.1 W Pair Production . . . 73
B.2 ZZ Production . . . 75
B.3 $e^+e^- \to \tau^+\tau^-\gamma$ . . . 76
B.4 $\mu^- \to e^-\nu_\mu\bar{\nu}_e$ . . . 78

C Electromagnetic Multipole Moments **82**
C.1 Magnetic Moments of Leptons . . . 82
C.2 The Magnetic Dipole Moment of the W Boson . . . 84
C.3 The Electric Quadrupole Moment of the W Boson . . . 86

D GENTLE v. 2.02 **88**
D.1 Description of the Program . . . 88
D.1.1 The CC-branch and Anomalous Triple Gauge Boson Couplings . . . 89
D.1.2 The NC-branch . . . 89
D.2 New Features . . . 90

E A Sample FORM File **91**

Bibliography **98**

Curriculum Vitae **109**

List of Publications and Talks **110**
Publications . . . 110
Talks . . . 111

Selbstständigkeitserklärung **112**

List of Figures

3.1 *The two Feynman diagrams contributing to final state radiation in τ pair production.* . . . 21
3.2 *A one loop correction to final state radiation.* . . . 24
3.3 *Contributions from terms linear and quadratic in a_τ constitute the effects of an anomalous magnetic moment on the total cross-section.* . . . 26
3.4 *Effects of the anomalous magnetic moment for different cuts to the angle between τ lepton and photon.* . . . 28
3.5 *The ratio of the contribution of anomalous terms compared to the Standard Model prediction depending on the minimal photon energy $E_{\min}$.* . . . 29

4.1 *The three signal diagrams contributing to the W pair production process.* . 31
4.2 *Four of the eight background diagrams contributing to the* `CC11` *process.* . 34
4.3 *The three gauge boson vertex.* . . . 40
4.4 *Differential cross-section for $e^+e^- \to \mu^-\bar{\nu}_\mu u\bar{d}$ with various corrections.* . . . 48
4.5 *The ratios* `CC09/CC03`*,* `CC10/CC03`*, and* `CC11/CC03` *at the center-of-mass energies of 190 GeV and 500 GeV.* . . . 49
4.6 *The ratio of cross-sections with anomalous coupling over the Standard Model prediction at a center-of-mass energy of 190 GeV.* . . . 52
4.7 *The ratio of cross-sections with anomalous coupling over the Standard Model prediction at a center-of-mass energy of 500 GeV.* . . . 53
4.8 *1σ-bounds at a center-of-mass energy of 500 GeV for $\mathcal{L} = 50 fb^{-1}$.* . . . 54

5.1 *The VZZ vertex with $V = \gamma, Z$.* . . . 56
5.2 *The total cross-section for ZZ production with anomalous couplings.* . . . 62
5.3 *The differential cross-section for ZZ production in the Standard Model and with anomalous couplings.* . . . 63
5.4 *Ratio of produced Z pairs with* `LL` *polarization.* . . . 63
5.5 *Ratio of produced Z pairs with* `LT` *polarization.* . . . 64
5.6 *Ratio of produced Z pairs with* `TT` *polarization.* . . . 64
5.7 *Ratio of produced Z pairs with certain polarization.* . . . 65

B.1 *The tree-level diagram for muon decay.* . . . 78

List of Tables

2.1 *The fermions of the Standard Model.* 9

4.1 *Number of Feynman diagrams contributing to the production of $\mathcal{CC}$ type final states.* 31
4.2 *Dependencies of the various background interferences on the seven kinematical functions.* 37
4.3 *Differential cross-sections without ISR.* 50
4.4 *Differential cross-sections with ISR.* 51

D.1 *Overview over the different branches and subbranches of* `GENTLE`. 88
D.2 *Number of diagrams in the* `CC`*-branch.* 89
D.3 *Number of diagrams in the* `NC`*-branch.* 89

Chapter 1

Introduction

1.1 Motivation

The Standard Model of electroweak interactions [1–3] represents the basic theory in particle physics. So far, no *significant* deviation from it could be found in any high energy physics experiment. Precision measurements at electron-positron colliders like the LEP collider at CERN and the SLC at SLAC were able to confirm the underlying symmetries in e^+e^-–annihilation processes at the Z resonance down to the per mil level[1]. At such high accuracies the quantum corrections can be seen. In addition, experiments at hadron-hadron and hadron-lepton colliders are supporting the theory and do not give any evidence for an inexactness of the Standard Model. Likewise, low energy experiments are in a fantastic agreement with the theory.

The exposed position of the Standard Model as the basis for all predictions requires permanent search for limitations. The goal is to increase the precision of already measured values and perform experiments in untested regions of the parameter space, for example at higher center-of-mass energies. Cross-checks between experiments using different methods to measure the same physical quantities must be performed to investigate the reliability of the Standard Model.

At the Z peak the couplings between the Z boson and fermions have been measured with an unmatched accuracy from the process

$$e^+e^- \to Z \to f^+f^-(\gamma). \tag{1.1}$$

With $\mathcal{O}(10^7)$ observed Z events the mass M_Z, the width Γ_Z, the weak mixing angle $\sin^2\theta_w$ in the on-shell scheme and the number of light neutrino types N_ν are known to be [4]:

$$M_Z = (91.1882 \pm 0.0022)\ \text{GeV}, \tag{1.2}$$

$$\Gamma_Z = (2.4952 \pm 0.0026)\ \text{GeV}, \tag{1.3}$$

$$\sin^2\theta_w = 0.22302 \pm 0.00040 \tag{1.4}$$

[1] "At the end of eleven years of running, LEP will be remembered as the machine that put the theory describing particle behavior - the Standard Model - on solid ground. Precision measurements made by the four LEP experiments have confirmed the Standard Model to an extraordinary degree of precision. They have also demonstrated conclusively that three and only three families of matter particles exist." from `http://press.web.cern.ch/Press/Releases00/PR14.00ELEPstop.html`

$$N_\nu \quad = \quad 2.994 \pm 0.012. \tag{1.5}$$

In addition, data allow for the investigation of the decay modes of produced particles.

The center-of-mass energy at the LEP collider had been increasing in the last years from about 91 GeV to more than 200 GeV. At energies above the production threshold of W boson pairs the creation of four fermions is studied:

$$e^+e^- \to W^+W^- \to 4f. \tag{1.6}$$

In these processes the mass of the W bosons, their width, and their gauge couplings are examined. The experiments could prove for the first time that the predicted non-abelian coupling between a Z boson and two W bosons exists. The measurement of the W-mass

$$m_W \quad = \quad (80.419 \pm 0.056)\ \text{GeV} \tag{1.7}$$

is in a perfect agreement with the results for the Z-mass in (1.2) and the weak mixing angle in (1.4).

At even higher center-of-mass energies the process

$$e^+e^- \to ZZ \to 4f \tag{1.8}$$

can be examined. To this process an anomalous ZZZ-vertex would contribute and limits to it can be found. In addition, (1.8) is an irreducible background process for the Higgs boson radiation process

$$e^+e^- \to ZH \to 4f \tag{1.9}$$

and should be precisely studied. Although process (1.9) might be used to discover the Higgs boson[2], it is also used to get a lower Higgs mass limit. It is (for the Standard Model Higgs) [4]:

$$m_H \quad > \quad 95.3\ \text{GeV}, \qquad \text{CL} = 95\%. \tag{1.10}$$

Despite of its extremely successful history the Standard Model is not regarded as the theory of everything. Its large number of free parameters gives the impression that there should be a more systematic theory beyond it. Further, the Standard Model fails in the attempt to include gravitation into the one theory together with other three forces. These flaws and the still undiscovered Higgs boson motivate the search for physical processes beyond the Standard Model.

In addition, there might be a slight indication for physics beyond the Standard Model. There is some evidence from neutrino physics that the neutrinos might have a small mass [5] and because they do not have electrical charge it might be that there are completely new phenomena in this sector. As an example, neutrinos might be Majorana particles instead of Dirac particles or maybe a mixture of both. However, up to now there is no confirmation of a behavior which is contrary to the Standard Model prediction except of the small neutrino mass.

[2] "LEP was scheduled to close at the end of September 2000 but tantalising signs of possible new physics led to LEP's run being extended until 2 November. At the end of this extra period, the four LEP experiments had produced a number of collisions compatible with the production of Higgs particles with a mass of around 115 GeV. These events were also compatible with other known processes." also from `http://press.web.cern.ch/Press/Releases00/PR14.00ELEPstop.html`

1.2 Structure

The comparisons of achieved and expected experimental results with the theoretical expectations have to rely on predictions which need to be precise enough. In this thesis some of these theoretical predictions are presented and extensions to the Standard Model are considered in the form of anomalous couplings.

A short overview over the particle content of the Standard Model and its symmetries and interaction lagrangian is given in chapter 2. Possible extensions, like supersymmetry, are also shortly discussed and the principles of anomalous couplings and effective theories are introduced for the γWW and ZWW vertices. It is shown that higher dimensional operators in effective theories contribute to anomalous couplings. The differences between linear and nonlinear realizations of the gauge symmetries are also demonstrated.

In chapter 3 we apply the method of anomalous couplings to the $\tau^+\tau^-\gamma$ vertex and investigate the effects of an anomalous magnetic moment of the τ lepton in the process of equation (1.1). It is studied how energy spectra and angular distributions of the final state radiation in τ pair production at LEP are influenced by the magnetic moment. The Fortran program `Anotau` was written to allow for these examinations. Predictions for various distributions of observables in the scattering process $e^+e^- \to Z \to \tau^+\tau^-\gamma$ are presented.

The main part of this work follows in chapter 4, where the process $e^+e^- \to 4f$ via W pair production, as in equation (1.6), is discussed. Analytic expressions for the differential cross-sections are presented for the signal diagrams and the `CC11` background class. The achieved expressions were implemented into the Fortran program `GENTLE` to give numerical predictions for the angular cross-section. In addition to the Standard Model results also the effects of non-standard γWW and ZWW couplings are determined for the complete `CC11` class and presented in section 4.3. Especially in the search for anomalous triple gauge boson couplings this class plays an important role since its final states offer the most complete kinematical information. Numerical calculations using the analytical results give a feeling for potential deviations from the Standard Model due to the anomalous couplings and may guide the search for them.

Radiative corrections to the W pair production process are considered for initial state radiation (ISR). For the angular cross-section the structure function approach as described in section 4.4 is used.

Anomalous contributions can also show up in new vertices which are not present in the Standard Model, like for example in γZZ or ZZZ vertices. These vertices would contribute to the process in equation (1.8) and can be studied in ZZ production. They become measurable at center-of-mass energies above the production threshold of two Z bosons. How the signature of anomalous γZZ and ZZZ vertices in ZZ production processes at LEP2 might look like is discussed in chapter 5, where analytical results and the numerical results from the program `ZAC` are presented.

The more technical parts of this work can be found in the appendices. The Feynman rules used for the calculations are presented in appendix A. A detailed description of the

phase space variables and their construction is given in appendix B. Appendix C contains a derivation of the magnetic dipole moment and of the electric quadrupole moment of the W boson. Also the magnetic dipole moment of leptons is derived there. A brief introduction into the FORTRAN program `GENTLE v. 2.02` can be found in appendix D. Newly implemented features are also described in this appendix. An extensive use was made of the `FORM` package [6] for analytic manipulation of formulae in order to derive the results presented in this thesis. Finally, a sample `FORM` file as used in the calculation in chapter 4 is explained in detail.

Throughout this thesis, natural units ($c = \hbar = 1$) are used.

Chapter 2

Standard Model of Electroweak Interactions and Beyond

The Standard Model is a theory based on quantized fields and its goal is the description of the interactions between all known elementary particles. For references are suggested e.g. the standard text books [7–12]. Particles are described by scalar, spinor, or vector fields and appear in this form in the scalar Lagrange function. Fermions, represented by spinor fields, can interact with each other via intermediate gauge bosons, represented by vector fields. Couplings between the particles are constructed by locally gauge invariant products of more than two particle fields in the Lagrangian. The only scalar field is the Higgs boson.

The Standard Model will be discussed in this chapter by mentioning some important parts of its history in section 2.1 and presenting its particle content in section 2.2. Further, potential extensions are mentioned in section 2.3 and at the end of this chapter there is a brief introduction to anomalous couplings.

2.1 Towards a Standard Model – Historical Overview

The Standard Model was constructed to unify the electromagnetic and the weak interaction. Also the strong interaction (QCD) can be included in a consistent way. However, until now the electroweak and strong interactions are described independently from each other. Their unification is left to future in a so-called GUT (Grand Unified Theory).

Electromagnetism was discovered centuries ago. On a macroscopic level it was first described mathematically by Maxwell in 1864 [13]. Later, in 1927 Dirac managed to express the force between charged point particles and photons in a quantized way [14]. Using his theory Dirac could explain the phenomenological factor $g = 2$ in the magnetic moment of the electron [15]. QED was further strengthened after Schwinger calculated the radiative one-loop correction to the magnetic moment of the electron [16], which was in very good agreement with the measured data. Nowadays, QED is the best verified theory.

The weak interaction represents the second branch of the Standard Model. Its history started with the discovery of β-decay by Becquerel in 1896 [17]. A theory explaining

the β-decay was invented by Fermi in 1934 [18]. One year later Yukawa published a meson theory and invented the idea of intermediate bosons for the strong and the weak interactions [19]. Doing this he was the first who assigned separate coupling constants to these two forces. At that time, the electron, the proton, and the neutron made up the set of known elementary particles[1] and β-decay was the only known aspect of weak interactions.

The muon, discovered in 1937 in cosmic rays [24,25], was first believed to be the meson that was predicted by Yukawa, but soon discrepancies were noticed. This problem was solved in 1947 when the charged π-mesons [26] and the strange particles [27] were discovered. The long lifetime of particles with strangeness made it impossible to assume that they decay in a strong interaction. Nishijima and Gell-Mann introduced independently a new quantum number "strangeness", which is conserved in electromagnetic and strong interactions but violated by the weak force. This could explain the long lifetime of the new particles, but another oddity remained. The K mesons decayed into different final states and some of them seemed to have the "wrong" parity. The solution was either that two particles with almost the same mass but different parity existed or that parity was violated. Yang and Lee proposed experiments to test parity conservation. Indeed, in the famous Wu experiment [28] parity violation was detected in 1957. The vector currents had to be given up for the weak interaction and had to be replaced by vector and axial-vector currents [29,30].

In 1960 Glashow picked up an idea of Schwinger to unify electromagnetic and weak interactions [3]. He used a Yang-Mills theory [31] with a non-abelian local gauge symmetry and proposed an additional neutral vector boson. He considered mixing between the photon and the additional neutral boson, but he could not explain the boson masses, since explicit masses for bosons break the desired gauge symmetries. Nambu and Jona-Lasinio showed how to produce boson masses with the mechanism of spontaneous symmetry breaking [32,33]. The problem with massless Goldstone bosons [34] produced by a spontaneous breaking of symmetries could be solved by Higgs in 1964 [35–37] with an idea which is now called the Higgs mechanism. The Goldstone bosons are just absorbed by the additional degrees of freedom of the massive gauge bosons.

In 1967 Weinberg and, independently, Salam suggested models to describe the electroweak theory [1,2]. This model became later the Standard Model, but it was not much noticed before 't Hooft and Veltman managed to prove its renormalizability four years later [38–42]. In Weinberg's model the left-handed electron and its neutrino, respectively the left-handed muon and the corresponding neutrino were collected in weak iso-doublets. Although it was not realized immediately, the same kind of doublet can be constructed with the up and down quarks, which where introduced by Gell-Mann [43, 44] with his "eight-fold way" and Zweig [45] as the constituents of hadrons.

The violation of strangeness could be explained by the assumption of a mixing between the down and the strange quark. The size of the mixing was parameterized by the Cabbibo angle. Unfortunately, the mixing would also lead to a flavor change in neutral current processes, which was not observed. This puzzle could be solved by the so-called GIM

[1]Pauli had already postulated the neutrino [20] to explain the non-conservation of energy and angular momentum in the β-decay. However, this particle was discovered only in 1956 by F. Reines and C. L. Cowan [21–23]. They used a nuclear reactor as a neutrino source.

mechanism invented by Glashow, Iliopoulous and Maiani in 1970 [46]. They introduced an additional quark: the charm quark. After summing the flavor changing neutral currents over the up-type quarks their effects canceled each other in tree level processes. Not much later, the charm quark was discovered in the production of J/ψ mesons and, soon after that, mesons with open charm were produced [47–50]. With the known particles two so-called particle families (or generations) could be formed. Each of them contained a neutrino, a charged lepton, and two quarks.

A first experimental consolidation of the Standard Model was given by the discovery of neutral currents in neutrino-scattering experiments at CERN in 1973 [51, 52]. In 1973 Kobayashi and Maskawa [53] assumed the existence of a third family in order to explain the violation of $\mathcal{CP}$ symmetry discovered in 1964 by Cronin and Fitch [54]. The 2×2 Cabbibo mixing matrix would be extended to a 3×3 Cabbibo-Kobayashi-Maskawa (CKM) matrix and instead of only one free mixing angle there are three angles and one phase needed to construct the most general unitary matrix. A non-vanishing phase in the CKM matrix would introduce $\mathcal{CP}$ violation into the Standard Model Lagrangian in a natural way.

Three years later in 1976 the τ lepton was discovered by Perl et al. [55, 56]. It was the first particle of the announced third generation. Shortly after that followed the discovery of the b-quark in 1977 [57]. And only some years ago the last missing quark of the third family the, top quark, was found at Fermilab [58] after its mass was predicted by the analysis of radiative corrections to the LEP measurements at the Z resonance. The τ-neutrino was directly observed recently in the DONUT experiment at Fermilab [59].

Two important experimental confirmations of the Standard Model could be achieved before the discovery of the top quark. In 1978 the mixing between the neutral gauge bosons in the Weinberg-Salam model was verified by the observation of the interference between weak and electromagnetic interactions in the scattering of polarized electrons on deuterium. And maybe the most important observation was the direct production of W and Z bosons in the UA1 and UA2 experiments at CERN [60, 61]. Experimental data from LEP indicates that the number of light neutrinos is three. This may lead to the assumption that all fermion families are discovered and that only the Higgs boson remains to be discovered in the Standard Model. We will come back to this in section 2.3.

2.2 The Particle Content of the Standard Model

In this section we present the particles of the Standard Model and their description by fields in a Lagrangian. Not only the physical particles like e.g. leptons, but also the unphysical particles like the Faddeev-Popov ghosts are introduced.

The Standard Model Lagrangian can be split up in parts to pronounce the different sectors of the model:

$$\mathscr{L} = \mathscr{L}_{\text{fermion}} + \mathscr{L}_{\text{gauge}} + \mathscr{L}_{\text{Higgs}} + \mathscr{L}_{\text{Yuk}} + \mathscr{L}_{\text{g.f.}} + \mathscr{L}_{\text{F.P.}}. \tag{2.1}$$

In the following, the various sectors will be described.

2.2.1 Fermions

The fermions are described by $\mathscr{L}_{\text{fermion}}$. This part of the Lagrangian contains the kinematic terms of the fermions and their interactions with the gauge fields. The interactions are introduced as minimal couplings via covariant derivatives:

$$\begin{aligned}\mathscr{L}_{\text{Fermion}} &= i \sum_{i=e,\mu,\tau} \overline{\psi}^i_L \not{D} \psi^i_L + i \sum_{i=e,\mu,\tau} \overline{l}^i_R \not{D} l^i_R \\ &\quad + i \sum_{i=u,c,t} \overline{\psi}^i_L \not{D} \psi^i_L + i \sum_{i=u,d,c,s,t,b} \overline{q}^i_R \not{D} q^i_R. \end{aligned} \tag{2.2}$$

Here, ψ_L denotes a doublet of left-handed leptons:

$$\psi^l_L = \begin{pmatrix} \nu_l \\ l \end{pmatrix}_L, \tag{2.3}$$

or quarks:

$$\psi^q_L = \begin{pmatrix} u_q \\ d'_q \end{pmatrix}_L. \tag{2.4}$$

The right-handed singlet fields are denoted by l^i_R for leptons and q^i_R for quarks. The fields u_q in equation (2.2) are used for up-type quarks and the fields d'_q represent down-type quarks. The primes indicate that the down-type fields are not eigenstates of the mass matrix. They are a linear combination of the mass eigenstates and constitute the partners of the up-type quarks in the fundamental representation of the weak interaction.

The connection between the physical fields d_q and the unphysical fields d'_q is given by the Cabbibo-Kobayashi-Maskawa matrix [53]:

$$\begin{pmatrix} d' \\ s' \\ b' \end{pmatrix} = V_{\text{CKM}} \begin{pmatrix} d \\ s \\ b \end{pmatrix} \tag{2.5}$$

The unitary matrix V_{CKM} can be parameterized by three angles, which are generalized Cabbibo angles, and a phase. The hyper-charge Y_W of the fermions is chosen in a way that the Gell-Mann-Nishijima relation [62]

$$Q = I_3 + \frac{Y_W}{2} \tag{2.6}$$

holds. In equation (2.6) Q stands for the electric charge and I_3 represents the third component of the weak isospin. The hyper-charge and other quantum numbers are given for all fermions in table 2.1.

We assume the neutrinos to be massless. This has the consequence that the lepton families do not mix and a mixing matrix similar to (2.5) is not needed for leptons. However, recent data suggest that neutrinos do mix [5]. This would imply masses for neutrinos and a mixing matrix as in equation (2.5) would be needed. The effects of the tiny neutrino masses are small and we will neglect them completely.

	Families			Q_f	I_3	Y_W
	1	2	3			
Leptons	$\begin{pmatrix} \nu_e \\ e \end{pmatrix}_L$	$\begin{pmatrix} \nu_\mu \\ \mu \end{pmatrix}_L$	$\begin{pmatrix} \nu_\tau \\ \tau \end{pmatrix}_L$	0 -1	$+\frac{1}{2}$ $-\frac{1}{2}$	-1 -1
	e_R	μ_R	τ_R	-1	0	-2
Quarks	$\begin{pmatrix} u \\ d' \end{pmatrix}_L$	$\begin{pmatrix} c \\ s' \end{pmatrix}_L$	$\begin{pmatrix} t \\ b' \end{pmatrix}_L$	$+\frac{2}{3}$ $-\frac{1}{3}$	$+\frac{1}{2}$ $-\frac{1}{2}$	$+\frac{1}{3}$ $+\frac{1}{3}$
	u_R	c_R	t_R	$+\frac{2}{3}$	0	$+\frac{4}{3}$
	d'_R	s'_R	b'_R	$-\frac{1}{3}$	0	$-\frac{2}{3}$

Table 2.1: *The fermions of the Standard Model.*

The covariant derivatives D_μ in equation (2.2) are defined by:

$$D_\mu \psi_L^l = \left(\partial_\mu + i\frac{g}{2}\vec{\tau}\cdot\vec{W}_\mu + i\frac{g'}{2}Y_W B_\mu\right)\psi_L^l, \tag{2.7}$$

$$D_\mu l_R^i = \left(\partial_\mu + i\frac{g'}{2}Y_W B_\mu\right) l_R^i, \tag{2.8}$$

$$D_\mu \psi_L^q = \left(\partial_\mu + i\frac{g}{2}\vec{\tau}\cdot\vec{W}_\mu + i\frac{g'}{2}Y_W B_\mu + i\frac{g_s}{2}G_\mu^a\lambda_a\right)\psi_L^q, \tag{2.9}$$

$$D_\mu q_R^i = \left(\partial_\mu + i\frac{g'}{2}Y_W B_\mu + i\frac{g_s}{2}G_\mu^a\lambda_a\right) q_R^i. \tag{2.10}$$

In the last two equations the parameter a runs from 1 to 8 and corresponds to the sum over all gluons. The Pauli matrices are denoted by $\vec{\tau}$ and λ_a are the Gell-Mann matrices. The constants g, g', and g_s represent the coupling constants for the $\mathrm{SU(2)_L}$, the $\mathrm{U(1)_Y}$ gauge symmetries and the strong interaction, respectively. The gauge boson fields are given by $\vec{W}_\mu$, B_μ, and G_μ^a.

Equation (2.2) defines the kinematics and the gauge couplings of the fermions in the Standard Model with the covariant derivatives defined in (2.7) – (2.10). The coupling between fermions and the Higgs boson will be treated in section 2.2.3.

2.2.2 Gauge Fields

The kinematics of the gauge fields introduced in the equations (2.7) – (2.10) is described in $\mathscr{L}_{\text{gauge}}$. It is given by:

$$\mathscr{L}_{\text{gauge}} = -\frac{1}{4}\vec{W}_{\mu\nu}\cdot\vec{W}^{\mu\nu} - \frac{1}{4}B_{\mu\nu}B^{\mu\nu} - \frac{1}{4}G^a_{\mu\nu}G_a^{\mu\nu}, \tag{2.11}$$

with the field-strength tensors

$$W^i_{\mu\nu} = \partial_\mu W^i_\nu - \partial_\nu W^i_\mu - g\epsilon^{ijk}W^j_\mu W^k_\nu, \tag{2.12}$$

$$B_{\mu\nu} = \partial_\mu B_\nu - \partial_\nu B_\mu, \tag{2.13}$$
$$G^a_{\mu\nu} = \partial_\mu G^a_\nu - \partial_\nu G^a_\mu - g_s f^{abc} G^b_\mu G^c_\nu, \tag{2.14}$$

where f^{abc} are the structure constants of the group SU(3). The indices i, j, k represent the numbers 1, 2, 3 and the letters a, b, c represent the numbers 1 to 8.

Note that there are no mass terms in equation (2.11). An explicit mass term, like

$$\mathscr{L}_{\text{mass}} = m_B^2 B^\mu B_\mu \tag{2.15}$$

would violate the gauge symmetry and has to be omitted.

With the expressions (2.2) and (2.11) all interactions of the already discovered elementary particles can be described. However, so far the theory contains only massless particles, since mass terms like

$$\mathscr{L}_M = m_e \bar{\psi}_L \psi_R + \text{h.c.}, \tag{2.16}$$

or the term in (2.15) are not invariant under the gauge transformations. A violation of the invariance would spoil the renormalizability of the theory.

2.2.3 Higgs sector

To keep the renormalizability of the Standard Model and introduce masses for the gauge bosons the $\mathrm{SU(2)_L} \times \mathrm{U(1)_Y}$ gauge symmetries must be broken spontaneously. This is achieved by the Higgs mechanism. The ansatz for the locally gauge invariant Lagrangian density of the Higgs sector reads:

$$\mathscr{L}_{\text{Higgs}} = (D^\mu \phi)^\dagger D_\mu \phi + \mu^2 \phi^\dagger \phi - \lambda \left(\phi^\dagger \phi\right)^2, \tag{2.17}$$

where μ^2 and λ are positive constants. The covariant derivative is:

$$D_\mu \phi = \left(\partial_\mu + i\frac{g}{2}\vec{\tau} \cdot \vec{W}_\mu + i\frac{g'}{2} Y_W B_\mu\right) \phi. \tag{2.18}$$

The field ϕ is a complex doublet transforming under the group $\mathrm{SU(2)_L} \times \mathrm{U(1)_Y}$ with the hyper-charge $Y_W(\phi) = 1$. Using the Gell-Mann-Nishijima relation (2.6) it follows that the upper component of ϕ has the electric charge $Q = +1$, while the lower component is a neutral field with $Q = 0$. This suggests the notation

$$\phi = \begin{pmatrix} \phi^+ \\ \phi^0 \end{pmatrix} \tag{2.19}$$

for the Higgs doublet. The covariant derivative in (2.18) leads to a coupling to the gauge fields W^i_μ and B_μ. There is no coupling to the gluon fields G^a_μ, since the Higgs field is a singlet under the SU(3) transformation. The minimum of the Higgs boson potential $\mu^2(\Phi^\dagger\Phi) - \lambda(\Phi^\dagger\Phi)^2$ is

$$\langle\phi\rangle^2 = \frac{v^2}{2}, \tag{2.20}$$

with $v = \sqrt{\mu^2/\lambda}$. It is the vacuum expectation value of the quantized Higgs field. Using gauge invariance of equation (2.17) under $\mathrm{SU}(2) \times \mathrm{U}(1)$ rotations the vacuum expectation value can be chosen in a way that the only non-vanishing term is real and contained in the neutral part of the doublet. This condition leads to:

$$\langle \phi \rangle = \begin{pmatrix} 0 \\ \sqrt{\mu^2/2\lambda} \end{pmatrix} = \begin{pmatrix} 0 \\ v/\sqrt{2} \end{pmatrix}. \tag{2.21}$$

The non-symmetrical choice of the phase in (2.21) is a global gauge fixing and breaks the gauge symmetry spontaneously. Although the symmetry disappeared, some of its features are still present and ensure the renormalizability of the Standard Model. The physical Higgs field should have a vacuum expectation value which is zero. This can be achieved by the field substitution:

$$\phi = \begin{pmatrix} \phi^+ \\ \frac{1}{\sqrt{2}}(v + h + i\chi) \end{pmatrix}. \tag{2.22}$$

The field h represents the Higgs boson and the fields χ, ϕ^+, and $\phi^- = (\phi^+)^\dagger$ are the Goldstone boson fields. The latter are unphysical degrees of freedom and can be absorbed by the gauge boson fields with an appropriate choice of the gauge, the unitary gauge.

Then the Higgs doublet has the form

$$\phi = \begin{pmatrix} 0 \\ \frac{1}{\sqrt{2}}(v + h) \end{pmatrix}. \tag{2.23}$$

When we introduce the vacuum expectation value v of the Higgs doublet in (2.17), we get mass terms for the gauge bosons. The expression relevant for the gauge boson masses is:

$$\frac{v^2}{2}\left[g^2 \left|W_\mu^1 - iW_\mu^2\right|^2 + \left(g'B_\mu - gW_\mu^3\right)^2\right]. \tag{2.24}$$

The charged W bosons are constructed from the fields W^1 and W^2 by

$$W_\mu^\pm = \frac{W_\mu^1 \mp iW_\mu^2}{\sqrt{2}}. \tag{2.25}$$

The identification of the right-hand-side of equation (2.25) with the corresponding term in (2.24) leads to the mass term

$$\frac{g^2 v^2}{4} W^+ W^-, \tag{2.26}$$

which yields a mass for the $W^\pm$ bosons

$$m_W = \frac{gv}{2}. \tag{2.27}$$

By measuring g and m_W the parameter v is also known. Its value is

$$v \approx 246 \text{ GeV}. \tag{2.28}$$

In equation (2.24) it is obvious that the third component of the $\vec{W}_\mu$ mixes with the field B_μ. With the definition of the orthogonal combinations

$$Z_\mu = \frac{gW_\mu^3 - g'b_\mu}{\sqrt{g^2 + g'^2}}, \tag{2.29}$$

and

$$A_\mu = \frac{gb_\mu + g'W_\mu^3}{\sqrt{g^2 + g'^2}}, \tag{2.30}$$

a mass term for the Z boson appears with

$$m_Z = \sqrt{g^2 + g'^2}v/2. \tag{2.31}$$

The photon does not get a mass term and remains massless.

By the mixing of the photon and the Z boson a new parameter is introduced: the weak mixing angle [3]. It is defined by

$$\tan\theta_W = \frac{g'}{g}. \tag{2.32}$$

Using the weak mixing angle and the W mass, we can express the Z boson mass:

$$m_Z = \frac{m_W}{\cos\theta_W}. \tag{2.33}$$

This relation is valid at tree-level and is changed by radiative corrections.

Equation (2.17) contains also a mass term for the Higgs boson:

$$m_H = \sqrt{\frac{\lambda}{2}}v. \tag{2.34}$$

The parameter λ cannot be determined so far and therefore the Higgs mass is still unconstrained.

Also the fermions get their masses from couplings to the Higgs boson. The Yukawa coupling is:

$$\begin{aligned}
\mathscr{L}_{\text{Yuk}} \;=\; & -\begin{pmatrix} \overline{e}_R \\ \overline{\mu}_R \\ \overline{\tau}_R \end{pmatrix}^T C_l \begin{pmatrix} \phi^\dagger \begin{pmatrix} \nu_e \\ e \end{pmatrix}_L \\ \phi^\dagger \begin{pmatrix} \nu_\mu \\ \mu \end{pmatrix}_L \\ \phi^\dagger \begin{pmatrix} \nu_\tau \\ \tau \end{pmatrix}_L \end{pmatrix} + \begin{pmatrix} \overline{u}_R \\ \overline{c}_R \\ \overline{t}_R \end{pmatrix}^T C'_q \begin{pmatrix} \phi^T\epsilon \begin{pmatrix} u \\ d' \end{pmatrix}_L \\ \phi^T\epsilon \begin{pmatrix} c \\ s' \end{pmatrix}_L \\ \phi^T\epsilon \begin{pmatrix} t \\ b' \end{pmatrix}_L \end{pmatrix} \\
& -\begin{pmatrix} \overline{d'}_R \\ \overline{s'}_R \\ \overline{b'}_R \end{pmatrix}^T C_q \begin{pmatrix} \phi^\dagger \begin{pmatrix} u \\ d' \end{pmatrix}_L \\ \phi^\dagger \begin{pmatrix} c \\ s' \end{pmatrix}_L \\ \phi^\dagger \begin{pmatrix} t \\ b' \end{pmatrix}_L \end{pmatrix} + \text{h.c.},
\end{aligned} \tag{2.35}$$

where C_l, C'_q, and C_q denote 3×3 matrices. The two-dimensional antisymmetric tensor is denoted as ϵ. In the Standard Model the second term in (2.35) couples the up-type components of the left-handed quark doublets to the vacuum expectation value in the Higgs doublet. The neutrinos are assumed to be massless and no coupling between them and the Higgs fields is introduced. Using unitary transformations it is possible to transform the matrices C_l, C'_q, and C_q without changing the physical content. The result is just a rotation in the fermion fields, which is without observable effects, since the rotated fermions have the same quantum numbers.

The invariance under the unitary transformations allows to diagonalize the matrices C_l and C'_q. The matrix C_q cannot be diagonalized at the same time as C'_q since they are multiplied by the same quark fields from the right side. With the unitary matrix V, C_q can be written as:

$$C_q = V \begin{pmatrix} c_d & 0 & 0 \\ 0 & c_s & 0 \\ 0 & 0 & c_b \end{pmatrix} V^\dagger. \tag{2.36}$$

The matrix V is the Cabbibo-Kobayashi-Maskawa matrix introduced in (2.5).

Note that the vacuum expectation value of the doublet ϕ produces fermion masses in (2.35) which are proportional to the elements of the diagonalized matrices C_l, C'_q, and C_q. The matrix elements are not predictable and have to be put in by hand using the experimentally known masses.

2.2.4 Gauge Fixing and Ghosts

The quantization of the Standard Model cannot be performed without fixing a gauge. The calculation of boson propagators requires additional terms in the Lagrangian. These terms, the gauge fixing terms, break the gauge symmetry, but they have no influence on observables. The physical content of the theory remains the same. For the photon we choose the R_ξ gauge [63]:

$$\mathscr{L}_{\text{g.f.}\gamma} = -\frac{\xi_\gamma}{2} \left(\partial^\mu A_\mu\right)^2 . \tag{2.37}$$

The term in equation (2.37) fixes the gauge with the parameterization ξ_γ. The same kind of gauge fixing term can be used for the gluons:

$$\mathscr{L}_{\text{g.f.G}} = -\frac{\xi_G}{2} \left(\partial^\mu G^a_\mu\right)^2 . \tag{2.38}$$

For practical reasons the 't Hooft-Feynman gauge with $\xi_W = 1$ and $\xi_Z = 1$ is often used for the massive gauge bosons[2]:

$$\mathscr{L}_{\text{g.f.W}} = -\xi_W \left| \partial^\mu W^+_\mu - i\frac{m_W}{\xi_W}\phi^+ \right|^2 , \tag{2.39}$$

and

$$\mathscr{L}_{\text{g.f.Z}} = -\frac{\xi_Z}{2} \left(\partial^\mu Z_\mu - \frac{m_Z}{\xi_Z}\chi \right)^2 . \tag{2.40}$$

[2]Another common choice for the gauge is the unitary gauge with $\xi = \infty$.

In (2.39) and (2.40) the Goldstone boson fields appear again. The gauge fixing is chosen in a way that there is no mixing between the gauge boson and the Higgs boson fields. However, it introduces unphysical longitudinal degrees of freedom into the theory. In the non-abelian groups a coupling between the physical and the unphysical degrees of freedom leads to a mixing among them. This problem can be solved by introducing additional fields to cancel contributions from unphysical states. The new terms are the Faddeev-Popov ghosts [64]. These ghost fields behave like scalar fermions and there occurrence in loops allows for cancellations with the other unphysical contributions.

The Lagrangian of the Faddeev-Popov ghosts depends on the gauge fixing terms. In the Feynman gauge ($\xi = 1$) for electroweak interactions they are:

$$\begin{aligned}
\mathscr{L}_{\text{F.P.}} &= -\overline{\eta}^{+}\left(\partial^{\mu}\partial_{\mu} + m_W^2\right)\eta^{+} + igc_W\overline{\eta}^{+}\partial^{\mu}\left(Z_{\mu}\eta^{+}\right) - ie\overline{\eta}^{+}\partial^{\mu}\left(A_{\mu}\eta^{+}\right) \\
&\quad - g\overline{\eta}^{+}\partial^{\mu}\left(W^{+}\left(\eta_Z c_W - \eta_A s_W\right)\right) \\
&\quad - m_W\overline{\eta}^{+}\left[g\frac{c_W^2 - s_W^2}{2c_W}\eta_Z\phi^{+} - e\eta_A\phi^{+} + \frac{g}{2}\eta^{+}\left(h + i\chi\right)\right] \\
&\quad + \left(\eta^{+} \to \eta^{-}, W^{+} \to W^{-}, i \to -i\right) \\
&\quad - \overline{\eta}_Z\left(\partial^{\mu}\partial_{\mu} + m_Z^2\right)\eta_Z - igc_W\overline{\eta}_Z\partial^{\mu}\left(\eta^{+}W_{\mu}^{-} - \eta^{-}W+_{\mu}\right) \\
&\quad - m_Z\overline{\eta}_Z\left(-\frac{g}{2}\eta^{-}\phi^{+} - \frac{g}{2}\eta^{+}\phi^{-} + \frac{g}{2c_W}\eta_Z h\right) \\
&\quad - \overline{\eta}_A\partial^{\mu}\partial_{\mu}\eta_A + ie\overline{\eta}_A\partial^{\mu}\left(\eta^{+}W_{\mu}^{-} - \eta^{-}W_{\mu}^{+}\right), \qquad (2.41)
\end{aligned}$$

and for the gluons:

$$\mathscr{L}_{\text{F.P.}} = -\overline{\eta}^{a}\partial^{\mu}\partial_{\mu}\eta_a + ig_s\overline{\eta}^{a}\partial^{\mu}f_{abc}G_{\mu}^{b}\eta^{c}. \qquad (2.42)$$

The fields η_V describe the Faddeev-Popov ghosts. The indices a, b, and c are used for the gauge group SU(3), with the structure constants f^{abc}. In equation (2.41) the abbreviations:

$$c_W = \cos\theta_W \qquad (2.43)$$

$$s_W = \sin\theta_W \qquad (2.44)$$

are used.

The Standard Model, as presented in this chapter, is complete in the sense that it describes all known particles and interactions except gravitation. Its renormalizability and consistency are ensured by gauge symmetries, which are not explicitly broken.

However, despite the great success of the Standard Model some features remain unsatisfactory. Up to now, there is no experimental evidence for the Higgs mechanism as the origin of spontaneously symmetry breaking. Another point is the large number of parameters, which cannot be predicted but have to be experimentally determined.

2.3 Theories beyond the Standard Model

Neither in high-energy nor in low-energy experiments a significant deviation from the Standard Model predictions has been detected. Nevertheless, some still unsolved problems, e.g. the failing attempts to include gravitation in a consistent way, indicate that

the Standard Model might have to be extended. Furthermore, the fact that the Higgs boson is still undiscovered provides some space for speculations about the mechanism of symmetry breaking.

Due to these reasons a bunch of theories beyond the Standard Model exists. It is impossible to mention them all and I will not give more than a small excerpt of them here.

The most prominent and popular theories beyond the Standard Model are supersymmetry [65,66] and string theory [67,68]. In the supersymmetric approach a new symmetry between fermions and bosons is introduced and all fermions in the Standard Model get supersymmetric sfermions as partners. The sfermions obey Bose statistics and are bosons. Similarly the Standard Model bosons get fermions, the bosinos, as supersymmetric partners. In the supersymmetric models a more extended Higgs sector is needed than in the Standard Model. At least two Higgs doublets are necessary to keep the theory anomaly free [69–71]. The two doublets are equivalent to eight real particle fields of which three can be absorbed by the longitudinal modes of the massive gauge bosons. This leaves five Higgs bosons and they should appear as physical particles. There are several reasons why supersymmetry is an attractive extension to the Standard Model. Some of them will become clear in the following discussion.

One of the major goals of particle physics is to explain many or even all phenomena by the simplest possible theory and the smallest possible amount of parameters. This motivates the search for a Grand Unified Theory (GUT), see e.g. refs. [72, 73]. After the unification of the electromagnetic and the weak interactions into a $\mathrm{SU}(2)_L \times \mathrm{U}(1)_Y$ gauge symmetry it is desired to incorporate also the strong interaction. By examining the running of the various coupling constants of the three gauge groups it becomes apparent that they do not meet at the same point in the Standard Model. In supersymmetric models this becomes possible.

A somehow natural extension in particle physics is to change the "size" of particles. Instead of only point-like particles also one-dimensional strings or objects with even higher dimension can be assumed. This approach is used in the theory of strings and superstrings, see e.g. [67, 68]. There is a hope that it will be possible to incorporate gravity into the theory of elementary particles. However, usual string theories are embedded in a ten or eleven-dimensional space and the problem how to compactify the higher dimensions in a unique way is still unsolved.

In supersymmetry and grand unified theories it is usually assumed that with increasing energy more and more symmetries will appear. In contrast to this hypothesis the opposite might be true. The observed symmetries might be just the low energy behavior of a more complicated world at much higher energies [74].

Since the Standard Model Higgs boson has not yet been discovered, there is still some room for new physics in this sector. One idea to produce particle masses without destroying the gauge symmetries is called Technicolor [75–82]. Here, a strong QCD-like interaction is assumed, which creates condensates and in this way substitutes the Higgs boson. Most Technicolor models predict measurable resonances at energies that are already ruled out. However, some "post-modern" models, see e.g. ref. [83], are still alive.

It is not surprising that all of these models change the experimental observables in

their specific way. Model dependent calculations must be performed in the comparison of theoretical predictions and experimental measurements. In the next section I will present a model-independent method of calculating cross-sections and other observables. Anomalous couplings are used to mimic the potential effects of new physics and a given model predicts the size of the anomalous parameters. When the anomalous parameters are measured well enough it will be possible to disentangle various theories.

2.4 Anomalous Triple Gauge Boson Couplings

In this section the most general form of the Lagrangian describing the VW^+W^- coupling with $V = \gamma, Z$ is presented. It is demonstrated that the requirement of invariance under various symmetries can be used to reduce the number of unknown parameters. With the assumption that the scale of new physics is far above the accessible energies the number of parameters can be further reduced in two different scenarios of effective theories.

Let us consider the most general Lagrangian $\mathscr{L}^{\rm ano}_{\rm gen}$ that describes vertices with two W bosons and one neutral boson that is invariant under Lorentz transformations [84–86]:

$$\begin{aligned} i\mathscr{L}^{\rm ano}_{\rm gen} &= g_{VWW}\Big[g_1^V V^\mu (W^-_{\mu\nu}W^{+\nu} - W^+_{\mu\nu}W^{-\nu}) + \kappa_V W^+_\mu W^-_\nu V^{\mu\nu} + \frac{\lambda_V}{m_W^2} V^{\mu\nu} W^{+\rho}_\nu W^-_{\rho\mu} \\ &\quad + ig_5^V \epsilon_{\mu\nu\rho\sigma}((\partial^\rho W^{-\mu})W^{+\nu} - W^{-\mu}(\partial^\rho W^{+\nu}))V^\sigma + ig_4^V W^-_\mu W^+_\nu (\partial^\mu V^\nu + \partial^\nu V^\mu) \\ &\quad - \frac{\tilde\kappa_V}{2} W^-_\mu W^+_\nu \epsilon^{\mu\nu\rho\sigma} V_{\rho\sigma} - \frac{\tilde\lambda_V}{2m_W^2} W^-_{\rho\mu} W^{+\mu}{}_\nu \epsilon^{\nu\rho\alpha\beta} V_{\alpha\beta}\Big]. \end{aligned} \tag{2.45}$$

As in (2.25) the fields W^μ denote the W boson, while V^μ represents the photon or Z boson field. The abbreviations $W_{\mu\nu} = \partial_\mu W_\nu - \partial_\nu W_\mu$ and $V_{\mu\nu} = \partial_\mu V_\nu - \partial_\nu V_\mu$ are used.

The fourteen parameters g_1^V, κ_V, λ_V, g_5^V, g_4^V, $\tilde\kappa_V$, and $\tilde\lambda_V$ are not restricted by Lorentz invariance. The Standard Model, however, predicts the precise structure of VWW vertices and delivers therefore fourteen couplings without a direct measurement. With the normalization conditions $g_{\gamma WW} = e$ and $g_{ZWW} = e\cot\theta$ the Standard Model couplings are:

$$g_1^V = \kappa_V = 1, \tag{2.46}$$

and

$$\lambda_V = g_5^V = g_4^V = \tilde\kappa_V = \tilde\lambda_V = 0. \tag{2.47}$$

By measuring the couplings in (2.46) and (2.47) the Standard Model can be tested. Unfortunately, the measurement of all fourteen coupling constants requires a huge number of observed events and it is therefore for practical purposes desirable to reduce the number of parameters. One strategy is to assume that the vertex factor (2.45) is invariant under certain symmetry transformations, like $\mathcal{C}$ (charge transformation), $\mathcal{P}$ (parity transformation) or their product $\mathcal{CP}$.

Assuming invariance under $\mathcal{CP}$ transformations leads to the shorter Lagrangian:

$$\begin{aligned} i\mathscr{L}^{\rm ano} &= g_{VWW}\Big[g_1^V V^\mu (W^-_{\mu\nu}W^{+\nu} - W^+_{\mu\nu}W^{-\nu}) + \kappa_V W^+_\mu W^-_\nu V^{\mu\nu} \\ &\quad + \frac{\lambda_V}{m_W^2} V^{\mu\nu} W^{+\rho}_\nu W^-_{\rho\mu} + ig_5^V \epsilon_{\mu\nu\rho\sigma}((\partial^\rho W^{-\mu})W^{+\nu} - W^{-\mu}(\partial^\rho W^{+\nu}))V^\sigma\Big]. \end{aligned} \tag{2.48}$$

The six anomalous parameters g_4^V, $\tilde{\kappa}_V$, and $\tilde{\lambda}_V$ disappear, because the according operators do not have the correct behavior under the symmetry transformations. The coupling proportional to g_5^V violates both $\mathcal{C}$ and $\mathcal{P}$ but is invariant under $\mathcal{CP}$ transformations. With the stricter assumption that $\mathcal{C}$ and $\mathcal{P}$ should be conserved separately also g_5^V can be eliminated.

In the case of electromagnetic interactions also gauge symmetry should be conserved. This demand leads to $g_1^\gamma = 1$ and $g_5^\gamma = 0$, and only the two parameters κ_γ and λ_γ will give anomalous contributions to the γWW vertex.

Using all these assumptions we end up with six anomalous couplings, which is still too many for present data. A further reduction of the number of couplings is possible by examining how physics beyond the Standard Model may look like.

Since no deviations from the Standard Model predictions were measured up to date we can expect that existing deviations are small if any. This implies that new physics can be described by effective theories in the presently accessible energy range. In an effective approach new terms are added to the Standard Model Lagrangian in a specific way. These new terms can contain all possible operators that keep a required symmetry invariant. The additional Lagrangian is written as a power series:

$$\mathscr{L}_{\mathrm{NR}} = \frac{1}{\Lambda}\sum_i \alpha_i^{(5)}\mathcal{O}_i^{(5)} + \frac{1}{\Lambda^2}\sum_i \alpha_i^{(6)}\mathcal{O}_i^{(6)} + \dots\,, \tag{2.49}$$

where $\mathcal{O}_i^{(N)}$ denotes an operator of mass dimension N. The large parameter Λ is the mass scale of the new physics. The typical contribution of the operators is expected to be of the order of $\alpha_i^{(N)}(\sqrt{s}/\Lambda)^{N-4}$, where s is the squared center-of-mass energy. If we assume that new physics behaves "natural", the parameters $\alpha_i^{(N)}$ will be of order one. With this requirement the contributions from operators with a higher N will be smaller than others as long as the condition $\Lambda \gg \sqrt{s}$ is valid. In such a case an expansion in the mass dimension is valid. However, the expansion will break down when $\sqrt{s}$ reaches the scale Λ.[3]

If the expansion in (2.49) cannot be limited by a maximal value for N, any interaction term in (2.45) can be rendered to be $\mathrm{SU}(2)_L\times\mathrm{U}(1)_Y$ gauge invariant by adding interactions with additional gauge bosons, additional would-be Goldstone bosons, and the Higgs boson [87–91]. However, in a low energy approximation, where we consider only operators with $N \leq N_{\mathrm{max}}$, a gauge-invariant parameterization of the triple-gauge boson coupling can be used to constrain the form of (2.45). In the following, we will assume that operators with mass dimension larger than six can be neglected. Further we presume that lepton number and baryon number are conserved. Then all operators with mass dimension five vanish. Still, more than eighty operators with mass dimension six remain [92–95]. However, not all of them will contribute to a particular process.

Using the $\mathrm{SU}(2)_L \times \mathrm{U}(1)_Y$ gauge-symmetry as a guideline there exist two possible scenarios. If the Higgs boson is light, a linear realization of the symmetry is used. A heavy Higgs or no Higgs boson at all will require a nonlinear realization of the symmetry.

[3] A well-known example of such a behavior is the Fermi theory of the weak decays. At low energies ($\sqrt{s} << M_W$) the decay can be treated as a four-particle interaction. In the region of the Z peak, however, this approach fails and the weak boson propagators must be considered.

As the low energy degrees of freedom with direct interactions with the new physics we consider the $\mathrm{SU}(2)_L \times \mathrm{U}(1)_Y$ gauge bosons and the would-be Goldstone bosons, which contribute to the degrees of freedom of the massive gauge bosons. The two possible scenarios will be discussed in the following.

2.4.1 Linear Realization

For the construction of gauge invariant operators the Higgs doublet field ϕ, the covariant derivatives D_μ and the field strength tensors $\hat{W}_{\mu\nu} = W_{\mu\nu} - gW_\mu \times W_\nu$ and $B_{\mu\nu}$ can be used. With these building blocks eleven $\mathcal{CP}$ conserving operators with mass dimension six can be constructed [88–90, 92, 94, 95]. Four of these operators have strict constraints due to low energy data, since they contribute to well measured gauge boson propagators. Four other operators describe anomalous Higgs couplings and are neglected in the present analysis. These operators can only be constrained by measuring the couplings between Higgs and gauge bosons.

The three remaining operators are [86]:

$$\mathscr{L}_{d=6}^{TGC} = ig' \frac{\alpha_{B\phi}}{m_W^2} (D_\mu \Phi)^\dagger B^{\mu\nu} (D_\nu \Phi) + ig \frac{\alpha_{W\phi}}{m_W^2} (D_\mu \Phi)^\dagger \vec{\tau} \vec{W}^{\mu\nu} (D_\nu \Phi) + g \frac{\alpha_W}{6 m_W^2} \vec{W}^\mu{}_\nu (\vec{W}^\nu{}_\rho \times \vec{W}^\rho{}_\mu), \tag{2.50}$$

where the coupling constants g and g' correspond to the $\mathrm{SU}(2)_L$ and $\mathrm{U}(1)_Y$ gauge groups. The operators in (2.50) describe interactions between three gauge bosons, interactions between four gauge bosons, and interactions between Higgs bosons and gauge bosons. Note that the factors $1/\Lambda^2$ appearing in (2.49) are here included in the parameters α_i.

After setting the Higgs field to its vacuum expectation value we get the contributions to the anomalous gauge boson couplings. The relations of $\alpha_{B\Phi}$, $\alpha_{W\Phi}$, and α_W to the anomalous couplings are then given by:

$$\Delta g_1^Z = \frac{\alpha_{W\phi}}{c_W^2}, \qquad \Delta\kappa_\gamma = -\frac{c_W^2}{s_W^2} \left(\Delta\kappa_Z - \Delta g_1^Z \right) = \alpha_{W\phi} + \alpha_{B\phi}, \qquad \lambda_\gamma = \lambda_Z = \alpha_W. \tag{2.51}$$

With the chosen symmetry requirements we managed to reduce the set of anomalous couplings from fourteen parameters to three. However, we are not completely model independent anymore and it should be stressed that if the condition $\Lambda \gg s$ is not fulfilled the relations in (2.51) will not be valid anymore.

2.4.2 Nonlinear Realization

If the Higgs boson is too heavy or if it is not present at all, a nonlinear realization is used to construct an effective Lagrangian. The Higgs doublet ϕ should be expressed by the unitary and dimensionless matrix U:

$$U = e^{i \frac{\vec{\omega} \cdot \vec{\tau}}{v}}, \tag{2.52}$$

with the would-be Goldstone bosons denoted as ω_i and v is the vacuum expectation value of the Higgs field as introduced in (2.20).

Using the "naive dimensional analysis" of ref. [96] the dependence of the scale of new physics Λ_{NP} can be determined and the operators can be compared with contributions from the linear realization. The dependence is given by:

$$\mathcal{O}(\Lambda_{NP}) \propto \Lambda_{NP}^2 \frac{1}{\Lambda_{NP}^d} \frac{1}{\Lambda_{NP}^w}, \tag{2.53}$$

where d is the number of derivatives and w gives the number of gauge fields in the operator. Applying (2.53) on the anomalous couplings in (2.45) it appears that the parameters Δg_1^V and κ_V are suppressed by a power $1/\Lambda_{NP}^2$ and effectively of the dimension six. This means that they can be produced by operators of the dimension six as in the case of the linear realization. The term $V^{\mu\nu} W_\nu^{+\rho} W_{\rho\mu}^-$ producing the anomalous coupling proportional to λ_V is of the "naive" dimension eight and for large Λ_{NP} expected to be much smaller than the couplings Δg_1^V and κ_V.

Chapter 3

The Anomalous Magnetic Moment of the τ Lepton

Dirac's famous prediction $\mu = e/2m$ [15] for the magnetic moment of spin $\frac{1}{2}$ point-like particles was a great success of his theory. This result and the calculation of the one-loop correction to μ by Schwinger [16] were convincing arguments for QED. Today, the magnetic moments of the two light leptons e^- and μ^- are among the best measured physical quantities and are determined with the spin-precession method to be [97]:

$$\mu_e = (1.001159652193 \pm 0.000000000010)\frac{e\hbar}{2m_e}, \tag{3.1}$$

$$\mu_\mu = (1.0011659230 \pm 0.0000000084)\frac{e\hbar}{2m_\mu}. \tag{3.2}$$

These values are in a very good agreement with the theoretical predictions.

To measure the magnetic moment of the τ lepton the spin-precession method cannot be applied, since the τ lifetime is to short. However, the value of the magnetic moment is of some interest, since a difference to the theoretical prediction would indicate new physics in form of new particles or a composite τ. The proton and the neutron are nice examples, where the magnetic dipole moments differ strongly from the theoretical prediction by Dirac because of their compositeness.

In this chapter we discuss measurements of the magnetic dipole moment of the τ lepton and derive analytical predictions for its determination in the e^+e^--annihilation processes at LEP. For other aspects in τ physics, please refer to recent overviews [98–101] and the references therein.

Let us start with flashing briefly the basics on magnetic dipole moments of leptons. A more detailed discussion of equation (3.3) and the derivation of equation (3.4) can be found in appendix C.1. The general form for the matrix element of the electromagnetic current of a lepton is of the form

$$j^\mu = e\bar{u}(p',s')\left[\gamma^\mu F_1(q^2) + \frac{i}{2m}\sigma^{\mu\nu}q_\nu F_2(q^2) + \gamma_5\sigma^{\mu\nu}q_\nu F_3\right]u(p,s), \tag{3.3}$$

with $q = p' - p$ and $\sigma^{\mu\nu} = \frac{i}{2}[\gamma^\mu, \gamma^\nu]$.

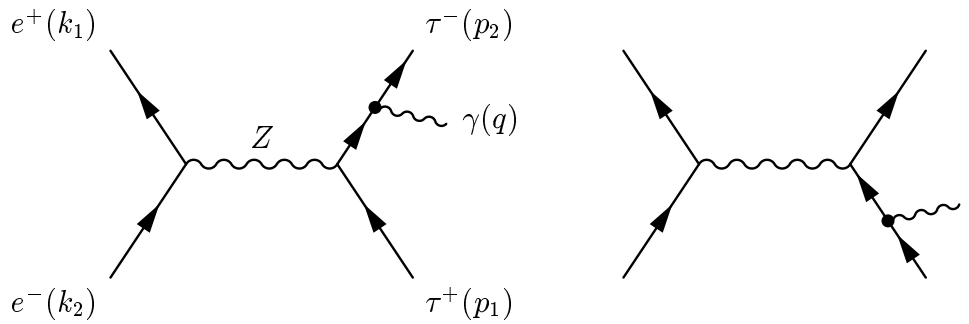

Figure 3.1: *The two Feynman diagrams contributing to final state radiation in τ pair production.*

The functions F_1 and F_2 contribute to the magnetic moment of the lepton

$$\mu_l = \frac{e\hbar}{2m}\left[F_1(0) + F_2(0)\right], \tag{3.4}$$

while F_3 generates the electric dipole moment

$$d_l = eF_3(0), \tag{3.5}$$

which should vanish as long as $\mathcal{CP}$ symmetry is valid. A derivation of equation (3.4) is given in appendix C.1. For spin $\frac{1}{2}$ particles, $F_1(0) = 1$. The anomalous magnetic moment is defined as

$$a_l = \frac{2m}{e\hbar}\mu_l - 1 = F_2(0). \tag{3.6}$$

Without radiative corrections $F_2(0)$ disappears for point-like spin $\frac{1}{2}$ particles. Including radiative corrections the theoretical prediction in the Standard Model is [102]:

$$a_\tau^{\text{th}} = 0.001177. \tag{3.7}$$

The first measurements of the form factor $F_2(q^2 > 0)$ were performed in the process of τ pair production with an intermediate photon. This was done in the e^+e^- annihilation experiments at PETRA [103]. The obtained limit was $F_2(q^2 > 0) \leq 0.02$ (95% CL) in the range of $(5 - 37\ \text{GeV})^2$ for q^2.

Another possibility to get limits to $F_2(m_Z^2)$ is to measure the $Z\tau^+\tau^-$ vertex and assuming $\text{SU(2)}_\text{L} \times \text{U(1)}_\text{Y}$ symmetry. This model dependent analysis was done by Escribano and Massó and they got the limit $-0.04 < F(m_Z^2) < 0.06$ [104].

A way to measure the parameter $F_2(0)$ is to look at final state radiation in the process of τ pair production. The corresponding Feynman diagrams are shown in figure 3.1. In figure 3.1 also the particle momenta are defined. The observed photons are on-shell, which implies $q^2 = 0$. The measured $F_2(0)$ is not exactly equivalent to the anomalous magnetic moment, since one of the τ leptons is off-shell.

Final state radiation was first applied to restrict the anomalous magnetic moment in an analysis by Grifols and Méndez [105]. They used the effect of an anomalous term on the Z decay width in their calculation and evaluated the expression

$$\Gamma\left[Z^0 \to \tau^+\tau^-\gamma\right] = \Gamma_0 + \Gamma_{\text{ano}}, \tag{3.8}$$

with

$$\Gamma_{\text{ano}} = \frac{\alpha^2 a_\tau^2 M_Z^3}{1024\pi m_\tau^2 \sin^2\theta_W \cos^2\theta_W}\left[(v^2+a^2) - \frac{1}{9}(v^2-a^2)\right]. \tag{3.9}$$

The Standard Model contribution is denoted with Γ_0 and $v = 1 - 4\sin^2\theta_W^{eff}$, $a = 1$ are the common abbreviations for the coupling constants. Grifols and Méndez got the limit $|a_\tau| \leq 0.11$ (95% CL). Note that terms linear in a_τ are neglected in equation (3.9). This is justified for large values of a_τ, since linear terms always appear together with a spin flip, which is proportional to m_τ^2/m_Z^2. However, the actual size of the linear term can only be determined in an explicit calculation as presented in section 3.1.

Recent measurements at LEP, using final state radiation and the linear terms in a_τ as discussed in section 3.1, give the best limit to the magnetic dipole moment [106, 107]. It is currently [97, 107]:

$$-0.052 < \frac{\mu_\tau}{e\hbar/2m_\tau} < 0.058. \tag{3.10}$$

This limit is about five times bigger than the theoretical prediction.

3.1 Analytical Predictions

For the Standard Model process we assume all known corrections, like initial state radiation and interferences between initial state and final state radiation, to be taken already into account. Their effects are proportional to the presumably small value of $a_\tau = F_2$ and can be safely neglected. The contributions of the photon exchange diagram is suppressed by the denominator in the s-channel propagator and is not considered here. Figure 3.1 shows the two remaining diagrams, used in this calculation.

To perform a precise determination of a_τ it is useful to look at more than the total cross-section, e.g. to examine distributions. The parameters of physical relevance are the production angle of the photon $\cos\theta_\gamma$, and the photon energy E_γ. For an experimental cut $\cos\theta_1$, the angle between photon and τ lepton, is important. This cut is treated in section 3.2, where numerical results are presented.

The matrix elements were evaluated applying the Feynman rules given in appendix A and checked using the program `CompHEP` [108, 109] with modified Feynman rules. The analytical integrations over the phase space, described in appendix B.3, were performed using `FORM` [6]. The integrals over the production angle of the τ leptons were done first. The only non-polynomial contribution in $\cos\theta_1$ and ϕ_1 came from the denominators of the τ propagators:

$$t_+ = 2p_1q = \frac{s}{2}(1-x')(1-\beta'\cos\theta_1), \tag{3.11}$$

$$t_- = 2p_2q = \frac{s}{2}(1-x')(1+\beta'\cos\theta_1), \tag{3.12}$$

where x' is related to the photon energy given by:

$$x' = \frac{(p_1+p_2)^2}{s} = 1 - \frac{2E_\gamma}{\sqrt{s}}, \tag{3.13}$$

and the velocity of the τ leptons in their center-of-mass system:

$$\beta' = \sqrt{1 - \frac{4m_\tau^2}{x's}} \tag{3.14}$$

is used.

The integrals of these propagators are:

$$\frac{1}{2}\int_{-1}^{1} \mathrm{d}\cos\theta_1 \frac{m_\tau^2}{t_\pm^2} = \frac{x'}{s(1-x')^2}, \tag{3.15}$$

$$\frac{1}{2}\int_{-1}^{1} \mathrm{d}\cos\theta_1 \frac{1}{t_\pm} = \frac{1}{\beta' s(1-x')} \ln\frac{1+\beta'}{1-\beta'} \approx \frac{1}{\beta' s(1-x')} \ln\frac{x's}{m_\tau^2}. \tag{3.16}$$

Note that the approximation in equation (3.16) is only used for integrations over x'.

After integrating over the two τ angles we get the distribution:

$$\begin{aligned}
\frac{\mathrm{d}^2\sigma}{\mathrm{d}x'\mathrm{d}\cos\theta_\gamma} = {} & \beta' C\left\{\frac{3}{8}(1-x')\left[(v^2+a^2)\frac{1}{\beta'}\ln\frac{1+\beta'}{1-\beta'}(1+\cos^2\theta_\gamma) - 4a^2\right]a_\tau \right. \\
& + \frac{1}{32}(1-x')\left[a^2[(1-x')^2(1-\cos^2\theta_\gamma)+8x'] \right. \\
& \left. + 3(v^2-a^2)x'(1+\cos^2\theta_\gamma)\right]\frac{s}{m_\tau^2}a_\tau^2 \\
& + \frac{3(v^2+a^2)}{8(1-x')}\left[(1+\cos^2\theta_\gamma)(1+x'^2)\frac{1}{\beta'}\ln\frac{1+\beta'}{1-\beta'}\right. \\
& \left.\left. - (1+\cos^2\theta_\gamma)(1-x')^2 - 8x'\cos^2\theta_\gamma\right]\right\},
\end{aligned} \tag{3.17}$$

where the abbreviation

$$C = \frac{\alpha}{\pi}\frac{G_\mu^2 M_Z^4}{96\pi}\frac{s}{\left|s - M_Z^2 + iM_Z\Gamma_Z(s)\right|^2}(v^2+a^2), \tag{3.18}$$

contains the s-channel propagator and the coupling constants.

The integration over the remaining angle $\cos\theta_1$ is simple and yields:

$$\begin{aligned}
\frac{\mathrm{d}\sigma}{\mathrm{d}x'} = {} & \beta' C\left\{(1-x')\left[(v^2+a^2)\frac{1}{\beta'}\ln\frac{1+\beta'}{1-\beta'} - 3a^2\right]a_\tau \right. \\
& + \frac{1}{4}(1-x')\left[a^2\frac{(1-x')^2}{6} + (v^2+a^2)x'\right]\frac{s}{m_\tau^2}a_\tau^2 \\
& \left. + \frac{v^2+a^2}{1-x'}(1+x'^2)\left(\frac{1}{\beta'}\ln\frac{1+\beta'}{1-\beta'} - 1\right)\right\}.
\end{aligned} \tag{3.19}$$

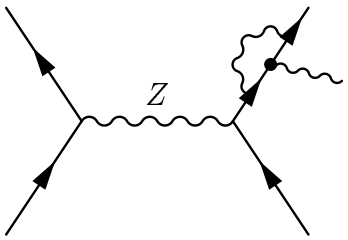

Figure 3.2: *A one loop correction to final state radiation.*

For small photon energies ($x' \to 1$) the Standard Model part of equation (3.19) shows the known infrared singularity. The anomalous terms have got an additional factor q_ν from the vertex factor in equation (3.3) and are infrared safe. With an upper cut x for the x' integration, the cross-section

$$\sigma_{hard}(x) = \int_0^x \mathrm{d}x' \frac{\mathrm{d}\sigma}{\mathrm{d}x'} \tag{3.20}$$

is finite. The cut-off x corresponds to a minimal photon energy

$$E_\gamma^{\min} = \frac{\sqrt{s}}{2}(1-x). \tag{3.21}$$

The cross-section for hard photons is then:

$$\begin{aligned}
\sigma_{hard}(x) \;=\; & C\Bigg\{-\frac{x}{2}\Bigg[(v^2+a^2)\left((x-2)\ln\frac{xs}{m_\tau^2}+2-\frac{x}{2}\right)-3a^2(x-2)\Bigg]a_\tau \\
& +\frac{1}{24}\Bigg[a^2\frac{1-(1-x)^4}{4}+(v^2+a^2)x^2(3-2x)\Bigg]\frac{s}{m_\tau^2}a_\tau^2 \\
& +(v^2+a^2)\Bigg[\frac{3}{4}x^2-\frac{x}{2}(2+x)\ln\frac{xs}{m_\tau^2}+2x+2\,\mathrm{Li}_2(1-x)-2\,\mathrm{Li}_2(1) \\
& +2\ln\frac{1}{1-x}\left(\ln\frac{s}{m_\tau^2}-1\right)\Bigg]\Bigg\},
\end{aligned} \tag{3.22}$$

where the Euler dilogarithm Li_2 is used. It is $\mathrm{Li}_2(1) = \pi^2/6$ and $\mathrm{Li}_2(0) = 0$.

As mentioned before only the Standard Model contribution is singular for $x \to 1$, so the singularity can be removed in the usual way. The contributions of soft photon radiation and virtual diagrams, which are of the same order in the coupling constant, have to be added. These corrections are [110]:

$$\sigma_{s+v}(x) = C(v^2+a^2)\left\{2\left(\ln\frac{s}{m_\tau^2}-1\right)\left[\ln(1-x)+\frac{3}{4}\right]+2\,\mathrm{Li}_2(1)-\frac{1}{2}\right\}. \tag{3.23}$$

The total cross-section for $\tau^+\tau^-(\gamma)$ production is given by the sum

$$\sigma_{tot} = \sigma_{hard}(x) + \sigma_{s+v}(x). \tag{3.24}$$

and is

$$\begin{aligned}\sigma_{tot} &= C\Bigg\{(v^2+a^2)\left[\frac{3}{4}-\frac{1}{2}\left(3-\ln\frac{s}{m_\tau^2}\right)a_\tau+\frac{3}{64}\frac{s}{m_\tau^2}a_\tau^2\right] \\ &\quad +(a^2-v^2)\left(-\frac{3}{4}a_\tau+\frac{1}{192}\frac{s}{m_\tau^2}a_\tau^2\right)\Bigg\}. \end{aligned} \tag{3.25}$$

The total cross-section in equation (3.25) is independent of the cutoff parameter x as desired. The infrared singularities in equation (3.22) and equation (3.23) cancel each other. The terms proportional to a_τ^2 were published in [104, 111]. The terms linear in a_τ were first presented in ref. [112].

The range in which equation (3.25) can be applied might be estimated with the theoretical prediction, for a_τ. When the limit for a_τ is close to the theoretical prediction contributions from loop diagrams as shown in figure 3.2 become important and cannot be neglected anymore.

It is easy to extend the calculation from above to the presence of a non-vanishing electric dipole moment as introduced in equation (3.3). The results can be extended by the simple replacement:

$$\frac{a_\tau^2}{m_\tau^2} \to \frac{a_\tau^2}{m_\tau^2} + 4\frac{d_\tau^2}{e^2}. \tag{3.26}$$

There appear no terms linear in d_τ, so a_τ and d_τ have different contributions to the cross-sections and can in principle be disentangled.

3.2 Numerical Results

All numerical results obtained in this section were produced with the Fortran program `Anotau` [113]. We used the value $\sin^2\theta_W = 0.2320$ and the τ mass $m_\tau = 1.777$ GeV for the calculations.

The result for the anomalous contribution to the total cross-section is shown in figure 3.3. To demonstrate the effects of the terms linear and quadratic in a_τ their separate contributions are plotted in the same figure. The figure shows that linear terms are of the same order as the quadratic terms at $|a_\tau| < 0.01$. For smaller $|a_\tau|$ they even give the dominating contribution to the anomalous effects and they are still of the order of 20% for values of $|a_\tau| < 0.05$.

Experimentally, it is impossible to identify photons when they are collinear with the τ leptons. This would require an additional cut on θ_1^*, the angle between the photon momentum and the τ momenta in the detector system. The angle θ_1 introduced in (B.44) – (B.46) is defined in the center-of-mass system of the τ leptons and cannot be used directly to apply this cut. However, it is possible to express θ_1 as a function of θ_1^* and the photon energy:

$$\theta_1 = \theta_1(\theta_1^*, x'). \tag{3.27}$$

The easiest way to calculate this dependency is by expressing the scalar product $(p_1 k)$ by the phase space variables defined in appendix B.3 and to compare this with the definition

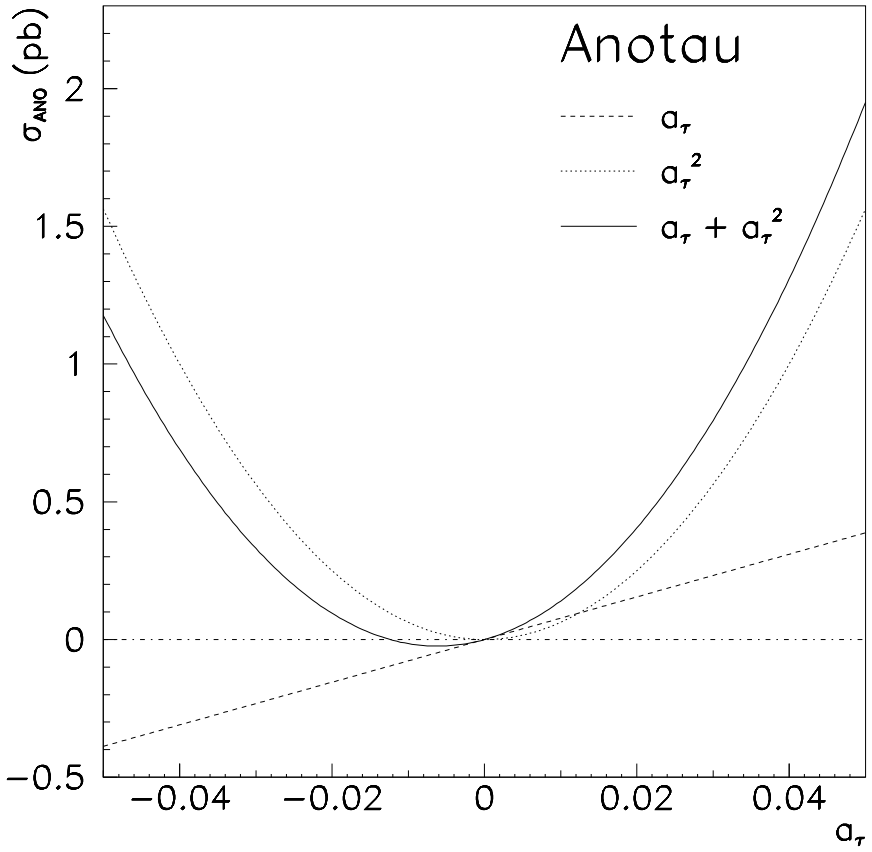

Figure 3.3: *Contributions from terms linear and quadratic in a_τ constitute the effects of an anomalous magnetic moment on the total cross-section.*

of θ_1^* in the detector system:

$$p_1 k = p_1^0 k^0 - \sum_{i=1}^{3} p_1^i k^i = p_1^0 k^0 \left[1 - \beta_1 \cos\theta_1^*\right], \tag{3.28}$$

where the velocity of the τ^+ in the detector system is:

$$\beta_1 = \sqrt{1 - \frac{m_\tau^2}{(p_1^0)^2}} = \left(1 - \frac{4m_\tau^2}{s} \frac{1}{\frac{1}{4}\left[(1+x') \mp (1-x')\beta' \cos\theta_1\right]^2}\right). \tag{3.29}$$

With (3.28) and (3.29) it is easy to get an expression for $\cos\theta_1^*$:

$$\cos\theta_1^* = \frac{1}{\beta_1}\left[1 - \frac{1 \mp \beta' \cos\theta}{\frac{1}{2}\left[(1+x') \mp (1-x')\beta' \cos\theta\right]}\right], \tag{3.30}$$

and an explicit dependence of $\cos\theta_1$:

$$\cos\theta_{1/2}^* = \frac{\pm A \cos\theta_1 - B}{\sqrt{D(1-\cos^2\theta_1) + A^2\cos^2\theta_1 \mp 2AB\cos\theta_1 + B^2}}, \tag{3.31}$$

where the abbreviations

$$A = \beta'(1+x'), \tag{3.32}$$

$$B = 1-x', \tag{3.33}$$

$$D = 4x'\beta'^2, \tag{3.34}$$

$$E = A^2-(A^2-D)\cos^2\theta^*_{1/2}, \tag{3.35}$$

are used.

To apply the discussed boost and get the required form of (3.27) it is necessary to invert equation (3.31) and express $\cos\theta_1$ in dependence of $\cos\theta^*_1$. This leads to a quadratic equation with two solutions:

$$\cos\theta_1 = \frac{AB(1-\cos^2\theta^*_1)\pm\sqrt{A^2B^2(1-\cos^2\theta^*_1)^2-E(B^2-(B^2+D)\cos^2\theta^*_1)}}{E}. \tag{3.36}$$

The correct solution of equation (3.36) is found by considering the limit $x'\to 1$ which corresponds to the case where the two Lorentz systems are identical. In this limit also the angles θ^*_1 and θ_1 must be equal. Inserting $x'=1$ in (3.32) – (3.35) exhibits that the sign in front of the square root is the same as the sign of $\cos\theta^*_1$.

To apply the cut it is useful to switch the order of integration and treat the scattering angles of the photon first. We get then the distribution:

$$\begin{aligned}\frac{d^2\sigma}{dx'd\cos\theta_1} = {}& \beta' C\Bigg\{(1-x')\left[\frac{1+x'^2}{2(1-x')}\left(\frac{1}{t_+}+\frac{1}{t_-}\right)-\frac{m_\tau^2}{s}\left(\frac{1}{t_+^2}+\frac{1}{t_-^2}\right)-1\right](v^2+a^2)\\ &+\frac{1-x'}{2}\left[(1-x')\left(\frac{1}{t_+}+\frac{1}{t_-}\right)(v^2+a^2)-6a^2\right]a_\tau\\ &+\frac{1-x'}{16}\left[4x'(v^2+a^2)+(1-\cos^2\theta_1)(1-x')^2\right]\frac{s}{m_\tau^2}a_\tau^2\Bigg\}.\end{aligned} \tag{3.37}$$

Now, the integration of (3.37) over $\cos\theta_1$ can be performed analytically for arbitrary limits and equation (3.36) can be used to determine the integration limits for the desired cuts. The cuts will be applied for both leptons and therefore the integration limits will remain symmetric.

The limits for the integrals presented in (3.15) and (3.16) are changed and the integrals yield now with new limits:

$$\frac{1}{2}\int_{-c}^{c}\mathrm{d}\cos\theta_1\frac{m_\tau^2}{t_\pm^2} = \mathcal{O}(\frac{m_\tau^2}{s})\to 0, \tag{3.38}$$

$$\frac{1}{2}\int_{-c}^{c}\mathrm{d}\cos\theta_1\frac{1}{t_\pm} = \frac{1}{(1-x')s}\ln\frac{1+c}{1-c}. \tag{3.39}$$

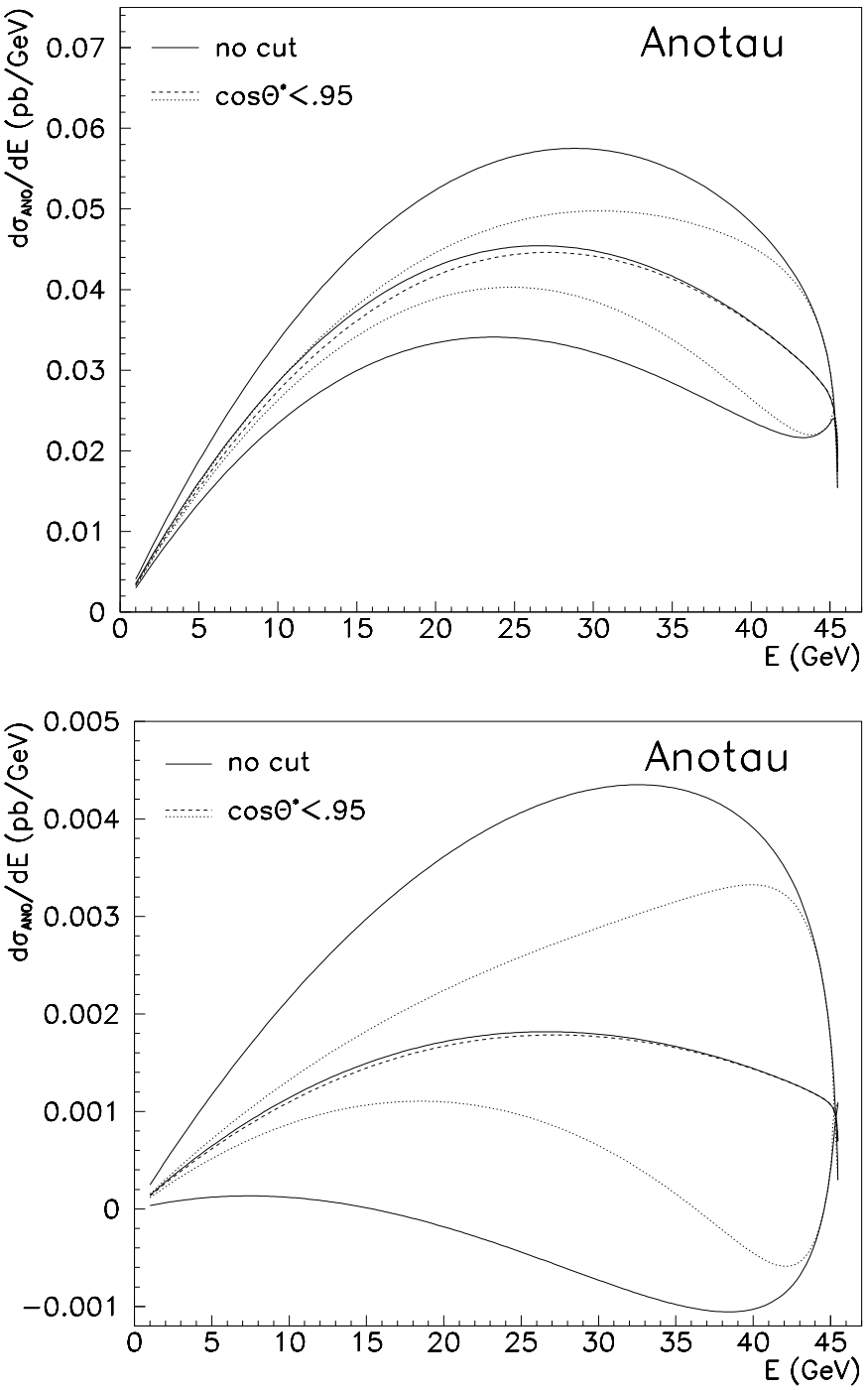

Figure 3.4: *Effects of the anomalous magnetic moment for different cuts to the angle between τ lepton and photon. The upper figure shows $|a_\tau| = 0.05\%$ and the lower figure shows $|a_\tau| = 0.01\%$.*

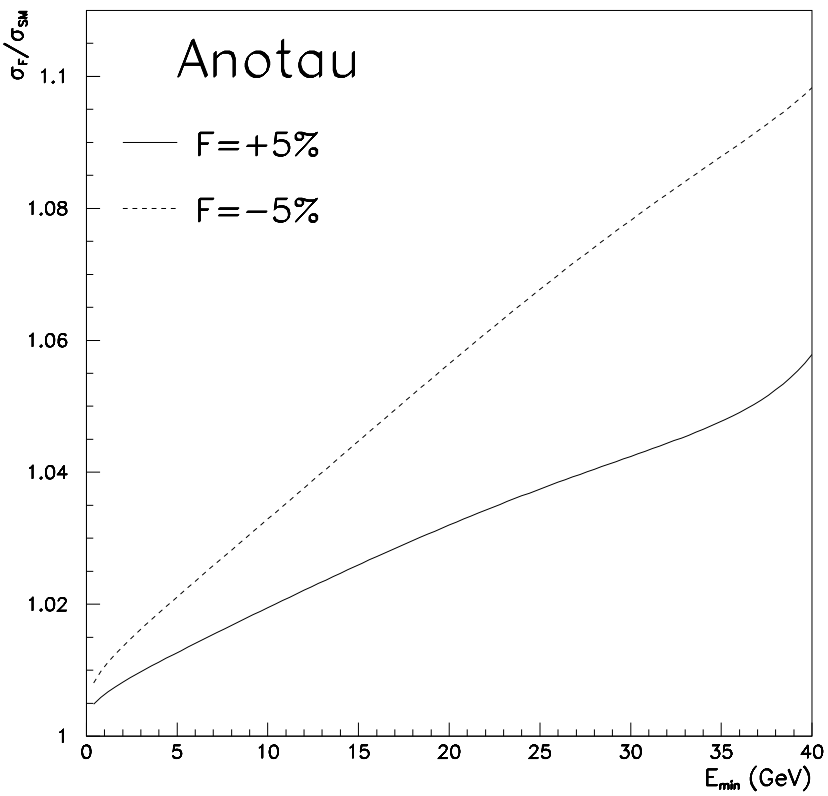

Figure 3.5: *The ratio of the contribution of anomalous terms compared to the Standard Model prediction depending on the minimal photon energy* $E_{\min}$.

In figure 3.4 the effects of this important cut are shown in the energy distribution of the emitted photon. Clearly, the anomalous signal is reduced. However, for high photon energies the anomalous contributions are less sensitive to the cut.

In figure 3.5 the ratio of the anomalous contribution over the Standard Model prediction is shown as a function of the minimal photon energy. The ratio increases for higher photon energies, but on the other hand the number of events is reduced drastically.

Acknowledgement

Using their Monte Carlo program to estimate the effects of an anomalous magnetic moment of the τ J. Swain, L. Taylor, T. Paul and S. Gau from L3 found out that the anomalous contributions linear in a_τ were much larger than expected. We decided to perform an analytical calculation of the scattering process to find out why the natural suppression by the factor of m_τ^2/m_Z^2 for the linear contributions is absent. We are grateful for the communication with the L3 group and for comparisons of our results, see e.g. [114, 115].

Chapter 4

W Pair Production

W pair production processes have been studied in theory since several decades. The first cross-section calculations were performed already before the Standard Model became known. With this kind of process the non-abelian gauge structure of the Standard Model can be tested. Especially, a more precise determination of the W mass [116–118] and the measurement of the triple gauge boson couplings [86] become possible with W pair production.

The first calculations for the process of W pair production in the Standard Model were done in the seventies for the total cross-section [119] and for the total and differential cross-section [120]. These calculations were done for the signal process

$$e^+e^- \to W^+W^-. \tag{4.1}$$

The produced bosons were assumed to be on-shell and the width of the W bosons was neglected. The three contributing diagrams in the process (4.1) are shown in figure 4.1. The cross-section for this process is a function of s, the center-of-mass energy squared, and m_W, the mass of the W boson:

$$\sigma = \sigma(s, m_W^2). \tag{4.2}$$

Ten years before, it was shown that the decay width Γ_W of the W boson will lead to large corrections if the W is much heavier than the proton [121]. Therefore, it is necessary to consider the finite decay width to make precise predictions. This may be done by convoluting the cross-section with Breit-Wigner factors [122]:

$$\sigma(s) = \int_0^s \mathrm{d}s_1 \rho(s_1) \int_0^{\left(\sqrt{s}-\sqrt{s_1}\right)^2} \mathrm{d}s_2 \rho(s_2) \sigma_0(s, s_1, s_2). \tag{4.3}$$

The Breit-Wigner factors are:

$$\rho(s_i) = \frac{1}{\pi} \frac{\sqrt{s_i}\Gamma_W(s_i)}{(s_i - m_W^2)^2 + s_i\Gamma_W^2(s_i)} \times B(f), \tag{4.4}$$

where $B(f)$ denotes the branching fraction for the decay of a W into the fermion doublet f. The expression $\sigma_0(s, s_1, s_2)$ in (4.3) describes the process of W pair production with the masses $\sqrt{s_1}$ for the W^- and $\sqrt{s_2}$ for the W^+. It is a generalization of $\sigma(s, m_W^2)$ in (4.2).

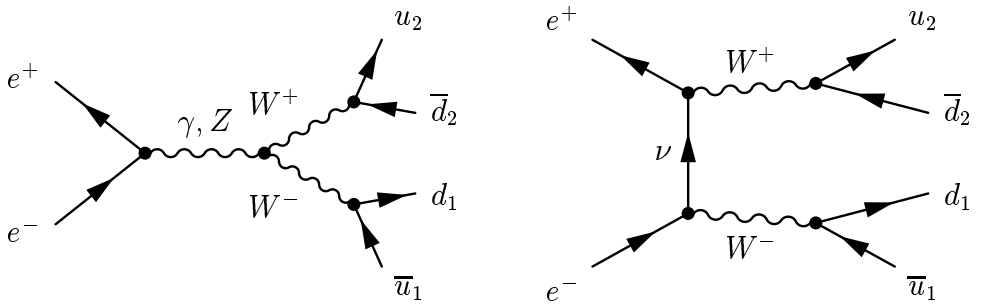

Figure 4.1: *The three signal diagrams contributing to the W pair production process. The s-channel Higgs boson diagram is neglected in the calculations. The diagrams constitute the* `CC03` *process.*

Since the W bosons decay almost immediately, the process

$$e^+e^- \to W^-W^+ \to (f_1, f_1{}')(f_2, f_2{}') \tag{4.5}$$

is observed. s_1 and s_2 can be reconstructed by the invariant masses of the produced weak doublets $(f_1, f_1{}')$ and $(f_2, f_2{}')$.

Additional diagrams, the so called background diagrams, contribute also to the same final state fermions. Their number depends only on the final state fermions. Therefore, one can easily classify all processes $e^+e^- \to 4f$ by their final state fermions [123]. Table 4.1 taken from reference [123] shows the number of diagrams for the various final states. We will restrict ourself to the `CC11` class. The `CC11` class is defined in section 4.2, where also the cross-sections are presented.

All results derived in this chapter are implemented in the Fortran program `GENTLE` [124] and were presented partially already in [125–128]. `GENTLE` is mainly applied for total cross-section predictions, nevertheless the package was also used in experimental studies of anomalous couplings [129, 130].

4.1 The Signal Cross-Section

In this section, the analytic expressions for the `CC03` cross-section are presented. They correspond to processes where only the signal diagrams contribute. We split the cross-section formula in a sum of products of coefficient functions $\mathcal{C}$ and kinematical functions

	$\bar{d}u$	$\bar{s}c$	$\bar{e}\nu_e$	$\bar{\mu}\nu_\mu$	$\bar{\tau}\nu_\tau$
$d\bar{u}$	*43*	**11**	20	**10**	**10**
$e\bar{\nu}_e$	20	20	*56*	18	18
$\mu\bar{\nu}_\mu$	**10**	**10**	18	*19*	**9**

Table 4.1: *Number of Feynman diagrams contributing to the production of CC type final states.*

$\mathcal{G}$:

$$\begin{aligned}\frac{\mathrm{d}\sigma_{\mathtt{CC03}}}{\mathrm{d}\cos\theta} &= \frac{\sqrt{\lambda}}{2\pi s^2}\int \mathrm{d}s_1\mathrm{d}s_2\ \Big[\mathcal{C}^t\mathcal{G}^t(s;s_1,s_2,\cos\theta)+\mathcal{C}^s\mathcal{G}^s(s;s_1,s_2,\cos\theta)\\ &\quad +\mathcal{C}^{st}\mathcal{G}^{st}(s;s_1,s_2,\cos\theta)\Big]. \qquad (4.6)\end{aligned}$$

The coefficient functions are [131]:

$$\begin{aligned}\mathcal{C}^t &= \frac{2}{(6\pi^2)^2}\mathrm{Re}\frac{1}{|D_W(s_1)|^2|D_W(s_2)|^2}\\ &\quad \times L^4(e,W))L^2(F_1,W)L^2(F_2,W)N_c(F_1)N_c(F_2), \qquad (4.7)\\ \mathcal{C}^{st} &= \sum_{k=\gamma,Z}\frac{2}{(6\pi^2)^2}\mathrm{Re}\frac{1}{|D_W(s_1)|^2|D_W(s_2)|^2D_k(s)}\\ &\quad \times g_kL(e,l)L^2(F_1,W)L^2(F_2,W)L^2(e,W)N_c(F_1)N_c(F_2), \qquad (4.8)\\ \mathcal{C}^s &= \sum_{k,l=\gamma,Z}\frac{2}{(6\pi^2)^2}\mathrm{Re}\frac{1}{|D_W(s_1)|^2|D_W(s_2)|^2D_k(s)D_l^*(s)}\\ &\quad \times g_kg_l[L(e,k)L(e,l)+R(e,k)R(e,l)]\\ &\quad \times L^2(F_1,W)L^2(F_2,W)N_c(F_1)N_c(F_2), \qquad (4.9)\end{aligned}$$

with the abbreviation

$$D_V(s) = s - M_V^2 + i\sqrt{s}\Gamma_V(s), \qquad (4.10)$$

for the denominators of the s-channel boson propagators. It can be seen from (4.7) - (4.9) that the coefficient functions are rather simple. They are constructed by the s-channel propagators and the coupling constants.

As coupling constants we used:

$$\begin{aligned} g_\gamma &= gs_W = e, & g_Z &= gc_W,\\ L(f,W) &= \frac{g}{2\sqrt{2}}, & R(f,W) &= 0,\\ L(f,\gamma) &= \frac{eQ_f}{2}, & L(f,Z) &= \frac{e}{4s_Wc_W}(2I_3^f - 2Q_fs_W^2),\\ R(f,\gamma) &= \frac{eQ_f}{2}, & R(f,Z) &= \frac{e}{4s_Wc_W}(-2Q_fs_W^2). \end{aligned} \qquad (4.11)$$

with $Q_e = -1$ and $I_3^e = -\frac{1}{2}$. The kinematical functions are then calculated to be:

$$\mathcal{G}^s = \frac{1}{32}\lambda\left[2s(s_1+s_2)+\left(3s_1s_2+\frac{\lambda}{4}\right)\sin^2\theta\right], \qquad (4.12)$$

$$\begin{aligned}\mathcal{G}^{st} &= \frac{1}{8}\left[(s-s_1-s_2)\left(2s(s_1+s_2)+\frac{\lambda}{4}\sin^2\theta\right)\right.\\ &\quad \left.-\frac{s_1s_2}{t_\nu}\left(4s(s_1+s_2)-\lambda\sin^2\theta\right)\right], \qquad (4.13)\end{aligned}$$

$$\mathcal{G}^t = \frac{1}{8}\left[2s(s_1+s_2)+\frac{\lambda}{4}\sin^2\theta+\frac{\lambda s_1s_2\sin^2\theta}{t_\nu^2}\right], \qquad (4.14)$$

with

$$\lambda = s^2 + s_1^2 + s_2^2 - 2ss_1 - 2ss_2 - 2s_1s_2 \tag{4.15}$$

and the denominator of the neutrino propagator t_ν:

$$t_\nu = \frac{1}{2}\left(s - s_1 - s_2 - \sqrt{\lambda}\cos\theta\right). \tag{4.16}$$

Note, that the integration of equations (4.12), (4.13), and (4.14) leads to the corresponding functions (2.2), (2.3), and (2.4) for the total cross-section in [131].

4.2 A Classification: Background Contributions of the `CC11` Class

The `CC11` class is defined by the final state fermions. It is required that two different weak iso-doublets are produced and that no electrons nor electron neutrinos are found in the final state. Up to eleven diagrams, the three signal diagrams and eight additional background diagrams, can contribute to such a process. In the following the notation `CCn` *process* is used when a better discrimination between the final states is desired. The number `n` determines the total number of Feynman diagrams contributing to the considered *process*. If it does not matter, whether the produced doublets consist of leptons or quarks, we will speak of the `CC11` *class*.

Four of the eight background diagrams in the `CC11` class are shown in figure 4.2. The total number of Feynman diagrams for four fermion production depends on the number of leptons in the final state. The following three cases can be distinguished:

- The `CC09` process with pure leptonic final states.
- The `CC10` process with semi-leptonic final states.
- The `CC11` process with pure hadronic final states.

The various background diagrams can be denoted by the final state fermion coupling to the neutral gauge boson in the s-channel propagator. For example the left diagram in figure 4.2 is denoted as a d_2-diagram since the down-type fermion of the positive charged doublet couples to the γ or Z. In this context we will not distinguish whether the final state fermion is a quark or a lepton.

It is useful to split up the background contributions into three parts. The first two parts are the interferences of the s-channel and the t-channel signal diagrams with the background diagrams in figure 4.2. The corresponding cross-section contributions are denoted by σ_{sb} and σ_{tb}. The third part contains the pure background and is denoted by σ_{bb}.

$$\frac{\mathrm{d}\sigma_b}{\mathrm{d}\cos\theta} = \frac{\mathrm{d}\sigma_{sb}}{\mathrm{d}\cos\theta} + \frac{\mathrm{d}\sigma_{tb}}{\mathrm{d}\cos\theta} + \frac{\mathrm{d}\sigma_{bb}}{\mathrm{d}\cos\theta}. \tag{4.17}$$

The expressions for each part in equation (4.17) can be presented in a similar way as it is done for the signal diagram results in equation (4.6). However, in contrast to the

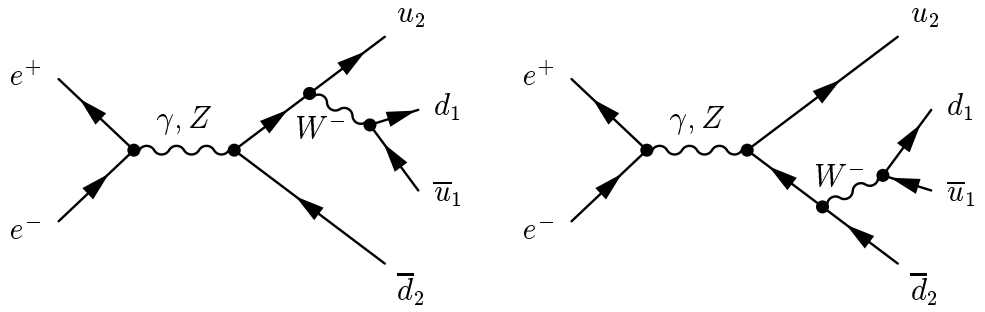

Figure 4.2: *Four of the eight background diagrams contributing to the* `CC11` *process.*

`CC03` expressions, we need in general two contributions from each interference, since more coupling constant combinations can appear.[1] An exception are the interferences with the t-channel diagram. Here only one combination of coupling constants is needed.

4.2.1 The Background-s-channel Interference

For the s-channel background interference we get:

$$\frac{\mathrm{d}\sigma_{sb}}{\mathrm{d}\cos\theta} = \frac{\sqrt{\lambda}}{2\pi s^2}\int \mathrm{d}s_1\mathrm{d}s_2 \sum_{i=1,2}\sum_{a=u,d}\left[\mathcal{C}_+^{sa_i}\mathcal{G}_+^{sa_i} + \mathcal{C}_-^{sa_i}\mathcal{G}_-^{sa_i}\right]. \tag{4.18}$$

The lower symbols + and − indicate the two coupling constant combinations.

The coefficient functions are:

$$\begin{aligned}\mathcal{C}_\pm^{sa_i} &= \sum_{k,l=\gamma,Z}\frac{2}{(6\pi^2)^2}\mathrm{Re}\frac{1}{D_k(s)D_l^*(s)D_W(s_1)D_W(s_2)D_W^*(s_{3-i})}\\ &\quad\times g_k\left[L(e,k)L(e,l)\pm R(e,k)R(e,l)\right]\\ &\quad\times L^2(F_1,W)L^2(F_2,W)L(f_a^i,l)N_c(F_1)N_c(F_2).\end{aligned} \tag{4.19}$$

For the su_1-interference we get the kinematical functions:

$$\mathcal{G}_-^{su_1}(s,s_1,s_2) = \frac{3}{16}\frac{\cos\theta}{\sqrt{\lambda}}ss_2\left\{2s\left[s(s_1+s_2)-s_1^2-s_2^2\right]\mathcal{L}(s_1;s_2,s)+(s+s_1)^2-s_2^2\right\}, \tag{4.20}$$

$$\begin{aligned}\mathcal{G}_+^{su_1}(s,s_1,s_2) &= \frac{3}{16}\frac{1-3\cos^2\theta}{\lambda}s^2s_1s_2\left[2ss_2\mathcal{L}(s_1;s_2,s)+s-s_1+s_2\right]\\ &\quad-\frac{3ss_2}{16}\left[s(s_1+s_2)(1+\cos^2\theta)+2s_1s_2\sin^2\theta\right]\mathcal{L}(s_1;s_2,s)\\ &\quad+\frac{ss_1}{8}(s_1-s-4s_2)+\frac{3s_2}{32}\left[s(3s_1-s_2-s)(1+\cos^2\theta)\right.\\ &\quad\left.+2s_1(s_1-s_2)\sin^2\theta\right]+\frac{\lambda\sin^2\theta}{64}(s_1-s-s_2),\end{aligned} \tag{4.21}$$

with

$$\mathcal{L}(s;s_1,s_2) = \frac{1}{\sqrt{\lambda}}\ln\frac{s-s_1-s_2+\sqrt{\lambda}}{s-s_1-s_2-\sqrt{\lambda}}. \tag{4.22}$$

[1] This effect is evoked by the additional spin dependent $Zf\bar{f}$-coupling in the background diagrams. Consequently the coefficient functions $\mathcal{C}_-$ vanish when only photons are exchanged.

The remaining kinematical functions can be easily obtained by the relation:

$$\mathcal{G}_{\pm}^{sd_1}(s,s_1,s_2) = \mathcal{G}_{\pm}^{sd_2}(s,s_2,s_1) = \mp\mathcal{G}_{\pm}^{su_2}(s,s_2,s_1) = \mp\mathcal{G}_{\pm}^{su_1}(s,s_1,s_2). \tag{4.23}$$

After an integration over $\cos\theta$, expression (4.21) leads to (3.1) of [131]. $\mathcal{G}_{-}^{su_1}$ is proportional to $\cos\theta$ and does not contribute to the total cross-section.

4.2.2 The Background-t-channel Interference

Since only left-handed fermions appear in the t-channel exchange in the interference of t-channel and background, only one coefficient function per interference term occurs:

$$\frac{\mathrm{d}\sigma_{tb}}{\mathrm{d}\cos\theta} = \frac{\sqrt{\lambda}}{2\pi s^2}\int \mathrm{d}s_1\mathrm{d}s_2 \sum_{i=1,2}\sum_{a=u,d} \mathcal{C}^{ta_i}\mathcal{G}^{ta_i}. \tag{4.24}$$

The coefficient functions are:

$$\begin{aligned}\mathcal{C}^{ta_i} &= \sum_{k=\gamma,Z}\frac{2}{(6\pi^2)^2}\mathrm{Re}\frac{1}{D_W(s_1)D_W(s_2)D_k^*(s)D_W^*(s_{3-i})} \\ &\quad\times L^2(E,W)L(e,k)L(f_i^a,k)L^2(F_1,W)L^2(F_2,W)N_c(F_1)N_c(F_2).\end{aligned} \tag{4.25}$$

and the kinematical function for tu_1 is:

$$\begin{aligned}&\mathcal{G}^{tu_1}(s,s_1,s_2) = \\ &\frac{-1}{\lambda}\left\{\frac{3}{4}\frac{\cos\theta}{\sqrt{\lambda}}\, s^2 s_1 s_2^2(5\sin^2\theta-2)\left[\frac{1}{t_\nu}(s+s_1-s_2)+2s\mathcal{L}(s_1;s_2,s)\right]\right. \\ &+\lambda\left[\frac{\sin^2\theta}{8t_\nu}[2s_1s_2(s_2-s_1)-6s^2s_2(s_1+s_2)\mathcal{L}(s_1;s_2,s)-3ss_2(s+s_2)]\right. \\ &\left.+\frac{\sin^2\theta}{16}[(s-s_1)^2-s_2^2]+\frac{ss_1}{2}\right]+\frac{ss_1s_2}{t_\nu}\left[-\frac{3}{4}ss_2\mathcal{L}(s_1;s_2,s)(5s\sin^4\theta+4s_1\right. \\ &+4s_2)-\frac{1}{8}(3s_2^2-2ss_1+4s_1s_2-7s_1^2+30ss_2+9s^2)\sin^2\theta-\frac{1}{2}(3s_2^2-2s_1^2 \\ &\left.-s_1s_2+2ss_1)\right]+\frac{3s^2s_2}{4}\mathcal{L}(s_1;s_2,s)([4s_1s_2+s_1^2+s_2^2-s(s_1+s_2)]\sin^2\theta \\ &-4[s_1s_2+s_1^2+s_2^2-s(s_1+s_2)])+\frac{ss_2\sin^2\theta}{8}(2s_1s_2-5s_1^2+3s_2^2 \\ &\left.-14ss_1-3s^2)+\frac{s}{2}(5s_1^2s_2-2s_1s_2^2-3s_2^3+5ss_1s_2+3s^2s_2)\right\}.\end{aligned} \tag{4.26}$$

For the td_1-interference we get:

$$\begin{aligned}\mathcal{G}^{td_1}(s,s_1,s_2) &= -\mathcal{G}^{tu_1}(s,s_1,s_2) \\ &\quad-\frac{3ss_2}{\lambda}\left[\frac{\sin^2\theta}{4t_\nu}\left\{(s+s_1+s_2)[s_1(2s_1-s-s_2)-(s-s_2)^2]\right.\right. \\ &\quad\left.-2\left[ss_1(s-s_1)^2+ss_2(s-s_2)^2+s_1s_2(s_1-s_2)^2\right]\mathcal{L}(s_1;s_2,s)\right\} \\ &\quad\left.+s\left[s(s_1+s_2)-s_1^2-s_2^2\right]\mathcal{L}(s_1;s_2,s)+\frac{1}{2}\left[(s+s_1)^2-s_2^2\right]\right].\end{aligned} \tag{4.27}$$

The kinematical functions for the second fermion doublet is obtained by the symmetry relations

$$\mathcal{G}^{tu_2}(s,s_1,s_2) = \mathcal{G}^{tu_1}(s,s_2,s_1), \tag{4.28}$$

and

$$\mathcal{G}^{td_2}(s,s_1,s_2) = \mathcal{G}^{td_1}(s,s_2,s_1). \tag{4.29}$$

4.2.3 The Pure Background Contribution

The pure background contribution contains the squares and interferences of eight Feynman diagrams. This leads to 64 interferences and, therefore, to 128 coefficient functions and kinematical functions:

$$\frac{\mathrm{d}\sigma_{bb}}{\mathrm{d}\cos\theta} = \frac{\sqrt{\lambda}}{2\pi s^2}\int \mathrm{d}s_1\mathrm{d}s_2 \sum_{a,b=u,d}\sum_{i,j=1,2}\left[\mathcal{C}_+^{a_ib_j}\mathcal{G}_+^{a_ib_j} + \mathcal{C}_-^{a_ib_j}\mathcal{G}_-^{a_ib_j}\right]. \tag{4.30}$$

The coefficient functions are:

$$\begin{aligned}\mathcal{C}_\pm^{a_ib_j} &= \sum_{k,l=\gamma,Z}\frac{2}{(6\pi^2)^2}\mathrm{Re}\frac{1}{D_k(s)D_l^*(s)D_W(s_{3-i})D_W^*(s_{3-j})}\\ &\quad\times\left[L(e,k)L(e,l)\pm R(e,k)R(e,l)\right]\\ &\quad\times L^2(F_1,W)L^2(F_2,W)N_c(F_1)N_c(F_2)\\ &\quad\times L(f_i^a,k)L(f_j^b,l).\end{aligned} \tag{4.31}$$

The γ and Z exchanges differ only in the coefficient functions, therefore, the number of independent kinematical functions can be reduced to 2×16. With the symmetry relation

$$\mathcal{G}_\pm^{a_ib_j} = \mathcal{G}_\pm^{b_ja_i}, \tag{4.32}$$

the number of independent kinematical functions can be further reduced. Only 2×10 independent $\mathcal{G}$-functions remain and have to be determined. To express all these kinematical functions only five new functions and two functions known from neutral current processes are needed. The functions are: $\mathcal{G}_+^{u_1u_1}$, $\mathcal{G}_-^{u_1u_1}$, $\mathcal{G}_+^{u_1d_2}$, $\mathcal{G}_-^{u_1d_2}$, $\mathcal{G}_-^{u_1u_2}$, $\mathcal{G}_{233}^{DD}$, and $\mathcal{G}_{422}^{DD}$. Table 4.2 gives an overview over the functions on which the various interferences depend.

Let us start with the simplest case: the square of the background diagrams. The u_1u_1 contributions are given by:

$$\mathcal{G}_-^{u_1u_1}(s,s_1,s_2) = \frac{3}{4}\frac{\cos\theta}{\sqrt{\lambda}}ss_2\left\{\frac{1}{2}\mathcal{L}(s_1;s_2,s)\left[(s-s_1)^2-s_2^2\right]+s-s_1-s_2\right\} \tag{4.33}$$

and

$$\begin{aligned}\mathcal{G}_+^{u_1u_1}(s,s_1,s_2) &= \frac{3}{8}\frac{1-3\cos^2\theta}{\lambda}ss_1s_2^2\left[\mathcal{L}(s_1;s_2,s)(s_2-s_1+s)+2\right]+\frac{1}{64}\lambda(1-\cos^2\theta)\\ &\quad+\frac{3}{16}s_2(1+\cos^2\theta)\left[s\mathcal{L}(s_1;s_2,s)(s_1-s_2-s)-2s-s_1\right]\\ &\quad+\frac{1}{8}s_1(s+3s_2).\end{aligned} \tag{4.34}$$

	u_1	u_2	d_1	d_2
u_1	$\mathcal{G}_+^{u_1u_1}$, $\mathcal{G}_-^{u_1u_1}$	$\mathcal{G}_-^{u_1u_2}$, $\mathcal{G}_+^{u_1d_2}$ $\mathcal{G}_{233}^{DD}$	$\mathcal{G}_+^{u_1u_1}$, $\mathcal{G}_{422}^{DD}$	$\mathcal{G}_+^{u_1d_2}$, $\mathcal{G}_-^{u_1d_2}$
u_2	$\mathcal{G}_-^{u_1u_2}$, $\mathcal{G}_+^{u_1d_2}$ $\mathcal{G}_{233}^{DD}$	$\mathcal{G}_+^{u_1u_1}$, $\mathcal{G}_-^{u_1u_1}$	$\mathcal{G}_+^{u_1d_2}$, $\mathcal{G}_-^{u_1d_2}$	$\mathcal{G}_+^{u_1u_1}$, $\mathcal{G}_{422}^{DD}$
d_1	$\mathcal{G}_+^{u_1u_1}$, $\mathcal{G}_{422}^{DD}$	$\mathcal{G}_+^{u_1d_2}$, $\mathcal{G}_-^{u_1d_2}$	$\mathcal{G}_+^{u_1u_1}$, $\mathcal{G}_-^{u_1u_1}$	$\mathcal{G}_-^{u_1u_2}$, $\mathcal{G}_+^{u_1d_2}$ $\mathcal{G}_{233}^{DD}$
d_2	$\mathcal{G}_+^{u_1d_2}$, $\mathcal{G}_-^{u_1d_2}$	$\mathcal{G}_+^{u_1u_1}$, $\mathcal{G}_{422}^{DD}$	$\mathcal{G}_-^{u_1u_2}$, $\mathcal{G}_+^{u_1d_2}$ $\mathcal{G}_{233}^{DD}$	$\mathcal{G}_+^{u_1u_1}$, $\mathcal{G}_-^{u_1u_1}$

Table 4.2: *Dependencies of the various background interferences on the seven kinematical functions.*

The kinematical functions for the squares of the other background diagrams are obtained by the symmetry relations:

$$\mathcal{G}_\pm^{u_2u_2}(s,s_1,s_2) = \mathcal{G}_\pm^{u_1u_1}(s,s_2,s_1), \tag{4.35}$$

$$\mathcal{G}_\pm^{d_1d_1}(s,s_1,s_2) = \pm\mathcal{G}_\pm^{u_1u_1}(s,s_1,s_2), \tag{4.36}$$

$$\mathcal{G}_\pm^{d_2d_2}(s,s_1,s_2) = \pm\mathcal{G}_\pm^{u_1u_1}(s,s_2,s_1). \tag{4.37}$$

After integrating equation (4.34) over $\cos\theta$ one gets the expression (3.3) as presented in reference [131]. The function $\mathcal{G}_-^{u_1u_1}$ in (4.33) does not contribute to the total cross-section, since it is an odd function of $\cos\theta$.

The kinematical functions for the interference terms between u_1 and d_1 diagram read:

$$\mathcal{G}_+^{u_1d_1}(s,s_1,s_2) = \mathcal{G}_+^{d_1d_1}(s,s_1,s_2) + \mathcal{G}_+^{u_1u_1}(s,s_1,s_2) - ss_2\mathcal{G}_{422}^{DD}(s,s_1,s_2), \tag{4.38}$$

and

$$\mathcal{G}_-^{u_1d_1}(s,s_1,s_2) = -\left[\mathcal{G}_-^{d_1d_1}(s,s_1,s_2) + \mathcal{G}_-^{u_1u_1}(s,s_1,s_2)\right] = 0. \tag{4.39}$$

The similar expressions for the other doublet are easily obtained by exchanging s_1 and s_2:

$$\mathcal{G}_\pm^{u_2d_2}(s,s_1,s_2) = \mathcal{G}_\pm^{u_1d_1}(s,s_2,s_1). \tag{4.40}$$

Note that the function $\mathcal{G}_{422}^{DD}(s,s_1,s_2)$ appears also in neutral-current processes [132] and is:

$$\begin{aligned}\mathcal{G}_{422}^{DD}(\cos\theta;s_1;s_2,s) &= \frac{3}{8}(1+\cos^2\theta)\mathcal{G}_{422}(s_1;s_2,s) \\ &\quad + \frac{1-3\cos^2\theta}{\lambda}s_1(s+s_2)\frac{3}{4}\left(1-2\mathcal{L}(s_1;s_2,s)\frac{ss_2}{s_1-s_2-s}\right),\end{aligned} \tag{4.41}$$

where $\mathcal{G}_{422}$ is $[123, 133, 134]$:

$$\mathcal{G}_{422}(s; s_1, s_2) = \frac{s^2 + (s_1 + s_2)^2}{s - s_1 - s_2}\mathcal{L}(s; s_1, s_2) - 2. \tag{4.42}$$

The contributions of interferences between diagrams where fermions from different doublets couple to the s-channel gauge boson have a more complicated structure. For the interference between u_1 and d_2 diagrams we get:

$$\mathcal{G}_{-}^{u_1 d_2}(s, s_1, s_2) = \frac{3}{8}\frac{\cos\theta}{\sqrt{\lambda}} s \left\{ 2s \left[s_2^2 \mathcal{L}(s_1; s_2, s) - s_1^2 \mathcal{L}(s_2; s, s_1) + \frac{s_2 - s_1}{2} \right] - s_1^2 + s_2^2 \right\}, \tag{4.43}$$

and

$$\begin{aligned}
\mathcal{G}_{+}^{u_1 d_2}(s, s_1, s_2) = & -18\frac{s^2 s_1^2 s_2^2}{\lambda^3}(1 + \sin^2\theta) s^2 s_1 s_2 \mathcal{L}(s_1; s_2, s)\mathcal{L}(s_2; s, s_1) \\
& - 3s \left[s_1^2 \mathcal{L}(s_2; s, s_1) + s_2^2 \mathcal{L}(s_1; s_2, s) \right] \\
& \times \left[\frac{\sin^2\theta}{8} + \frac{s\cos^2\theta}{4\lambda}(s - \sigma) + \frac{s^2 s_1 s_2 (1 + \sin^2\theta)}{2\lambda^2} \left(2 - 3s\frac{s - 3\sigma}{\lambda} \right) \right] \\
& - s(s_1 - s_2) \left[s_1^2 \mathcal{L}(s_2; s, s_1) - s_2^2 \mathcal{L}(s_1; s_2, s) \right] \\
& \times \left[\frac{3\sin^2\theta}{8\lambda}(s - \sigma) + \frac{3s s_1 s_2 (1 + \sin^2\theta)}{2\lambda^2} \left(1 - 3s\frac{s + \sigma}{\lambda} \right) \right] \\
& + \frac{3s^2 s_1 s_2 (1 + \sin^2\theta)}{4\lambda^2} \left[s^2 - s_1^2 - s_2^2 - \frac{12 s s_1 s_2 (s - \sigma)}{\lambda} \right] \\
& + \frac{s(1 + \cos^2\theta)}{16\lambda} \left[4 s s_1 s_2 + 3(s_1^3 + s_2^3) - (3s^2 + 7 s_1 s_2)\sigma \right] \\
& - \frac{\sin^2\theta}{32} \left[\frac{24 s s_1 s_2 (2s - \sigma)}{\lambda} + s^2 - s_1^2 - s_2^2 - 10 s_1 s_2 \right].
\end{aligned} \tag{4.44}$$

Expression (4.44) is used to write the kinematical function for the $u_1 u_2$ interference:

$$\begin{aligned}
\mathcal{G}_{-}^{u_1 u_2}(s, s_1, s_2) = & -\mathcal{G}_{-}^{u_1 d_2}(s, s_1, s_2) + \frac{s\cos\theta}{\sqrt{\lambda}} \left\{ \frac{27 s^2 s_1^2 s_2^2}{2\lambda^2} \Big[s(\sigma - s)\mathcal{L}(s_1; s_2, s)\mathcal{L}(s_2; s, s_1) \right. \\
& \left. + (s_1 - s - s_2)\mathcal{L}(s_1; s_2, s) + (s_2 - s - s_1)\mathcal{L}(s_2; s, s_1) - 2 \Big] \right. \\
& + \frac{9 s s_1 s_2}{2\lambda} \left[s[3 s_1 s_2 + s(\sigma - s)]\mathcal{L}(s_1; s_2, s)\mathcal{L}(s_2; s, s_1) \right. \\
& + \left[s(s_1 - s) + s_2 \left(s_1 - s_2 - \frac{s}{2} \right) \right] \mathcal{L}(s_1; s_2, s) \\
& + \left[s_2(s_2 - s - s_1) - \frac{5}{2} s s_1 \right] \mathcal{L}(s_2; s, s_1) - \frac{5}{4}(s + \sigma) \Big] \\
& + \frac{3 s_1}{4} \left[6 s^2 s_2 \mathcal{L}(s_1; s_2, s)\mathcal{L}(s_2; s, s_1) + 3 s s_2 \mathcal{L}(s_1; s_2, s) \right. \\
& \left. \left. - s(3 s_2 + 2 s_1)\mathcal{L}(s_2; s, s_1) - s + s_1 + \frac{3}{2} s_2 \right] \right\}.
\end{aligned} \tag{4.45}$$

The kinematical function $\mathcal{G}_+^{u_1u_2}$ can be expressed using the already derived function $\mathcal{G}_+^{u_1d_2}(s,s_1,s_2)$ and $\mathcal{G}_{233}^{DD}$:

$$\mathcal{G}_+^{u_1u_2}(s,s_1,s_2) = \frac{1}{2}ss_1s_2\mathcal{G}_{233}^{DD}(\cos\theta,s,s_1,s_2) - \mathcal{G}_+^{u_1d_2}(s,s_1,s_2). \tag{4.46}$$

Like $\mathcal{G}_{422}$ the function $\mathcal{G}_{233}^{DD}(\cos\theta,s,s_1,s_2)$ is also taken from neutral-current processes. It is [132]:

$$\begin{aligned}\mathcal{G}_{233}^{DD}(\cos\theta,s,s_1,s_2) &= \frac{3}{8}(1+\cos^2\theta)\mathcal{G}_{233}(s;s_1,s_2)\\ &\quad -\frac{3}{\lambda^2}\frac{3}{8}(1-3\cos^2\theta)s\left[\mathcal{L}(s_1;s_2,s)2s_2(s_1-s_2)+(s-s_1-3s_2)\right]\\ &\quad \times\left[\mathcal{L}(s_2;s,s_1)2s_1(s_2-s_1)+(s-s_2-3s_1)\right],\end{aligned} \tag{4.47}$$

with [135]:

$$\begin{aligned}\mathcal{G}_{233}(s;s_1,s_2) &= \frac{3}{\lambda^2}\{\mathcal{L}(s_2;s,s_1)\mathcal{L}(s_1;s_2,s)\\ &\quad 4s\left[ss_1(s-s_1)^2+ss_2(s-s_2)^2+s_1s_2(s_1-s_2)^2\right]\\ &\quad +(s+s_1+s_2)\left[\mathcal{L}(s_2;s,s_1)2s\left[(s-s_2)^2+s_1(s+s_2-2s_1)\right]\right.\\ &\quad\quad +\mathcal{L}(s_1;s_2,s)2s\left[(s-s_1)^2+s_2(s+s_1-2s_2)\right]\\ &\quad\quad \left.+5s^2-4s(s_1+s_2)-(s_1-s_2)^2\right]\}.\end{aligned} \tag{4.48}$$

The relations

$$\mathcal{G}_\pm^{d_1u_2}(s,s_1,s_2) = \mathcal{G}_\pm^{u_1d_2}(s,s_2,s_1), \tag{4.49}$$

and

$$\mathcal{G}_\pm^{d_1d_2}(s,s_1,s_2) = \pm\mathcal{G}_\pm^{u_1u_2}(s,s_1,s_2), \tag{4.50}$$

complete the set of kinematical functions for the pure background.

4.3 Anomalous Couplings in W Pair Production

In the process of W pair production triple gauge boson vertices, as shown in figure 4.3, appear in the two s-channel diagrams. In the Standard Model this vertex is described by the Lagrangian

$$\mathcal{L} = ig_{WWV}\left[\left(W^+_{\mu\nu}W^{-\mu}-W^{+\mu}W^-_{\mu\nu}\right)V^\nu + W^+_\mu W^-_\nu V^{\mu\nu}\right], \tag{4.51}$$

where all parameters are known. However, since there are only weak constraints to the possible parameters in this vertex, deviations may occur. The most general form for the γWW and ZWW vertices that is still compatible with Lorentz invariance was first considered in [84]. Later, the number of anomalous parameters for each vertex was reduced

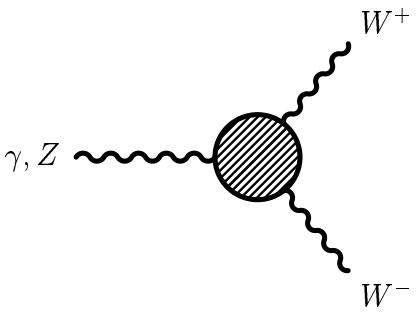

Figure 4.3: *The three gauge boson vertex.*

to seven in [85,89]. Several studies were performed to examine the influence of anomalous couplings on W pair production, see e.g. [136–139]. An overview can be found in [86].

The anomalous couplings used in this work are defined by the Lagrangian:

$$\begin{aligned}
\mathcal{L}_1 &= -ie\left[A_\mu\left(W^{-\mu\nu}W^+_\nu - W^{+\mu\nu}W^-_\nu\right) + F_{\mu\nu}W^{+\mu}W^{-\nu}\right] \\
&\quad - ie\left(\cot\theta_W + \delta_Z\right)\left[Z_\mu\left(W^{-\mu\nu}W^+_\nu - W^{+\mu\nu}W^-_\nu\right) + Z_{\mu\nu}W^{+\mu}W^{-\nu}\right] \\
&\quad - iex_\gamma F_{\mu\nu}W^{+\mu}W^{-\nu} - iex_Z Z_{\mu\nu}W^{+\mu}W^{-\nu} \\
&\quad - ie\frac{y_\gamma}{M_W^2}F^{\nu\lambda}W^-_{\lambda\mu}W^{+\mu}_\nu - ie\frac{y_Z}{M_W^2}Z^{\nu\lambda}W^-_{\lambda\mu}W^{+\mu}_\nu,
\end{aligned} \tag{4.52}$$

and

$$\mathcal{L}_2 = \frac{ez_Z}{M_W^2}\partial_\alpha\tilde{Z}_{\rho\sigma}\left(\partial^\rho W^{-\sigma}W^{+\alpha} - \partial^\rho W^{-\alpha}W^{+\sigma} + \partial^\rho W^{+\sigma}W^{-\alpha} - \partial^\rho W^{+\alpha}W^{-\sigma}\right). \tag{4.53}$$

The Lagrangian $\mathcal{L}_1$ in (4.52) defines anomalous couplings which conserve $\mathcal{C}$ and $\mathcal{P}$ symmetry separately. In the Lagrangian $\mathcal{L}_2$ of (4.53) the $\mathcal{C}$ and $\mathcal{P}$ violating, but $\mathcal{CP}$ conserving coupling z_Z is introduced. In the Standard Model the parameters δ_Z, x_γ, x_Z, y_γ, y_Z, and z_Z are zero.

The parameters z_γ and y_γ contribute to the magnetic dipole moment μ_W and the electromagnetic quadrupole moment q_W of the W boson [140]:

$$\mu_W = \frac{e}{m_W^2}(2 + x_\gamma + y_\gamma), \tag{4.54}$$

$$q_W = -\frac{e}{m_W^2}(1 + x_\gamma - y_\gamma). \tag{4.55}$$

A derivation of equations (4.54) and (4.55) can be found in appendices C.2 and C.3. The weak couplings x_Z and y_Z give contributions in a similar way as κ_γ and λ_γ in equation (4.54) and (4.55) to the weak moments of the W boson.

Before LEP2 reached the threshold for W pair production, there had been limits to the γWW vertex from Tevatron [141]:

$$-0.33 < x_\gamma < 0.45\,(y_\gamma = 0), \tag{4.56}$$

$$-0.20 < y_\gamma < 0.20\,(x_\gamma = 0), \tag{4.57}$$

where the relations

$$x_\gamma = x_Z \tan\theta_W, \tag{4.58}$$
$$y_\gamma = y_Z \tan\theta_W, \tag{4.59}$$
$$\delta_Z = 0, \tag{4.60}$$

are applied. Recent limits from LEP2 for anomalous couplings combined with results from D0 are [142]:

$$\alpha_{W\phi} = -0.03^{+0.06}_{-0.06}, \tag{4.61}$$
$$\alpha_W = -0.03^{+0.08}_{-0.08}, \tag{4.62}$$
$$\alpha_{B\phi} = -0.05^{+0.22}_{-0.20}, \tag{4.63}$$

where the α's are the coefficients of the three six-dimensional operators:

$$\mathcal{O}_{B\phi} = ig'\frac{\alpha_{B\phi}}{m_W^2}\left(D_\mu\Phi\right)^\dagger B^{\mu\nu}\left(D_\nu\Phi\right), \tag{4.64}$$
$$\mathcal{O}_{W\phi} = ig\frac{\alpha_{W\phi}}{m_W^2}\left(D_\mu\Phi\right)^\dagger \vec{\tau}\cdot\vec{W}^{\mu\nu}\left(D_\nu\Phi\right), \tag{4.65}$$
$$\mathcal{O}_W = g\frac{\alpha_W}{6m_W^2}\vec{W}^\mu{}_\nu\cdot\left(\vec{W}^\nu{}_\rho\times\vec{W}^\rho{}_\mu\right), \tag{4.66}$$

and imply the identities:

$$\alpha_{W\phi} = c_W s_W \delta_Z, \tag{4.67}$$
$$\alpha_W = y_\gamma = \frac{s_W}{c_W}y_Z, \tag{4.68}$$
$$\alpha_{B\phi} = x_\gamma - c_W s_W \delta_Z = -\frac{c_W}{s_W}\left(x_Z + s_W^2\delta_Z\right). \tag{4.69}$$

4.3.1 The CC03 Process with Anomalous Couplings

As mentioned before, the three gauge boson vertices appear in the s-channel signal diagrams. The occurrence of non-vanishing anomalous couplings will therefore change the cross-section of the CC03 process. The contributions of anomalous couplings to the differential cross-section is investigated in this section.

We present the results in the same way as in section 4.1 and 4.2 and introduce the functions $\mathcal{C}^s_{nm}$ and $\mathcal{G}^s_{nm}(s;s_1,s_2,\cos\theta)$ for the pure s-channel contribution and the functions $\mathcal{C}^{st}_n$ and $\mathcal{G}^{st}_n(s;s_1,s_2,\cos\theta)$ for the interferences between s-channel and t-channel:

$$\frac{\mathrm{d}\sigma^{\mathrm{ano}}_{\mathrm{CC03}}}{\mathrm{d}\cos\theta} = \frac{\sqrt{\lambda}}{2\pi s^2}\int \mathrm{d}s_1\mathrm{d}s_2\left[\sum_{nm}\mathcal{C}^s_{nm}\mathcal{G}^s_{nm}(s;s_1,s_2,\cos\theta) + \sum_n \mathcal{C}^{st}_n\mathcal{G}^{st}_n(s;s_1,s_2,\cos\theta)\right]. \tag{4.70}$$

With the Feynman rules of appendix A we get for the coefficient functions:

$$\mathcal{C}^s_{nm} = \sum_{k,l=\gamma,Z}\frac{2}{(6\pi^2)^2}\mathrm{Re}\frac{1}{|D_W(s_1)|^2|D_W(s_2)|^2 D_k(s)D_l^*(s)}$$

$$
\begin{aligned}
& \times g_k^n g_l^m [1 + (1 - \delta_m^n)\delta_l^k] A_{kl}^{nm} \\
& \times L^2(F_1, W) L^2(F_2, W) N_c(F_1) N_c(F_2), \qquad (4.71) \\
\mathcal{C}_n^{st} \;=\; & \sum_{k=\gamma,Z} \frac{2}{(6\pi^2)^2} \mathrm{Re} \frac{1}{|D_W(s_1)|^2 |D_W(s_2)|^2 D_k(s)} \\
& \times g_k^n L(e,l) L^2(F_1, W) L^2(F_2, W) L^2(e, W) N_c(F_1) N_c(F_2), \qquad (4.72)
\end{aligned}
$$

where the anomalous couplings

$$
\begin{aligned}
g_\gamma^x &= g s_W x_\gamma, & g_Z^x &= g s_W x_Z, \\
g_\gamma^y &= \frac{g s_W y_\gamma}{M_W^2}, & g_Z^y &= \frac{g s_W y_Z}{M_W^2}, \qquad (4.73) \\
g_Z^\delta &= g s_W \delta_Z, & g_Z^z &= \frac{g s_W z_Z}{M_W^2},
\end{aligned}
$$

are used. The Standard Model couplings are:

$$
g_\gamma^{\mathrm{SM}} = g s_W, \qquad g_Z^{\mathrm{SM}} = g c_W. \qquad (4.74)
$$

To include the parity violating coupling z_Z, we have to introduce the abbreviations:

$$
\begin{aligned}
A_{kl}^{zm} = A_{kl}^{mz} &= L(e,k)L(e,l) - R(e,k)R(e,l) \qquad \text{for } m \neq z \qquad (4.75) \\
A_{kl}^{nm} &= L(e,k)L(e,l) + R(e,k)R(e,l) \qquad \text{otherwise.} \qquad (4.76)
\end{aligned}
$$

The kinematical functions $\mathcal{G}^{st}$ for the interference between s-channel and t-channel are:

$$
\begin{aligned}
\mathcal{G}_x^{st} &= \frac{1}{8} s \left[(s_1 + s_2) \left(s - s_1 - s_2 - \frac{2 s_1 s_2}{t_\nu} \right) + \frac{\lambda}{4} \sin^2\theta \right], \qquad (4.77) \\
\mathcal{G}_y^{st} &= \frac{1}{4} s s_1 s_2 \left[s - s_1 - s_2 - \frac{2 s_1 s_2}{t_\nu} \right], \qquad (4.78) \\
\mathcal{G}_z^{st} &= \frac{1}{16} \lambda s \left[2(s_1 + s_2) - \frac{\sin^2\theta}{t_\nu} (s_1(s - s_1) + s_2(s - s_2)) \right], \qquad (4.79)
\end{aligned}
$$

and for the s-channel squared diagrams:

$$
\begin{aligned}
\mathcal{G}_{xx}^{s} &= \frac{1}{128} \lambda s \left[(s_1 + s_2)(1 + \cos^2\theta) + s \sin^2\theta \right], \qquad (4.80) \\
\mathcal{G}_{xy}^{s} &= \frac{1}{64} \lambda s s_1 s_2 (1 + \cos^2\theta), \qquad (4.81) \\
\mathcal{G}_{sx}^{s} = \mathcal{G}_{x\delta}^{s} &= \frac{1}{128} \lambda s \left[4(s_1 + s_2) + (s - s_1 - s_2) \sin^2\theta \right], \qquad (4.82) \\
\mathcal{G}_{yy}^{s} &= \frac{1}{128} \lambda s s_1 s_2 \left[2s \sin^2\theta + (s_1 + s_2)(1 + \cos^2\theta) \right], \qquad (4.83)
\end{aligned}
$$

$$\mathcal{G}^s_{sy} = \mathcal{G}^s_{y\delta} = \frac{1}{16}\lambda s s_1 s_2, \tag{4.84}$$

$$\mathcal{G}^s_{zz} = \frac{1}{128}\lambda^2 s(s_1+s_2)(1+\cos^2\theta), \tag{4.85}$$

$$\mathcal{G}^s_{s\delta} = \mathcal{G}^s_{\delta\delta} = \frac{1}{32}\lambda\left[2s(s_1+s_2)+\left(3s_1s_2+\frac{\lambda}{4}\right)\sin^2\theta\right], \tag{4.86}$$

$$\mathcal{G}^s_{xz} = \frac{1}{64}\lambda^{\frac{3}{2}} s(s_1+s_2)\cos\theta, \tag{4.87}$$

$$\mathcal{G}^s_{yz} = \frac{1}{32}\lambda^{\frac{3}{2}} s s_1 s_2 \cos\theta, \tag{4.88}$$

$$\mathcal{G}^s_{sz} = \mathcal{G}^s_{z\delta} = -\frac{1}{32}\lambda^{\frac{3}{2}} s(s_1+s_2)\cos\theta. \tag{4.89}$$

4.3.2 The CC11 Process with Anomalous Couplings

There appears no triple gauge boson vertex in the background diagrams. However, anomalous couplings influence the background contributions due to interferences with the s-channel diagram.

The differential cross-section for this part of the background is:

$$\frac{\mathrm{d}\sigma^{\mathrm{ano}}_{sb}}{\mathrm{d}\cos\theta} = \frac{\sqrt{\lambda}}{2\pi s^2}\int \mathrm{d}s_1\mathrm{d}s_2 \sum_{a=u,d}\sum_{i=1,2}\sum_n \left[\mathcal{C}^{sa_i}_{+,n}\mathcal{G}^{sa_i}_{+,n} + \mathcal{C}^{sa_i}_{-,n}\mathcal{G}^{sa_i}_{-,n}\right], \tag{4.90}$$

with the coefficient functions:

$$\begin{aligned}\mathcal{C}^{sa_i}_{\pm,n} &= \sum_{k,l=\gamma,Z}\frac{2}{(6\pi^2)^2}\mathrm{Re}\frac{1}{D_k(s)D^*_l(s)D_W(s_1)D_W(s_2)D^*_W(s_{3-i})} \\ &\quad\times g^n_k\left[L(e,k)L(e,l)\pm R(e,k)R(e,l)\right] \\ &\quad\times L^2(F_1,W)L^2(F_2,W)L(f^i_a,l)N_c(F_1)N_c(F_2).\end{aligned} \tag{4.91}$$

In the interference between the s-channel and the u_1-background diagram the kinematical functions for the various anomalous couplings are:

$$\mathcal{G}^{su_1}_{-,x}(s,s_1,s_2) = \frac{3}{32}\frac{\cos\theta}{\sqrt{\lambda}}ss_2\left\{2s[s(s_1+s_2)-s_1^2-s_2^2]\mathcal{L}(s_1;s_2,s)+(s+s_1)^2-s_2^2\right\}, \tag{4.92}$$

$$\begin{aligned}\mathcal{G}^{su_1}_{+,x}(s,s_1,s_2) &= \frac{3}{32}\frac{1-3\cos^2\theta}{\lambda}s^2s_1s_2\left[2ss_2\mathcal{L}(s_1;s_2,s)+s-s_1+s_2\right] \\ &\quad-\frac{3s}{32}(1+\cos^2\theta)ss_2(s_1+s_2)\mathcal{L}(s_1;s_2,s) \\ &\quad+\frac{ss_2}{64}(1-3\cos^2\theta)(s+s_2-s_1)\end{aligned}$$

$$+\frac{s}{16}\left[s_1^2-s_2^2-s(s_1+s_2)-\frac{\lambda\sin^2\theta}{4}\right], \tag{4.93}$$

$$\begin{aligned}\mathcal{G}^{su_1}_{-,y}(s,s_1,s_2) &= \frac{3}{32}\frac{\cos\theta}{\sqrt{\lambda}}ss_1s_2\left\{2ss_2[2s-(s_1+s_2)]\mathcal{L}(s_1;s_2,s)-2s_2^2+2s_1s_2\right.\\ &\left.+3ss_2-ss_1+s^2\right\},\end{aligned} \tag{4.94}$$

$$\begin{aligned}\mathcal{G}^{su_1}_{+,y}(s,s_1,s_2) &= \frac{ss_1s_2}{64}\left\{6\frac{1-3\cos^2\theta}{\lambda}ss_2\left\{s[s-(s_1+s_2)]\mathcal{L}(s_1;s_2,s)+s+s_1-s_2\right\}\right.\\ &+(1-3\cos^2\theta)[s-2ss_2\mathcal{L}(s_1;s_2,s)]-16ss_2\mathcal{L}(s_1;s_2,s)\\ &\left.-8(s-s_1+s_2)\right\},\end{aligned} \tag{4.95}$$

$$\begin{aligned}\mathcal{G}^{su_1}_{-,z}(s,s_1,s_2) &= \frac{1}{32}\frac{\cos\theta}{\sqrt{\lambda}}s\left\{6ss_1s_2[2ss_2\mathcal{L}(s_1;s_2,s)+s-s_1+s_2]\right.\\ &\left.+\lambda\left[6ss_2(s_1+s_2)\mathcal{L}(s_1;s_2,s)+s(2s_1+3s_2)-s_1s_2-2s_1^2+3s_2^2\right]\right\},\end{aligned} \tag{4.96}$$

$$\begin{aligned}\mathcal{G}^{su_1}_{+,z}(s,s_1,s_2) &= \frac{3}{64}(1+\cos^2\theta)ss_2\left\{2s[s_1^2+s_2^2-s(s_1+s_2)]\mathcal{L}(s_1;s_2,s)\right.\\ &\left.+s_2^2-(s+s_1)^2\right\},\end{aligned} \tag{4.97}$$

$$\mathcal{G}^{su_1}_{-,\delta}(s,s_1,s_2) = \mathcal{G}^{sf_1^u}_{-}(s,s_1,s_2), \tag{4.98}$$

$$\mathcal{G}^{su_1}_{+,\delta}(s,s_1,s_2) = \mathcal{G}^{sf_1^u}_{+}(s,s_1,s_2). \tag{4.99}$$

The interferences of s-channel and the other background diagrams can be calculated using the relations:

$$\mathcal{G}^{sd_1}_{\pm,z}(s,s_1,s_2)=\mathcal{G}^{sd_2}_{\pm,z}(s,s_2,s_1)=\mp\mathcal{G}^{su_2}_{\pm,z}(s,s_2,s_1)=\mp\mathcal{G}^{su_1}_{\pm,z}(s,s_1,s_2). \tag{4.100}$$

4.4 Radiative Corrections – Initial State Radiation

Up to now, no complete electroweak one-loop calculation is available for the process $e^+e^-\to 4f$. However, much work has been invested on this field, see e.g. [116, 143–161] and references therein.

In the present analysis we consider only initial state radiation (ISR) as radiative corrections. These corrections are implemented in `GENTLE` for the total cross-section, but are also used, with the modifications described in this section, in calculations of the differential cross-section.

In total cross-section calculations radiative corrections lead to a change of the event rate. This effect is mostly due to the fact that the center-of-mass energy is reduced by the radiation of photons. A cross-section which strongly depends on the center-of-mass energy, might get large corrections in such a process. A well-known example is the cross-section for $e^+e^-\to Z\to\mu^+\mu^-$, where the radiation of hard photons increases the cross-section drastically at center-of-mass energies larger than m_Z.

The change of event rate can also be observed in the differential cross-section. In this case however, an additional effect appears. The momenta of e^- and e^+ are changed by radiating photons. As a consequence, the center-of-mass system is boosted along the beam axes. This Lorentz boost will also change the differential distribution of the W bosons, without an effect on the total event rate.

To calculate the ISR corrections the structure function approach as described in section 4.4.1 is used and in section 4.4.2 we describe the Lorentz boost necessary for the differential cross-section.

4.4.1 Structure Function Approach

Initial state radiation can be considered by the structure function approach [116, 162]. In this approach the Born cross-section is convoluted with two structure functions $D(x,s)$:

$$\frac{\mathrm{d}\sigma_{\mathrm{QED}}(s)}{\mathrm{d}s_1\mathrm{d}s_2\mathrm{d}\cos\theta} = \int_{x_1^{\min}}^{1}\mathrm{d}x_1\int_{x_2^{\min}}^{1}\mathrm{d}x_2 D(x_1,s)D(x_2,s)\sum_{i=1,2}\left|\frac{\mathrm{d}\cos\theta_i'}{\mathrm{d}\cos\theta}\right|\frac{\mathrm{d}\sigma(x_1x_2s,s_1,s_2)}{\mathrm{d}\cos\theta_i'}, \tag{4.101}$$

with $\theta_i' = \theta_i'(s,s_1,s_2,x_1,x_2,\theta)$ and the lower integration boundaries

$$x_1^{\min} \geq \frac{(\sqrt{s_1}+\sqrt{s_2})^2}{s}, \tag{4.102}$$

$$x_2^{\min} \geq \frac{(\sqrt{s_1}+\sqrt{s_2})^2}{x_1 s}. \tag{4.103}$$

The functions $D(x,s)$ are [131, 162]:

$$D(x,s) = (1-x)^{\beta_e/2-1}\frac{\beta_e}{2}(1+S)+H(x,s), \tag{4.104}$$

with

$$S = \frac{e^{(3/4-\gamma_E)\beta_e/2}}{\Gamma(1+\frac{\beta_e}{2})}-1, \tag{4.105}$$

$$H(x,s) = -\frac{1}{2}(1+x)\frac{\eta_e}{2}+\frac{1}{8}\left[-4(1+x)\ln(1-x)+3(1+x)\ln x - 4\frac{\ln x}{1-x}-5-x\right]\left(\frac{\eta_e}{2}\right)^2, \tag{4.106}$$

$$\eta_e = \frac{2\alpha}{\pi}(L_e-1), \tag{4.107}$$

and

$$\beta_e = \frac{2\alpha}{\pi}(L_e-1), \tag{4.108}$$

$$L_e = \ln\frac{s}{m_e^2}. \tag{4.109}$$

Note that the structure functions $D(x,s)$ are determined for the total cross-section and have to be considered as an approximation when applied to the differential cross-section.

The transformation of the angles (due to the Lorentz boost) leads to the introduction of the Jacobean $\left|\frac{\mathrm{d}\cos\theta_i'}{\mathrm{d}\cos\theta}\right|$ into equation (4.101). The transformation function $\theta'(\theta, x_1, x_2, s)$ and the corresponding Jacobean are derived in section 4.4.2.

For numerical applications, e.g. the analysis presented in section 4.5.2, and especially for comparisons with Monte Carlo programs [163,164] it is useful to calculate a bin-wise integrated cross-section:

$$\sigma = \sum_i \int_{\cos\theta'_{a_i}(\theta_a)}^{\cos\theta'_{b_i}(\theta_b)} \frac{d\sigma}{d\cos\theta'}. \tag{4.110}$$

The integration in (4.110) could be performed analytically for the `CC03` process and implemented into `GENTLE` also when ISR corrections are considered.

4.4.2 Lorentz Boost

Let us denote the detector system as Σ and the center-of-mass system of the produced W bosons as Σ'. The momenta of the electron and the positron in Σ are:

$$p_{e^-} = Ex_1(1,0,0,1), \tag{4.111}$$
$$p_{e^+} = Ex_2(1,0,0,-1). \tag{4.112}$$

$E = \sqrt{s}/2$ is the beam energy of the collider. The transformation of these momenta into their center-of-mass system (Σ') leads to:

$$p'_{e^-} = E\sqrt{x_1x_2}(1,0,0,1), \tag{4.113}$$
$$p'_{e^+} = E\sqrt{x_1x_2}(1,0,0,-1). \tag{4.114}$$

The boost velocity can be calculated by applying the transformation

$$p'_3 = \frac{p_3 - vp_0}{\sqrt{1-v^2}} \tag{4.115}$$

on the momenta in (4.111) and (4.113). Solving the equation

$$\sqrt{x_1x_2} = \frac{x_1 - vx_1}{\sqrt{1-v^2}} \tag{4.116}$$

for the boost velocity v we get:

$$v = \frac{x_1 - x_2}{x_1 + x_2}. \tag{4.117}$$

In their own center-of-mass system the momenta of the two W bosons are chosen to be:

$$p'_{W^-} = \left(\sqrt{\frac{\lambda'}{4s'} + s_1},\ \sqrt{\frac{\lambda'}{4s'}}\sin\theta',\ 0,\ \sqrt{\frac{\lambda'}{4s'}}\cos\theta'\right), \tag{4.118}$$

$$p'_{W^+} = \left(\sqrt{\frac{\lambda'}{4s'} + s_2},\ -\sqrt{\frac{\lambda'}{4s'}}\sin\theta',\ 0,\ -\sqrt{\frac{\lambda'}{4s'}}\cos\theta'\right), \tag{4.119}$$

with $s' = 4x_1x_2E^2$ as the reduced center-of-mass energy and the definition:

$$\lambda' \equiv \lambda(s', s_1, s_2). \tag{4.120}$$

Because of conservation of the 4-momentum, the energies and the momenta of the bosons are fixed. The direction of the W bosons defines the angle θ'.

Now, the momenta of the W^- boson in the frame Σ can be calculated by a Lorentz boost of the momentum (4.118) with velocity $-v$:

$$p_{W^-} = (Q_i, B_i \sin\theta, 0, B_i \cos\theta), \tag{4.121}$$

where Q_i and B_i are real and positive functions of s', s_1, s_2, $\cos\theta$ and v. The velocity of the W^--boson in the laboratory system is given by:

$$\beta_i = \frac{B_i}{Q_i}. \tag{4.122}$$

The lower index i indicates, that more than one solution may exist for the functions Q_i, B_i, and β_i.

Using

$$p_{e^-} + p_{e^+} = p_{W^-} + p_{W^+} \tag{4.123}$$

and the relations

$$p^2_{W^-} = s_1, \qquad\qquad p^2_{W^+} = s_2, \tag{4.124}$$

the functions Q_i and B_i of (4.121) can be determined. We get two sets of solutions

$$B_{1,2} = \frac{(s' - s_2 + s_1)\sqrt{1-v^2}\,(v\cos\theta \pm b)}{2\sqrt{s'}(1 - v^2\cos^2\theta)}, \tag{4.125}$$

$$Q_{1,2} = \frac{(s' - s_2 + s_1)\sqrt{1-v^2}\,(1 \pm bv\cos\theta)}{2\sqrt{s'}(1 - v^2\cos^2\theta)}, \tag{4.126}$$

with the abbreviation

$$b = \sqrt{1 - \frac{4s_1s'(1 - v^2\cos^2\theta)}{(s' - s_2 + s_1)^2(1-v^2)}}. \tag{4.127}$$

The number of solutions for (4.125) and (4.126) depends on $\cos\theta$, v and b. By definition, B is real and positive and therefore two solutions exit when $b < v\cos\theta$. No solution exists for $b < -v\cos\theta$ and there will be one solution for all remaining cases.

With the solutions in (4.125) and (4.126) and equation (4.115), the relation between the W production angles in the two Lorentz systems is:

$$\cos\theta' = \frac{B\cos\theta - vQ}{\sqrt{(1-v^2)B^2\sin^2\theta + (B\cos\theta - vQ)^2}}. \tag{4.128}$$

The transformation (4.128) is in accordance with the similar transformation derived in the limited case of on-shell W pair production published in reference [165] for on-shell

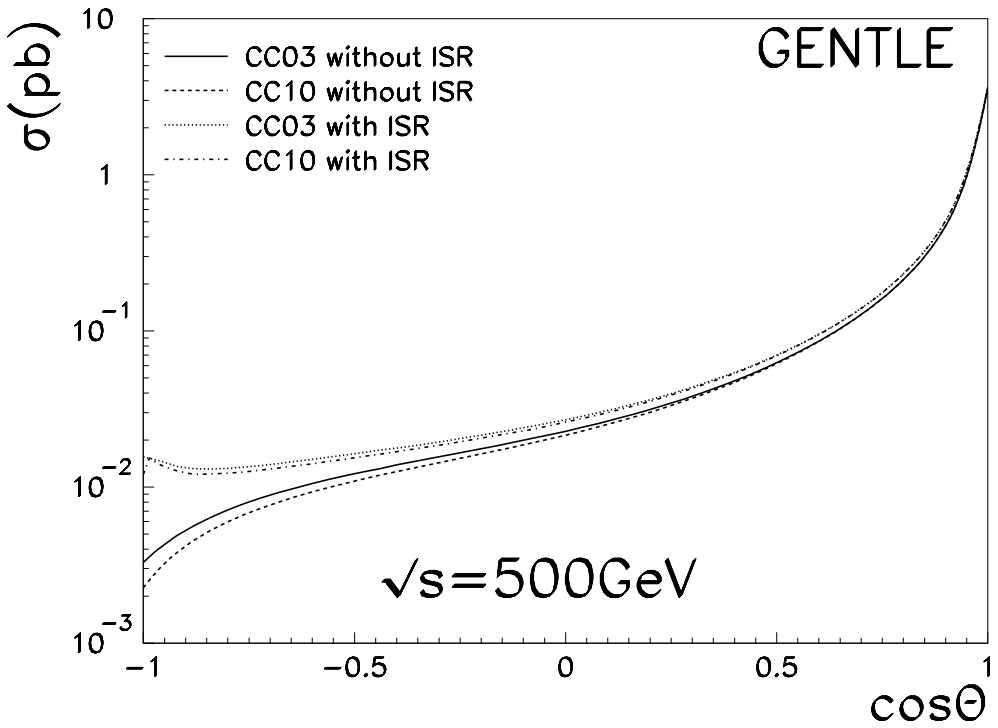

Figure 4.4: *Differential cross-section for* $e^+e^- \to \mu^-\bar{\nu}_\mu u\bar{d}$ *with various corrections.*

W pair production. The derivation of (4.128) with respect to $\cos\theta$ leads to the Jacobean included in equation (4.101):

$$\frac{\mathrm{d}\cos\theta'_{1,2}}{\mathrm{d}\cos\theta} = \frac{\beta_{1,2}(1-v^2)}{\left[\beta_{1,2}^2 + v^2(1-\beta_{1,2}^2\sin^2\theta) - 2v\beta_{1,2}\cos\theta\right]^{3/2}} \tag{4.129}$$

$$\times\left[\beta_{1,2} - v\cos\theta \pm v(1-\cos^2\theta)\frac{1-b^2}{b}\frac{v}{1\pm vb\cos\theta}\right]. \tag{4.130}$$

In the calculation of the bin-wise integrated differential cross-section it is easier to perform the integration over $\cos\theta$ in the center-of-mass system of the W pair, Σ', and consider the boost only for the integration limits as described in (4.128). In this way an analytical integration is still possible.

Note that for an angular bin in the laboratory system, there may be zero, one or two corresponding bins in Σ'.

4.5 Numerical Results

4.5.1 Standard Model Contributions

All numerical results presented in this chapter were produced with the program `GENTLE` [124]. The flag setting used for the calculations can be found in appendix D. Some of our results were already presented in the articles [125–127].

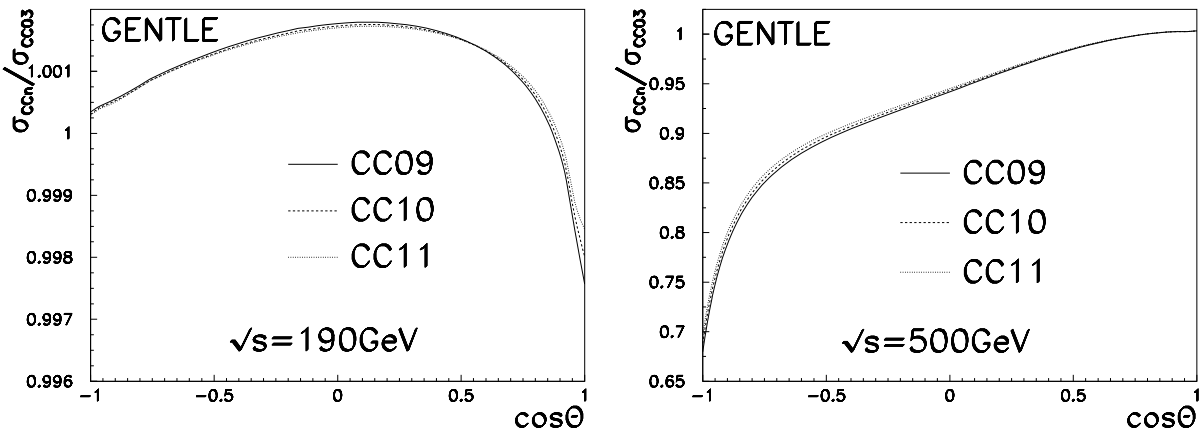

Figure 4.5: *The ratios* `CC09/CC03`, `CC10/CC03`, *and* `CC11/CC03` *at the center-of-mass energies of 190 GeV and 500 GeV without QED corrections. The numerical calculation was performed with an s-dependent width in the s-channel propagators.*

The differential cross-section for processes with semi-leptonic final states at a center-of-mass energy of 500 GeV is plotted in figure 4.4. The forward peaking character of the cross-section is obvious. This feature is even more pronounced at higher energies. It is produced by the t-channel diagram of figure 4.1. The four different curves in figure 4.4 show the cross-section with only the three signal diagrams with and without initial state radiation and the complete `CC10` process with and without initial state radiation. It is demonstrated that the largest deviation due to radiative and background corrections appears in the region of $\cos\theta < 0$, which is the region of backward-scattering. The effects of initial-state radiation are clearly much bigger than the corrections due to the `CC11` background contribution. The large corrections due to initial state radiation can be explained by the reduction of the center-of-mass energy. At lower energies the cross-section for backward scattering is much higher than at high energies, while the opposite holds for the forward peak.

The contributions of the various processes in the `CC11` class are studied in figure 4.5. In this figure the ratio of cross-sections with background effects over the cross-section of the signal diagrams is plotted for two center-of-mass energies. It is remarkable that the curves of the various processes, `CC09`, `CC10`, and `CC11` are similar to each other, although there are different couplings appearing and even a different number of Feynman diagrams contributing. At a center-of-mass of 190 GeV the background effects are small over the whole range of the scattering angle. The biggest deviations are here in the limit $\cos\theta \to 1$ and are of the order of three per mil. This situation changes drastically at a center-of-mass energy of 500 GeV. Here, corrections due to background are large in the region of backward scattering. The maximal deviation is at $\cos\theta = -1$. They are of the order of 30%.

In table 4.3 we present numerical values for the differential Born cross-section for three different scattering angles. With a semi-analytical program like `GENTLE` a high precision in the numerical integrations is easy to achieve. Therefore, the numbers for the cross-section are presented with their *numerical* precision. The differential cross-sections are given for

the CC03 signal diagrams with semi-leptonic final states and for all possible final states of the CC11 class. The ratios of CC11/CC10 and CC10/CC09 are both about three, which corresponds to the color factor appearing in the decay of the W bosons. The ratios deviate slightly from the color factor even for the signal diagrams, because of QCD corrections considered in the hadronic W decays.

The effects of initial-state radiation are considered in table 4.4. Apart from that the values presented are produced in the same way as the numbers in table 4.3. Since two additional numerical integrations are needed in the calculation of the cross-sections, we require a lower numerical precision and give less digits.

The influence of s-dependent and s-independent boson widths in the Z and W propagators is studied in tables 4.3 and 4.4. The effect of the s-dependence is small at low energies as expected. However at higher energies, like $\sqrt{s} = 500$ GeV, the gauge violating character of the s-dependent width becomes obvious and large deviations appear. They are especially strong for backward scattered W pairs since the gauge cancellations are strongest in this case. The s-dependent terms in the boson width destroy these cancellations. As a result the cross-sections can be almost twice as high as with intact gauge cancellations. Therefore, at energies well above the W threshold the s-independent calculation is supposed to be more reliable [116, 166, 167].

$\sqrt{s}$ (GeV)	$\cos\theta$	$\sigma_{\texttt{CC03}}$ (pb)	$\sigma_{\texttt{CC09}}$ (pb)	$\sigma_{\texttt{CC10}}$ (pb)	$\sigma_{\texttt{CC11}}$ (pb)
	–0.8	0.0944912	0.0303619	0.0945628	0.294524
	–0.8	0.0943803	0.0303466	0.0945159	0.294360
190	0.0	0.216782	0.0697249	0.217156	0.676333
190	0.0	0.216791	0.0697497	0.217241	0.676600
	0.8	0.790399	0.253913	0.790888	2.46346
	0.8	0.790432	0.253951	0.791012	2.46385
	–0.8	0.00712779	0.00191168	0.00598642	0.0187496
	–0.8	0.0064616	0.0017215	0.0053926	0.016888
500	0.0	0.0227606	0.00688311	0.0214732	0.0669960
500	0.0	0.0215908	0.00654501	0.0204228	0.0637232
	0.8	0.212756	0.0683217	0.212821	0.662936
	0.8	0.212368	0.0682179	0.212503	0.661957
	–0.8	0.00407742	0.000913816	0.00287169	0.00902554
	–0.8	0.00244188	0.000403725	0.00128268	0.00407275
1000	0.0	0.01001499	0.00276245	0.00860917	0.0268337
1000	0.0	0.00614750	0.00155423	0.00484706	0.0151154
	0.8	0.0550750	0.0175387	0.0546059	0.170015
	0.8	0.0535172	0.0170530	0.0530947	0.165310

Table 4.3: *Differential cross-sections without ISR. The* CC03 *cross-section is calculated with the branching ratios for the* CC10 *process. In the first rows the cross-section with an s-dependent boson width is given, while in the second rows the s-independent widths are used in the calculation.*

$\sqrt{s}$ (GeV)	$\cos\theta$	$\sigma_{\texttt{CC03}}$ (pb)	$\sigma_{\texttt{CC09}}$ (pb)	$\sigma_{\texttt{CC10}}$ (pb)	$\sigma_{\texttt{CC11}}$ (pb)
	–0.8	0.09075	0.02917	0.09083	0.2829
	–0.8	0.09064	0.02915	0.09077	0.2827
190	0.0	0.1971	0.06339	0.1974	0.6149
190	0.0	0.1971	0.06340	0.1975	0.6150
	0.8	0.6869	0.2206	0.6872	2.140
	0.8	0.6868	0.2206	0.6871	2.140
	–0.8	0.0131	0.003934	0.01228	0.03834
	–0.8	0.01248	0.003749	0.01170	0.0365
500	0.0	0.02698	0.008348	0.02603	0.08119
500	0.0	0.02590	0.008036	0.02506	0.0782
	0.8	0.2312	0.07427	0.2314	0.7207
	0.8	0.2308	0.07418	0.2311	0.7198
	–0.8	0.006844	0.001930	0.006032	0.01886
	–0.8	0.005282	0.001441	0.004510	0.01412
1000	0.0	0.01128	0.00333	0.01037	0.0323
1000	0.0	0.007757	0.00223	0.006939	0.02163
	0.8	0.06278	0.02010	0.06259	0.1949
	0.8	0.0613	0.01963	0.06114	0.1904

Table 4.4: *Differential cross-sections with ISR. The* `CC03` *cross-section is calculated with the branching ratios for the* `CC10` *process. In the first rows the cross-section with an s-dependent boson width is given, while in the second rows the s-independent widths are used in the calculation.*

4.5.2 Anomalous Couplings

In figures 4.6 and 4.7 the ratio of cross-sections with anomalous couplings over the Standard Model cross-section is presented for two different energies. The differential cross-section is divided into five bins. This allows for direct comparisons with Monte Carlo programs.

The figures show the influence of anomalous couplings when only one parameter differs from the Standard Model prediction. This oversimplified scenario is not suited to describe any realistic model beyond the Standard Model. It is nevertheless useful for comparisons with other calculations and shows some basic effects of anomalous couplings. The results in figure 4.6 are in good agreement with a similar figure in reference [168]. Additional checks with the Monte Carlo program `WOPPER` [169, 170] are also in nice agreement with the `GENTLE` calculation.

Both figures show that the influence of anomalous couplings to the differential cross-section are largest for backward scattering, i.e. in the region $\cos\theta < 0$. Note, that this is the same region where also corrections due to initial state radiation and background give important corrections. At a center-of-mass energy of 190 GeV and for absolute values of 0.5 for the anomalous couplings, the contributions linear in the anomalous parameters are dominating. This situation changes drastically at a center-of-mass energy of 500 GeV and an absolute value of 0.1. Here the quadratic terms are important and start to dominate

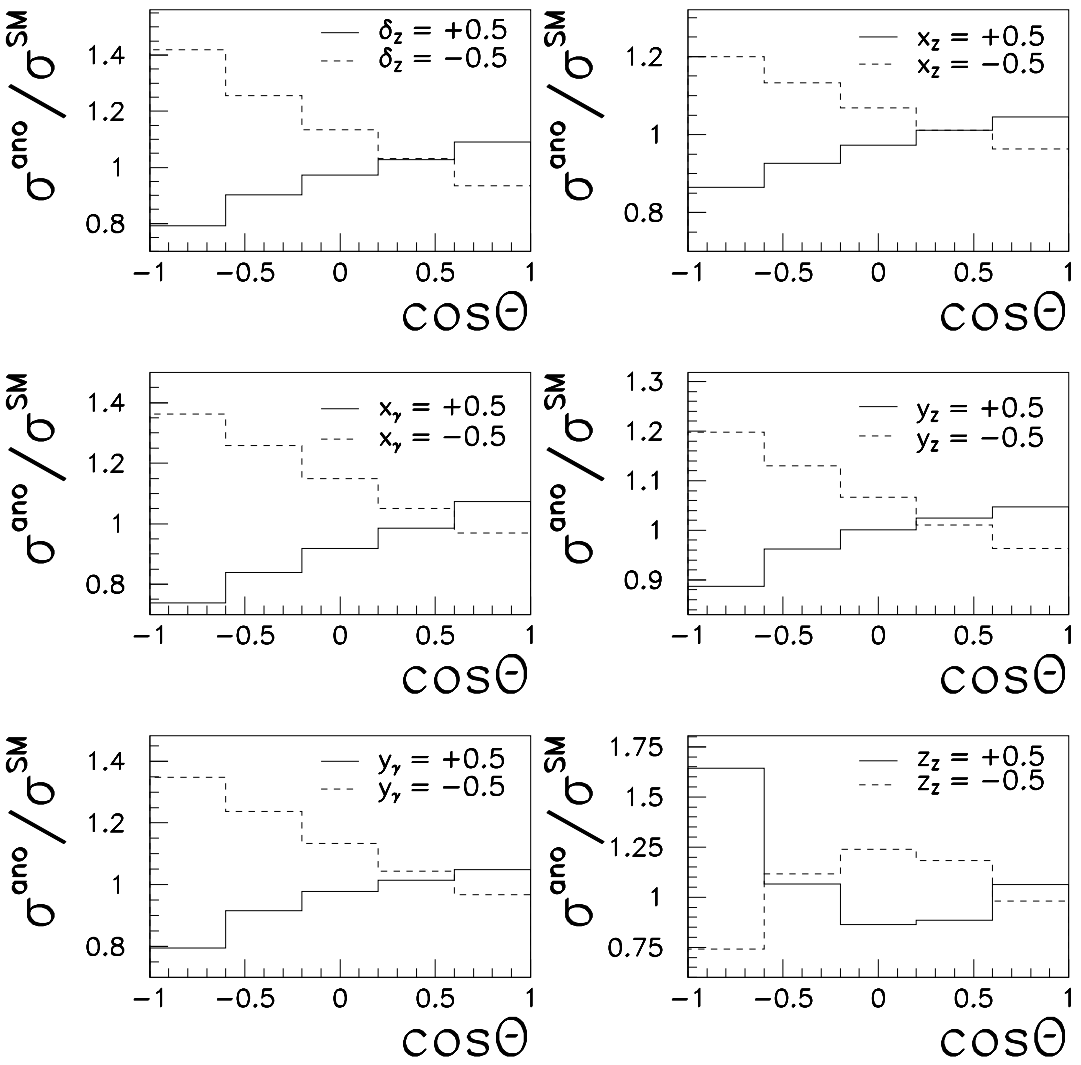

Figure 4.6: *The ratio of cross-sections with anomalous coupling over the Standard Model prediction at a center-of-mass energy of 190 GeV. In each figure only one anomalous parameter differs from zero.*

as it can be seen for the parameter z_Z, where the sign of z_Z is almost of no importance.

In figure 4.6 it is obvious, that most anomalous couplings lead to similar effects in the differential cross-section. This feature allows for strong cancellations in the differential cross-section between the different parameters. We conclude that it is necessary to investigate more than only one anomalous coupling at a time. Multi-parameter fits must be performed in a realistic analysis.

With `GENTLE` it is easy to extend the number of anomalous couplings. All of the six defined couplings can be used at the same time. A simple analysis is shown in figure 4.8.

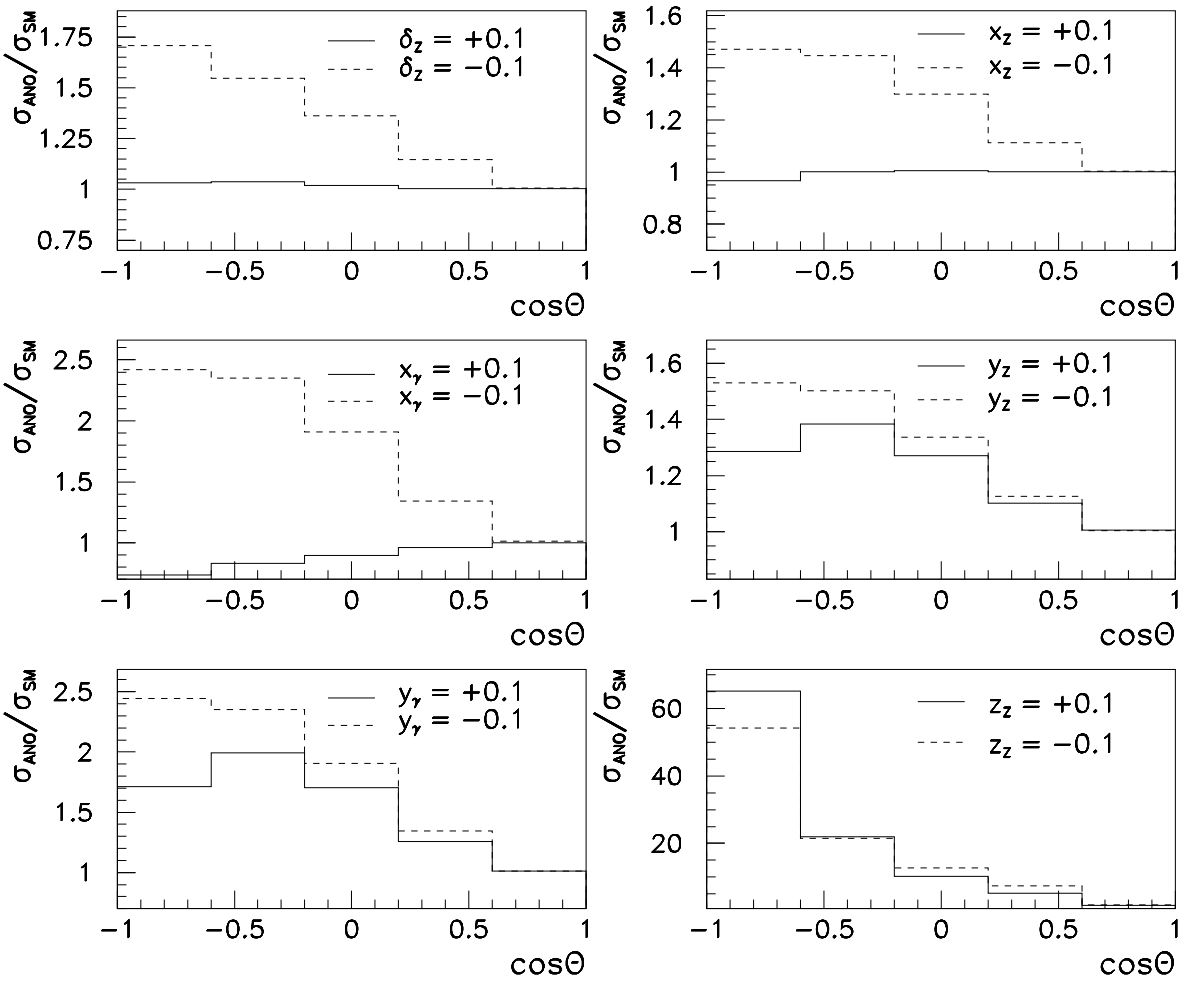

Figure 4.7: *The ratio of cross-sections with anomalous coupling over the Standard Model prediction at a center-of-mass energy of 500 GeV. In each figure only one anomalous parameter differs from zero.*

In each plot two anomalous parameters are allowed to differ from zero. The cross-section is split up into two areas. The forward cross-section is defined by:

$$\sigma_{\mathrm{F}} = \int_0^1 \mathrm{d}\cos\theta \frac{\mathrm{d}\sigma}{\mathrm{d}\cos\theta}, \tag{4.131}$$

and the backward cross-section by:

$$\sigma_{\mathrm{B}} = \int_{-1}^0 \mathrm{d}\cos\theta \frac{\mathrm{d}\sigma}{\mathrm{d}\cos\theta}. \tag{4.132}$$

The two cross-sections σ_{F} and σ_{B} can be used to express the total cross-section $\sigma_{\mathrm{T}} = \sigma_{\mathrm{F}} + \sigma_{\mathrm{B}}$ and the forward-backward asymmetry $A_{\mathrm{FB}} = (\sigma_{\mathrm{F}} - \sigma_{\mathrm{B}})/\sigma_{\mathrm{T}}$.

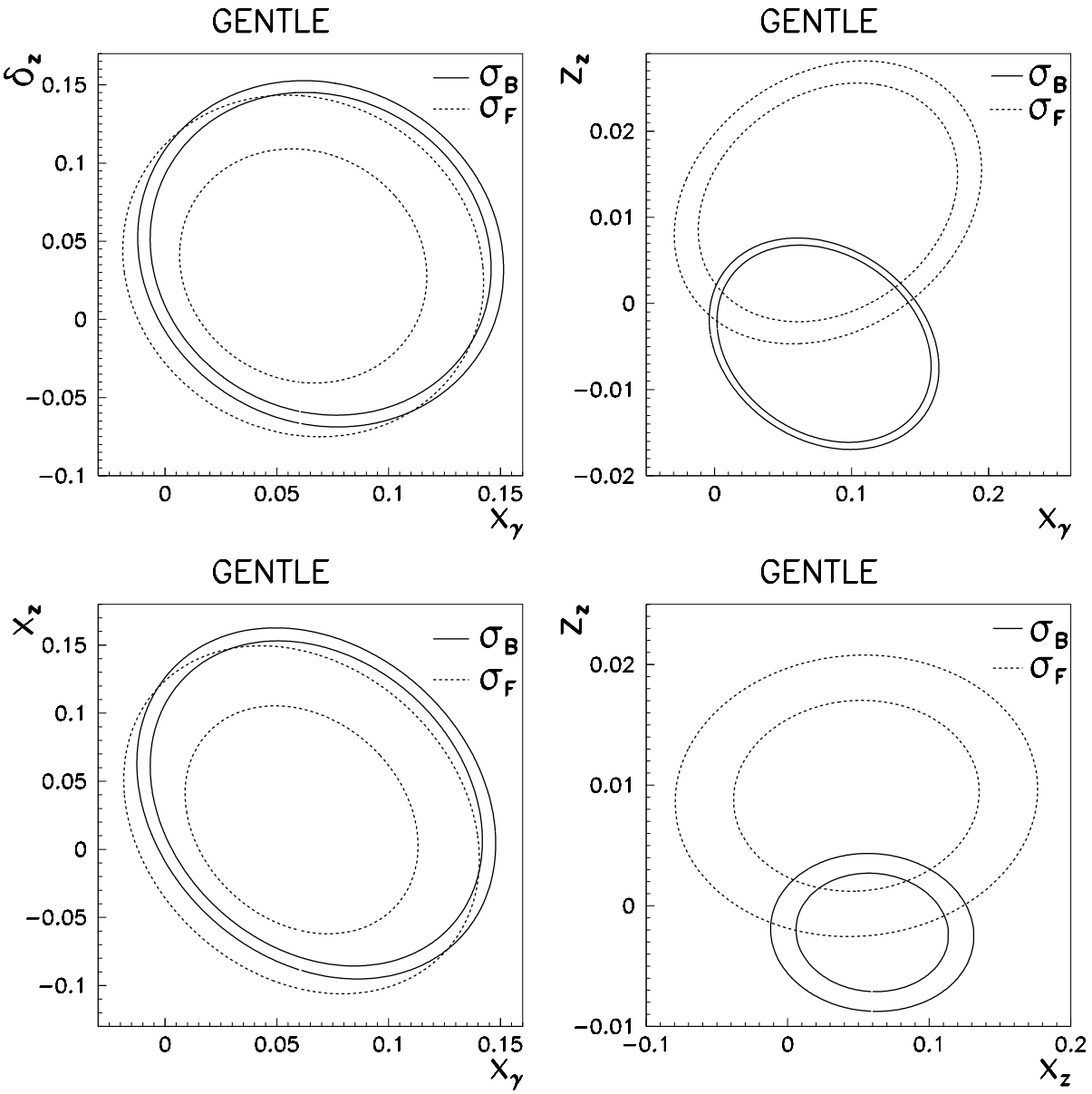

Figure 4.8: 1σ-*bounds at a center-of-mass energy of 500 GeV for* $\mathcal{L} = 50 fb^{-1}$.

The rings in figure 4.8 show the region for a pair of anomalous couplings where the cross-section differs less than a standard deviation from the Standard Model prediction. Although the cross-section for forward scattering ($\approx$ 1.6 pbn) is much bigger than the cross-section for backward scattering ($\approx$ 110 fbn), the rings resembling the backward scattering are more narrow. This effect demonstrates the higher sensitivity of the observable σ_{B} to anomalous couplings.

It is interesting to compare the sensitivity of the forward-backward asymmetry to the various anomalous couplings. It is obvious that the parity violating coupling z_Z can be better restricted in this analysis than the parity conserving couplings. In the latter case the forward and the backward ring have almost the same center and the narrow ring of the

backward scattering cross-section is almost completely contained in the ring of forward scattering.

Chapter 5

Anomalous Couplings in ZZ Production

LEP2 is at present running at energies above the ZZ production threshold and the first Z pairs have been observed. During the run of LEP2 several hundred events will be collected. This will be enough to provide limits for ZZZ and γZZ vertices, which are absent in the Standard Model of electroweak interactions at tree-level. However, physics beyond the Standard Model might give strong contributions to neutral gauge boson vertices [171–173].

Requiring only invariance under Lorentz transformations the most general VZZ vertex, see figure 5.1, with two on-shell Z bosons is given by [84, 85]:

$$\Gamma^{\alpha\beta\mu}_{VZZ} = \frac{p^2 - m_V^2}{m_Z^2}\left[if_4^V(p^\alpha g^{\mu\beta} + p^\beta g^{\mu\alpha}) + if_5^V \epsilon^{\mu\alpha\beta\rho}(q_1 - q_2)_\rho\right]. \tag{5.1}$$

In contrast to the VW^+W^- vertex with seven possible anomalous couplings [84, 85], compare also section 4.3, Bose symmetry forbids more couplings in (5.1). More anomalous couplings are allowed in (5.1) if one additional Z boson is off-shell (see e.g. [174]), but their contributions are suppressed by a factor $(q_1^2 - q_2^2)$. The anomalous parameter f_5^V in (5.1) leads to violation of $\mathcal{C}$ and $\mathcal{P}$ symmetry, but maintains invariance under $\mathcal{CP}$ transformations, while f_4^V would introduce $\mathcal{CP}$ violation in (5.1).

The differential Standard Model cross-section for ZZ production in e^+e^- annihilation has been known for almost 20 years [84, 175]. Also, the effects of anomalous neutral gauge boson couplings in the production of γZ, ZZ, and γ bosons have been studied, see

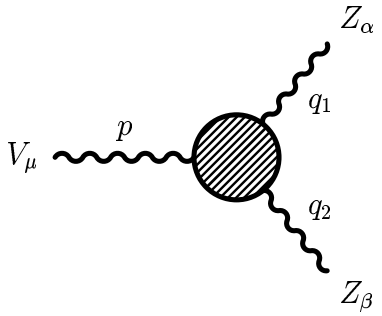

Figure 5.1: *The VZZ vertex with $V = \gamma, Z$. Two Z bosons with momenta q_i are on-shell, $q_i^2 = m_Z^2$.*

e.g. [176–180]. In $Z\gamma$ production processes at the Tevatron [181–183] and LEP [184–186], limits to the vertex $Z\gamma Z$ were obtained. However, they cannot be transferred to Z pair production, since the anomalous couplings in equation (5.1) are independent of couplings in $Z\gamma$ production.

Recent analysis of ZZ production processes could provide limits to the anomalous parameters f_4^V and f_5^V. They are [187]:

$$-3.6 \leq f_4^Z \leq 3.4, \quad -8.4 \leq f_5^Z \leq 7.9, \quad -2.1 \leq f_4^\gamma \leq 2.1, \quad -4.9 \leq f_5^\gamma \leq 4.8. \tag{5.2}$$

The total Standard Model cross-section for the process of ZZ production is already included in `GENTLE`. Compare also appendix D. The included background effects are based on the publications [135, 188], while the calculation of non-universal QED corrections follows the ones presented in reference [189]. The attempt of the next section is to prepare the installation of the differential cross-section with anomalous couplings into `GENTLE`. The numerical calculations were performed with the FORTRAN program `ZAC` [190] and the results were presented partially already in [191].

5.1 The Differential Cross-Section for ZZ Production

The differential cross-section for ZZ production is presented in this section. It is obtained for the various spin combinations of final state Z bosons. This allows to determine their sensitivity to the anomalous couplings.

The finite width effects of the produced Z bosons are considered by convoluting the cross-section for ZZ production with two Breit-Wigner functions. The differential cross-section is then expressed by the sum:

$$\frac{d\sigma}{d\cos\theta} = \sum_{\sigma\sigma'} \frac{d\sigma^{\sigma\sigma'}}{d\cos\theta}, \tag{5.3}$$

with

$$\frac{d\sigma^{\sigma\sigma'}}{d\cos\theta} = \int \mathrm{d}s_1 \int \mathrm{d}s_2 \, \frac{\sqrt{\lambda}}{64\pi s^2} \left|\mathcal{M}^{\sigma\sigma'}\right|^2 \rho(s_1)\rho(s_2), \tag{5.4}$$

where σ and σ' stand for the possible Z boson helicities $+$, $-$, and 0, which are defined by the vectors:

$$\epsilon_{1\pm} = \epsilon_{2\mp} = \frac{1}{\sqrt{2}}\left(0, \mp 1, -i, 0\right), \tag{5.5}$$

$$\epsilon_{10} = \frac{1}{2\sqrt{s s_1}}\left(\sqrt{\lambda}, 0, 0, (s + s_1 - s_2)\right), \tag{5.6}$$

$$\epsilon_{20} = \frac{1}{2\sqrt{s s_2}}\left(\sqrt{\lambda}, 0, 0, -(s - s_1 + s_2)\right). \tag{5.7}$$

The Källén function λ and other notations may be inferred from chapter 4. The Breit-Wigner factors $\rho(s_i)$ are:

$$\rho(s_i) = \frac{1}{\pi} \frac{m_Z \Gamma_Z(s_i)}{(s_i - m_Z^2)^2 + m_Z^2 \Gamma_Z^2(s_i)}. \tag{5.8}$$

The squared matrix element $\left|\mathcal{M}^{\sigma\sigma'}\right|^2$ in equation (5.4) can be expressed by the Standard Model part $\left|\mathcal{M}^{\sigma\sigma'}_{\mathrm{SM}}\right|^2$ and the anomalous contributions $A^{\sigma\sigma'}$:

$$\left|\mathcal{M}^{\sigma\sigma'}\right|^2 = \left|\mathcal{M}^{\sigma\sigma'}_{\mathrm{SM}}\right|^2 + A^{\sigma\sigma'}. \tag{5.9}$$

The squared amplitude in the Standard Model is:

$$\left|\mathcal{M}^{\sigma\sigma'}_{\mathrm{SM}}\right|^2 = \left(L_Z^4 + R_Z^4\right)\mathcal{G}^{\sigma\sigma'}_{\mathrm{SM}}(s_1,s_2) + \left(L_Z^4 - R_Z^4\right)\mathcal{G}^{\sigma\sigma'}_{\mathrm{SM}-}(s_1,s_2), \tag{5.10}$$

where the Zee couplings L_Z and R_Z can again be taken from chapter 4. The functions $\mathcal{G}^{\sigma\sigma'}_{\mathrm{SM}}$ are:

$$\begin{aligned}
\mathcal{G}^{00}_{\mathrm{SM}}(s_1,s_2) &= \frac{16s^2 s_1 s_2}{u^2t^2}\cos^2\theta\sin^2\theta, && (5.11)\\
\mathcal{G}^{\pm\pm}_{\mathrm{SM}}(s_1,s_2) &= \frac{\mathcal{G}^{00}}{4} + 2(s_1-s_2)^2\sin^2\theta\left(\frac{1}{u^2}+\frac{1}{t^2}\right), && (5.12)\\
\mathcal{G}^{\pm\mp}_{\mathrm{SM}}(s_1,s_2) &= \frac{s^2(u+t)^2}{u^2t^2}(1-\cos^4\theta), && (5.13)\\
\mathcal{G}^{0\pm}_{\mathrm{SM}}(s_1,s_2) &= \frac{2ss_1}{u^2t^2}\left\{8s_2^2\cos^2\theta + 4s_2\sin^2\theta\left(s_1 - s\cos^2\theta\right) + \lambda\sin^4\theta\right\}, && (5.14)\\
\mathcal{G}^{\pm 0}_{\mathrm{SM}}(s_1,s_2) &= \mathcal{G}^{0-}_{\mathrm{SM}}(s_2,s_1), && (5.15)
\end{aligned}$$

with the Mandelstam variables:

$$\begin{aligned}
t &= -\frac{1}{2}\left(s - s_1 - s_2 - \sqrt{\lambda}\cos\theta\right), && (5.16)\\
u &= -\frac{1}{2}\left(s - s_1 - s_2 + \sqrt{\lambda}\cos\theta\right). && (5.17)
\end{aligned}$$

It is worth to note that the coupling constant combination $(L_Z^4 - R_Z^4)$ gives contributions only to the various spin combinations of equation (5.10). These terms cancel each other for all measurable cross-sections, because the produced Z bosons are identical, and not all of the spin combinations in equations (5.11) – (5.15) are observable by themselves. As an example, the contribution of $\mathcal{G}^{+-}(s_1,s_2)$ cannot be distinguished from $\mathcal{G}^{-+}(s_2,s_1)$ and only their sum can be measured. For completeness the remaining $\mathcal{G}$-functions are given:

$$\begin{aligned}
\mathcal{G}^{00}_{\mathrm{SM}-}(s_1,s_2) &= 0, && (5.18)\\
\mathcal{G}^{0\pm}_{\mathrm{SM}-}(s_1,s_2) &= \mp\frac{32ss_1s_2}{\lambda^{3/2}}\left\{2\left[s - s_1 + s_2\right]\left(\frac{1}{u}-\frac{1}{t}\right)\right.\\
&\qquad \left. + s_2\left[s + s_1 - s_2\right]\left(\frac{1}{u^2}-\frac{1}{t^2}\right)\right\}, && (5.19)\\
\mathcal{G}^{\pm\pm}_{\mathrm{SM}-}(s_1,s_2) &= \mp\frac{16s_1s_2\left(s_1-s_2\right)}{\lambda^{3/2}}\left\{\left[4s + \frac{s_1+s_2}{s_1s_2}\lambda\right]\left(\frac{1}{u}-\frac{1}{t}\right)\right.\\
&\qquad \left. + \left[s(s-s_1-s_2) - \lambda\right]\left(\frac{1}{u^2}-\frac{1}{t^2}\right)\right\}, && (5.20)\\
\mathcal{G}^{\pm\mp}_{\mathrm{SM}-}(s_1,s_2) &= \pm\frac{4s^2(u+t)(u^2-t^2)}{\sqrt{\lambda}u^2t^2}\sin^2\theta, && (5.21)\\
\mathcal{G}^{\pm 0}_{\mathrm{SM}-}(s_1,s_2) &= \pm\mathcal{G}^{0-}_{\mathrm{SM}-}(s_2,s_1). && (5.22)
\end{aligned}$$

The contributions from the anomalous diagrams are:

$$
\begin{aligned}
A^{\sigma\sigma'} &= \sum_{V_k,V_l=\gamma,Z} \frac{1}{m_Z^4}\Big[(L_{V_k}L_{V_l}+R_{V_k}R_{V_l})\,\mathcal{G}_s^{\sigma\sigma'}(s_1,s_2;V_k,V_l) \\
&\qquad - (L_{V_k}L_{V_l}-R_{V_k}R_{V_l})\,\mathcal{G}_{s-}^{\sigma\sigma'}(s_1,s_2;V_k,V_l)\Big] \\
&\quad + \sum_{V=\gamma,Z} \frac{f_5^V}{m_Z^2}\Big[\left(L_V L_Z^2 - R_V R_Z^2\right)\mathcal{G}_i^{\sigma\sigma'}(s_1,s_2) \qquad (5.23)\\
&\qquad - \left(L_V L_Z^2 + R_V R_Z^2\right)\mathcal{G}_{i-}^{\sigma\sigma'}(s_1,s_2)\Big], \qquad (5.24)
\end{aligned}
$$

with the coupling constants $L_\gamma = R_\gamma = -e/2$ for the γee coupling. The denominators of the s-channel propagators $1/(s-m_V^2)$ cancel with the corresponding factors in the anomalous vertex function (5.1). Photon and Z exchange have the same s-dependence in (5.24).

The functions $\mathcal{G}_s^{\sigma\sigma'}$ for the s-channel diagrams squared are:

$$
\begin{aligned}
\mathcal{G}_s^{00}(s_1,s_2) &= \frac{\lambda\sin^2\theta}{4s_1s_2}(s_1-s_2)^2\, f_4^{V_k} f_4^{V_l}, && (5.25)\\
\mathcal{G}_s^{0\pm}(s_1,s_2) &= \frac{(1+\cos^2\theta)\,s}{8s_1}\left\{\lambda f_4^{V_k} f_4^{V_l} + (\lambda - 4s_1[s-2(s_1+s_2)])f_5^{V_k} f_5^{V_l}\right\}, && (5.26)\\
\mathcal{G}_s^{\pm\pm}(s_1,s_2) &= (s_1-s_2)^2\sin^2\theta f_5^{V_k} f_5^{V_l}, && (5.27)\\
\mathcal{G}_s^{\pm 0}(s_1,s_2) &= \mathcal{G}_s^{0-}(s_2,s_1), && (5.28)\\
\mathcal{G}_s^{\pm\mp}(s_1,s_2) &= 0. && (5.29)
\end{aligned}
$$

Similarly, the interferences $\mathcal{G}_i^{\sigma\sigma'}$ between t and u-channel diagrams and the s-channel diagram can be expressed by:

$$
\begin{aligned}
\mathcal{G}_i^{0\pm}(s_1,s_2) &= \frac{s(3s_1+s_2-s)}{ut}\left\{4s_2-(3s_2-s_1+s)\sin^2\theta\right\}, && (5.30)\\
\mathcal{G}_i^{\pm\pm}(s_1,s_2) &= \frac{2(s_1-s_2)^2(u+t)}{ut}\sin^2\theta, && (5.31)\\
\mathcal{G}_i^{\pm 0}(s_1,s_2) &= \mathcal{G}_i^{0-}(s_2,s_1), && (5.32)\\
\mathcal{G}_i^{00}(s_1,s_2) &= \mathcal{G}_s^{\pm\mp}(s_1,s_2) = 0. && (5.33)
\end{aligned}
$$

Again, as in equation (5.10), terms which disappear in physical observables are present. They are listed for completeness:

$$
\begin{aligned}
\mathcal{G}_{s-}^{0\pm}(s_1,s_2) &= \pm\frac{\cos\theta s}{4s_1}\left\{\lambda f_4^{V_k} f_4^{V_l} + (\lambda - 4s_1[s-2(s_1+s_2)])f_5^{V_k} f_5^{V_l}\right\}, && (5.34)\\
\mathcal{G}_{s-}^{\pm 0}(s_1,s_2) &= \mp\mathcal{G}_{s-}^{0-}(s_2,s_1), && (5.35)\\
\mathcal{G}_{s-}^{00}(s_1,s_2) &= \mathcal{G}_{s-}^{\pm\mp}(s_1,s_2) = \mathcal{G}_{s-}^{\pm\pm}(s_1,s_2) = 0, && (5.36)\\
\mathcal{G}_{i-}^{0\pm}(s_1,s_2) &= \mp s\left\{\left(\frac{1}{u}-\frac{1}{t}\right)\left(\frac{4ss_2-4s_2^2-8s_1s_2}{\sqrt{\lambda}}\right.\right.
\end{aligned}
$$

$$
\left. - \frac{8 s_1 s_2 (s_1 - s_2)(s - s_1 - s_2)}{\lambda^{3/2}} \right)
$$

$$
\left. + \cos\theta \left(8 \frac{(s_1 - s_2)(s - s_1 - s_2)}{\lambda} - 4 \right) \right\}, \tag{5.37}
$$

$$
\mathcal{G}_{i-}^{\pm 0}(s_1, s_2) = \pm \mathcal{G}_{i-}^{0-}(s_2, s_1), \tag{5.38}
$$

$$
\mathcal{G}_{i-}^{\pm\pm}(s_1, s_2) = \mp 8 \frac{(s_1 - s_2)\cos\theta}{\lambda} \left\{ \left(1 - \frac{s_1 s_2}{ut} \right) [\lambda - s(s - s_1 - s_2)] \right\}, \tag{5.39}
$$

$$
\mathcal{G}_{i\pm}^{00}(s_1, s_2) = \mathcal{G}_{s-}^{\pm\mp}(s_1, s_2) = 0. \tag{5.40}
$$

As expected there are no contributions of anomalous couplings to the spin combinations $(+-)$ and $(-+)$. These are spin 2 states and cannot be produced by the s-channel diagrams.

Equations (5.25) – (5.40) exhibit that the $\mathcal{CP}$ violating couplings proportional to f_4^V do neither interfere with the Standard Model terms nor with terms proportional to f_5^V. A further conclusion is that it is impossible to separate out the effects of the parameters f_4^Z and f_4^γ on the differential cross-section of the process $e^+e^- \to ZZ$. However, both parameters imply $\mathcal{CP}$ violation in a VZZ vertex.

In the limit of on-shell Z pair production only the combination with one longitudinally and one transversally polarized Z receives contributions from anomalous couplings.

With the given expressions for the various spin combinations, the differential cross-section (5.3) is obtained:

$$
\frac{d\sigma}{d\cos\theta} = \int \mathrm{d}s_1 \int \mathrm{d}s_2 \, \frac{\sqrt{\lambda}}{64\pi s^2} \rho(s_1)\rho(s_2) \left\{ S + A_i + A_s \right\}, \tag{5.41}
$$

with the functions

$$
S = 2 \frac{L_Z^4 + R_Z^4}{u^2 t^2} \left\{ 4\lambda \sin^2\theta (s\sigma + s_1 s_2) + \lambda^2 (1 - \cos^4\theta) + 16 s s_1 s_2 \sigma \right\}, \tag{5.42}
$$

$$
A_i = -\frac{4}{m_Z^2} \sum_{V=\gamma,Z} \frac{L_V L_Z^2 - R_V R_Z^2}{ut} f_5^V \left\{ 2s[(s - \sigma)\sigma - 4 s_1 s_2] - \lambda(s + \sigma)\sin^2\theta \right\}, \tag{5.43}
$$

$$
\begin{aligned}
A_s = \sum_{V_k, V_l = \gamma, Z} & \frac{L_{V_k} L_{V_l} + R_{V_k} R_{V_l}}{4 s_1 s_2 m_Z^4} \left\{ \lambda (1 + \cos^2\theta) \left[s\sigma f_4^{V_k} f_4^{V_l} + (s\sigma - 8 s_1 s_2) f_5^{V_k} f_5^{V_l} \right] \right. \\
& \left. + (s_1 - s_2)^2 \left[\lambda \sin^2\theta f_4^{V_k} f_4^{V_l} + 16 s_1 s_2 f_5^{V_k} f_5^{V_l} \right] \right\},
\end{aligned} \tag{5.44}
$$

where the abbreviation $\sigma = s_1 + s_2$ is used. The Standard Model part is described by S while the anomalous contributions are contained in A_i and A_s.

In the Standard Model limit the differential cross-section in (5.41) is in agreement with the result presented in reference [132]. Radiative corrections to (5.41) due to initial state radiation, see e.g. [189], can be applied in the structure function approach including a Lorentz boost of the scattering angle as described similarly in W pair production [127].

The presented analytical results demonstrate how potential anomalous couplings might change the differential ZZ production cross-section. Anomalous couplings will have their main effect in the production of a longitudinally and a transversally polarized Z boson. For on-shell ZZ production, these are the only spin combinations which are sensitive to

an anomalous signal. Effects of non-vanishing f_4^V and f_5^V on the final states with two transversally or two longitudinally polarized Z bosons are zero or suppressed by a factor $(s_1 - s_2)^2$. Therefore, a measurement of the final state spins might be used to increase the ratio of the anomalous signal over the Standard Model background. However, the spin analysis can not be used to disentangle the signals from the anomalous parameters f_4^V and f_5^V, since only one type of spin combination is sensitive to anomalous couplings. Due to the interference contribution of f_5^V in the equations (5.30) and (5.32). f_4^V and f_5^V have different angular distributions. It might be possible to separate out their effects at LEP2 by examine those characteristics if they would contribute substantially.

5.2 Numerical Results

The numerical calculations presented in this section were performed with the input values

$$m_Z^2 = 91.187 \text{ GeV}, \tag{5.45}$$
$$\Gamma_Z = 2.49 \text{ GeV}, \tag{5.46}$$
$$G_F = 1.16639 \cdot 10^{-5} \text{ GeV}^{-2}, \tag{5.47}$$
$$s_W^2 = 0.23124, \tag{5.48}$$

which were taken from reference [97].

Assuming that the anomalous couplings are large enough already the total cross-section alone will give a clear signal as shown in figure 5.2. Especially for energies much above the production threshold a huge deviation will arise. This behavior reflects the fact that there is no gauge cancellation for the anomalous diagrams and as a consequence unitarity is violated by them. However, at too high energies and large anomalous couplings the method of anomalous couplings is not applicable anymore and the results become senseless.

The differential cross-section for ZZ production is shown in figure 5.3 for two different center-of-mass energies. At $\sqrt{s} = 190$ GeV the cross-section is relatively flat for the Standard Model prediction. At higher energies like 500 GeV the Z bosons are produced in the direction of the beams or against it. As shown in the last section the contributions of an anomalous coupling f_4^V is quadratic in the parameter. The effect can only be an enhancement of the cross-section, since no negative contributions are allowed. For the anomalous coupling f_5^V interference terms are allowed and can lead to a reduction of the cross-section. This might lead to weaker limits on the parameters f_5^V.

To analyze the power of a spin-dependent measurement we define three spin combinations in the final state:

`LL`: both Z bosons are longitudinally polarized

`LT`: one Z is longitudinally, the other transversally polarized

`TT`: both Z bosons are transversally polarized

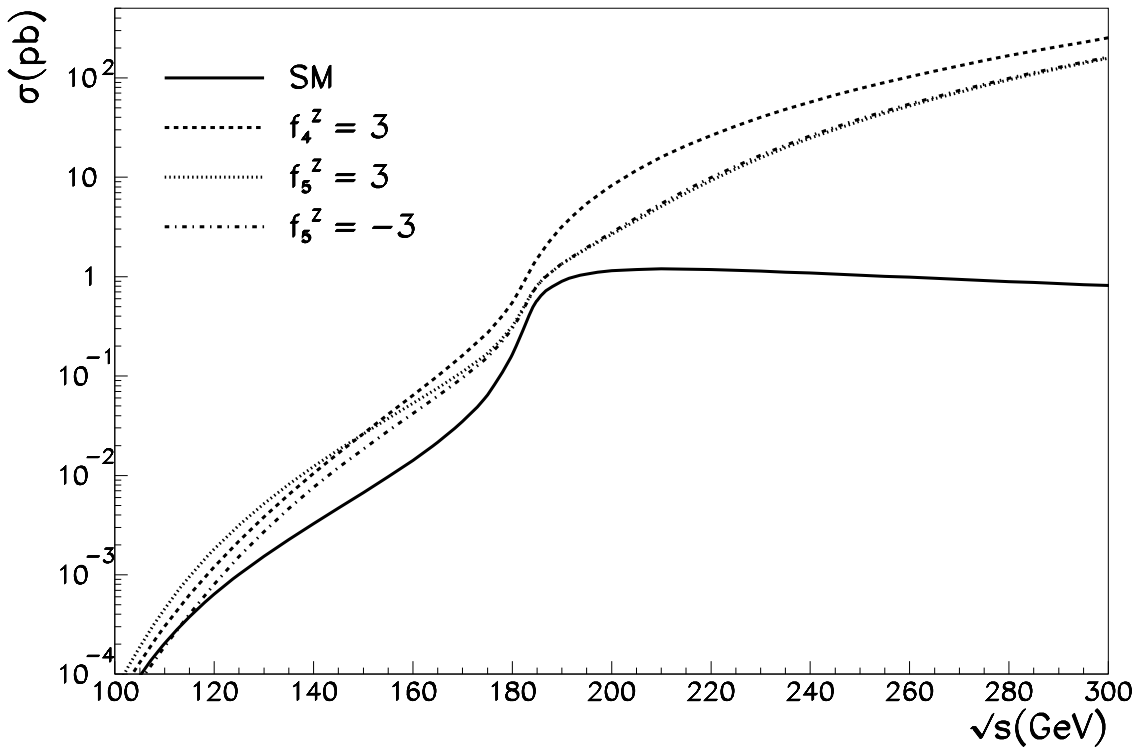

Figure 5.2: *The total cross-section for ZZ production with anomalous couplings.*

Which corresponds to

$$\sigma^{\mathtt{LL}} = \sigma^{00} \tag{5.49}$$

$$\sigma^{\mathtt{LT}} = \sigma^{0-} + \sigma^{0+} + \sigma^{-0} + \sigma^{+0} \tag{5.50}$$

$$\sigma^{\mathtt{TT}} = \sigma^{--} + \sigma^{-+} + \sigma^{+-} + \sigma^{++} \tag{5.51}$$

In figures 5.4, 5.5, and 5.6 the ratio of the cross-section for our three cases over the sum of all spins ($\sigma^{\mathtt{LL}}/\sigma$, $\sigma^{\mathtt{LT}}/\sigma$, and $\sigma^{\mathtt{TT}}/\sigma$) is plotted for a center-of-mass energy of $\sqrt{s} = 190$ GeV. In each diagram the solid line describes the Standard Model prediction, while the dashed curves show the cross-sections with anomalous couplings. In the figures on the right-hand side cuts are applied to the invariant masses of the decay particles.

The figures demonstrate that the average polarization of the Z bosons is different from the Standard Model expectation when anomalous couplings appear. This is mainly due to the large effects on the spin combination `LT`. The effects on the other combinations are suppressed by a factor $(s_1 - s_2)$, see section 5.1, and consequently the average polarization must change.

The behavior of the Z polarization at a center-of-mass energy of $\sqrt{s} = 500$ GeV is plotted in figure 5.7. The average polarization of the Z bosons is clearly sensitive to anomalous couplings. Especially the spin combination `LT` might be strongly changed. Since with the Standard Model vertices almost no longitudinally polarized Z bosons are

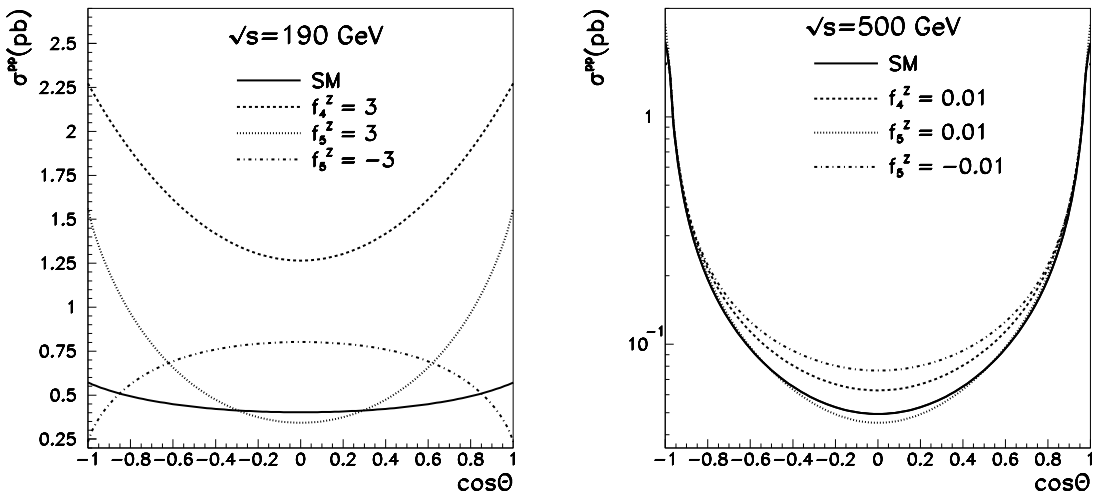

Figure 5.3: *The differential cross-section for ZZ production in the Standard Model and with anomalous couplings at center-of-mass energies of 190 GeV and 500 GeV.*

produced, an excess of them would be a clear signal for physics beyond the Standard Model. At these high energies a spin dependent analysis would be helpful in the search for anomalous couplings.

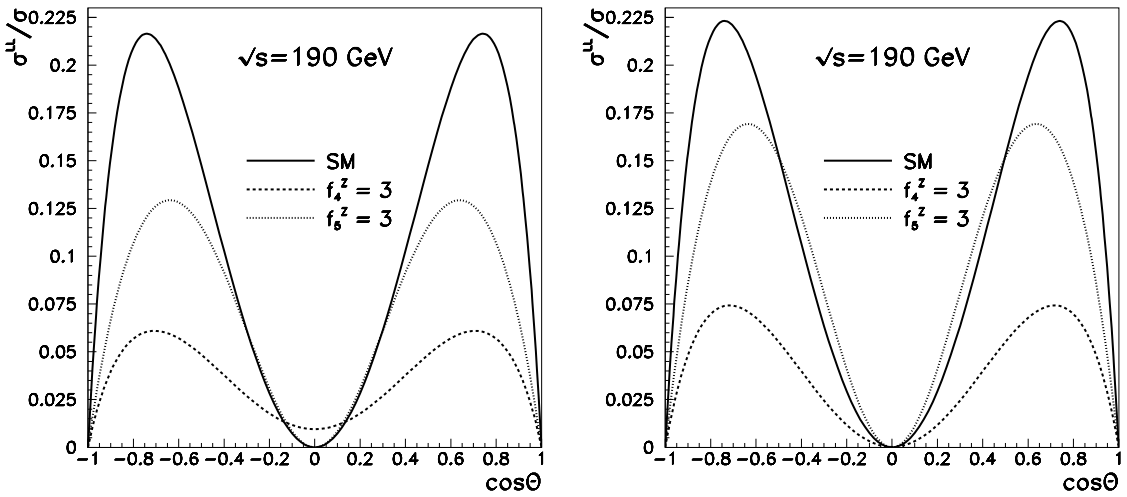

Figure 5.4: *The ratio of produced Z pairs, where both bosons are longitudinally polarized, over all produced Z pairs. The left-hand figure is without cuts, the right-hand figure is with cuts on the invariant masses:* $m_Z - 2\Gamma_Z < \sqrt{s_i} < m_Z + 2\Gamma_Z$.

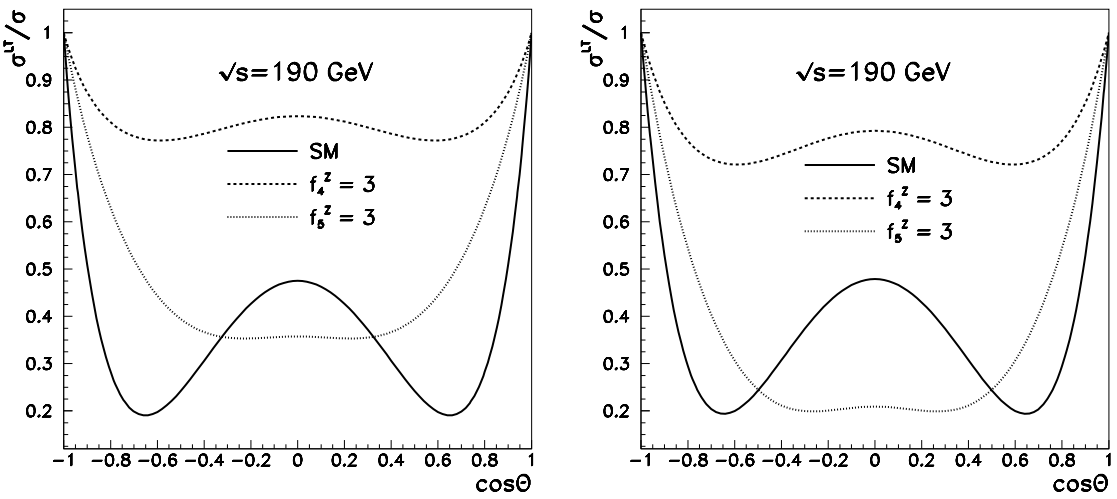

Figure 5.5: *Same as figure 5.4, but for a longitudinally and a transversally polarized Z.*

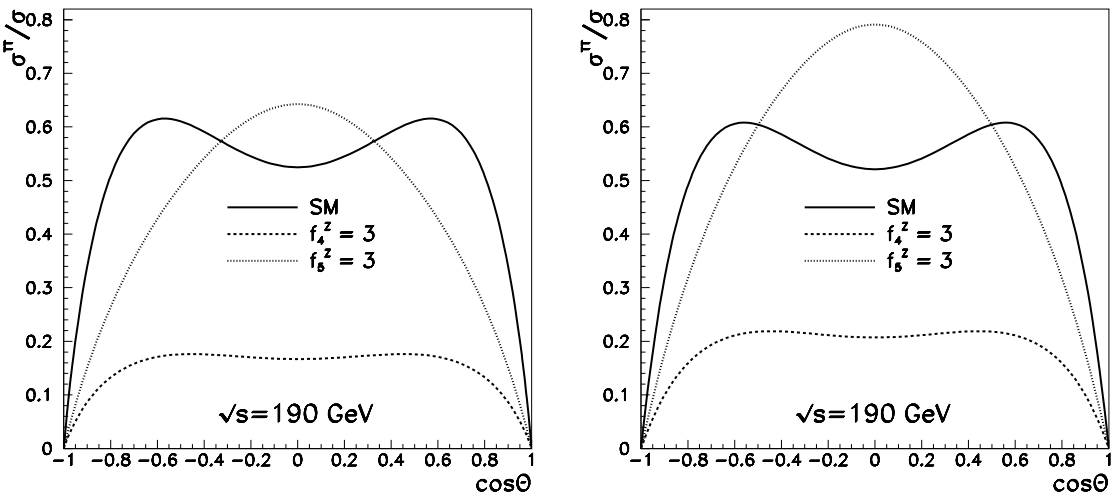

Figure 5.6: *Same as figure 5.4, but with both Z bosons transversally polarized.*

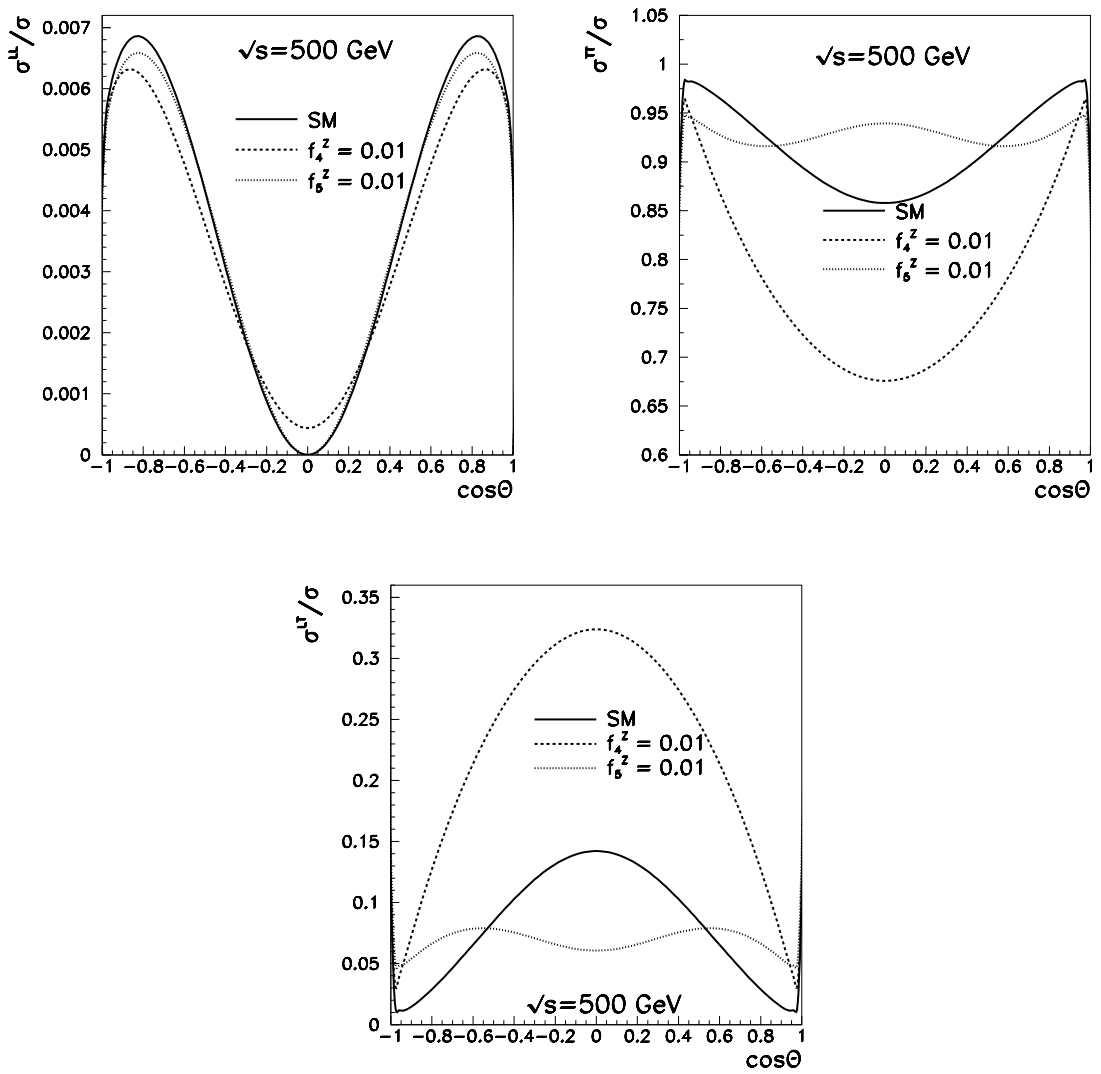

Figure 5.7: *The analog of figures 5.4, 5.5, and 5.6 without cuts to the invariant masses and at a center-of-mass energy of* $\sqrt{s} = 500$ *GeV. Note, the couplings are much smaller than for 190 GeV.*

Acknowledgement

I am grateful to T. Hebbeker and P. Molnár from L3 for drawing my attention to the experimental interest in the problem of anomalous ZZZ and $ZZ\gamma$ vertices. Their questions and the common discussions inspired this calculation. Thanks to J. Alcaraz for numerical comparisons and to W. Lohmann for providing me with information about the experimental situation.

Chapter 6

Conclusions

Summary

We used the formalism of anomalous couplings to determine various potential effects of physics beyond the Standard Model. In this approach new physics can be parameterized in a model independent way at energies well below the corresponding production threshold.

In chapter 3 we predicted the signal of a potential anomalous magnetic moment of τ leptons in the final state radiation spectrum at LEP. It was shown that terms that were believed to be small and negligible (terms with a linear dependence of the magnetic moment) cannot be neglected anymore, when the precision of the measurement reaches a limit in the order of 5% or even smaller. The current limit of the LEP analysis is now $-0.052 < \frac{\mu_\tau}{e\hbar/2m\tau} < 0.058$ and consequently the expressions with a pure quadratic dependence of a_τ as used in earlier analysis should not be applied anymore. Instead, the results derived in chapter 3 or the full Monte Carlo simulation [114] should be used.

In the main part of this thesis the process of four fermion production via two W boson exchange was investigated. The full set of kinematical functions, describing the differential cross-sections of the `CC11` class processes, was derived. The analytical results were implemented into `GENTLE` and used to study the effects of background diagrams and ISR corrections.

In addition, all anomalous couplings which are invariant under $\mathcal{CP}$ transformations were considered in the calculation and can be used to simulate physics beyond the Standard Model. This was done by experimentalists of the L3 collaboration especially in the starting phase of LEP2.

We calculated the bin-wise integrated differential cross-sections with an analytic integration over $\cos\theta$ for the `CC03` process with anomalous couplings. This feature simplifies and speeds up comparisons with Monte Carlo programs drastically. However, for the `CC11` background processes only the total and the differential cross-section are available and for the `CC11` processes with anomalous couplings only the differential cross-sections were calculated.

Since the ZZ production threshold has been reached at LEP2 also this process is subject for studies. ZZ production is the main irreducible background process in the search for a light Higgs boson, but also an anomalous triple gauge boson coupling could contribute to the process. It is natural to apply the methods used for W pair production

also here. Couplings of three Z bosons or two Z bosons and a photon are predicted to vanish in the Standard Model at all. Moreover, most of the anomalous couplings allowed in a ZWW vertex are forbidden by Bose symmetry in a ZZZ vertex. If only one Z is off-shell, only two anomalous couplings may exist. Their effects were studied in chapter 5. The derived results can be used in a determination of the anomalous couplings, respectively to determine limits to these couplings.

Outlook

It cannot be expected that the limits to the anomalous magnetic moment of the τ will improve much by using experiments with center-of-mass energies in the region of the production threshold. In these experiments the photons do not have enough energy to allow for a clear distinction between initial and final state radiation. However, a high luminosity run at Z peak energies at a future linear collider might deliver a much better statistics and could be used to increase to precision of the measurement.

After the era of LEP2, where the search for anomalous couplings was already performed, a very interesting collider for the search of anomalous gauge couplings will be one of the planned linear colliders[1]. In contrast to the case of the anomalous magnetic moment of the τ, where a center-of-mass energy at the Z-peak is best, the triple gauge boson couplings will be best examined at energies well above the W-pair production threshold. Considering the high energy and the large luminosity of the future linear colliders I see a large potential to discover new physics.

And besides the collider physics also in low energy particle physics experiments exist the hope to find deviations of the Standard Model and anomalous triple gauge boson couplings. For example, new and more precise measurements of the anomalous magnetic moment of the muon will allow a precise determination of the gauge boson couplings of the W boson, see e.g. [193, 194].

[1] For the physical potential of a 500-1000 GeV linear collider, see e.g. reference [192].

Appendix A

Feynman Rules

In this appendix we reproduce the Feynman rules used for our calculations. For a complete list of Feynman rules we refer to the literature, see e.g. [195–199].

A.1 External Particles

To describe fermions and bosons we use for the external lines the expressions:

incoming fermion

$$u(p) \qquad \overset{p}{\longrightarrow\!\bullet} \tag{A.1}$$

outgoing fermion

$$\overline{u}(p) \qquad \bullet\!\overset{p}{\longrightarrow} \tag{A.2}$$

incoming antifermion

$$\overline{v}(p) \qquad \overset{p}{\longleftarrow\!\bullet} \tag{A.3}$$

outgoing antifermion

$$v(p) \qquad \bullet\!\overset{p}{\longleftarrow} \tag{A.4}$$

incoming vector boson

$$\epsilon_\mu(k,\lambda) \qquad V_\mu \overset{k}{\sim\!\bullet} \tag{A.5}$$

outgoing vector boson

$$\epsilon^*_\mu(k,\lambda) \qquad \bullet\!\overset{k}{\sim} V_\mu \tag{A.6}$$

The spinors and antispinors are normalized to:

$$\sum_{\text{spin}} \overline{u}(p,s)u(p,s) = 2m, \tag{A.7}$$

$$\sum_{\text{spin}} \overline{v}(p,s)v(p,s) = -2m, \tag{A.8}$$

and

$$\sum_{\text{spin}} u(p,s)\overline{u}(p,s) = \not{p} + m, \tag{A.9}$$

$$\sum_{\text{spin}} v(p,s)\overline{v}(p,s) = \not{p} - m. \tag{A.10}$$

For the vector boson polarizations we have the properties:

$$k^\mu \epsilon_\mu(k,\lambda) = 0, \tag{A.11}$$

$$\epsilon_\mu(k,\lambda)\epsilon^{*\mu}(k,\lambda') = -\delta^\lambda_{\lambda'} \tag{A.12}$$

$$\sum_\lambda \epsilon_\mu(k,\lambda)\epsilon^*_\nu(k,\lambda) = -g_{\mu\nu} + \frac{k_\mu k_\nu}{k^2}. \tag{A.13}$$

Note that the right-hand side of (A.13) is identical with the numerator in (A.16). The use k^2 instead of m^2 on the right-hand-side of equation (A.13) allows to apply the formula also for off-shell particles.

A.2 Propagators

The particle propagators for fermions and spin one bosons are:

spin 1/2 fermion

$$\frac{i}{\not{p} - m_l + i\epsilon} = \frac{i(\not{p} + m)}{p^2 - m_l^2 + i\epsilon} \qquad p \tag{A.14}$$

massless vector boson

$$i\frac{-g_{\mu\nu}}{k^2 + i\epsilon} \qquad \mu \overset{k}{\sim} \nu \tag{A.15}$$

massive vector boson

$$i\frac{-g_{\mu\nu} + \dfrac{k_\mu k_\nu}{k^2}}{k^2 - m_V^2 + i\epsilon} \qquad \mu \overset{k}{\sim} \nu \tag{A.16}$$

Expression (A.16) is a special gauge, the Landau gauge ($\xi = 0$), of the more general propagator:

$$D_{\mu\nu} = \frac{-i}{k^2 - m^2 + i\epsilon}\left[g_{\mu\nu} - (1-\xi)\frac{k_\mu k_\nu}{k^2 - \xi m_V^2 + i\epsilon}\right]. \tag{A.17}$$

In equation (B.62) we use for convenience the unitary gauge ($\xi = \infty$) of (A.17):

$$D_{\mu\nu} = i\frac{-g_{\mu\nu} + \dfrac{k_\mu k_\nu}{m_V^2}}{k^2 - m_V^2 + i\epsilon} \tag{A.18}$$

to calculate the muon decay on the Born level.

By changing the sign of the four-momentum the fermion propagators can be used also for the description of antifermions.

A.3 Vertices

The vertices play an important role here since anomalous couplings might appear in them. The couplings between fermions and the massive gauge bosons are treated in the Standard Model. In three-gauge boson couplings anomalous contributions are taken into account. In addition, for the calculations in chapter 3, an anomalous magnetic dipole moment a_τ and an anomalous electric dipole moment d_τ are considered in (A.20). In all vertices all the momenta are assumed to be outgoing.

$$-iQ_f\gamma^\mu \tag{A.19}$$

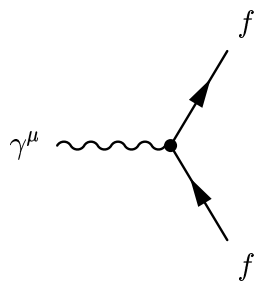

$$ie\left[\gamma^\mu + i\frac{a_\tau}{2m_\tau}\sigma^{\mu\nu}q_\nu + \frac{d_\tau}{2m_\tau}\gamma_5\sigma^{\mu\nu}q_\nu\right] \tag{A.20}$$

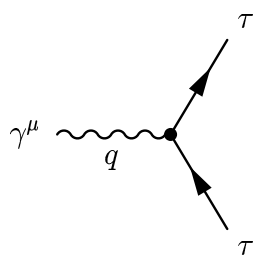

$$-ig_W\gamma^\mu(1-\gamma_5) \tag{A.21}$$

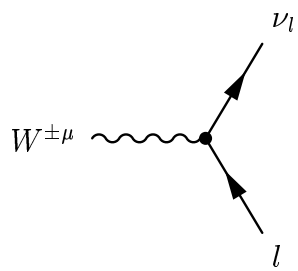

$$-\frac{ig_Z}{\sqrt{2}}\gamma^\mu\left[R_f(1+\gamma_5)+L_f(1-\gamma_5)\right] \qquad Z^\mu \qquad f,\ f \tag{A.22}$$

$$\Gamma_V^{\mu\nu\alpha}{}_{\rm SM}+\Gamma_V^{\mu\nu\alpha}{}_{\rm ano} \qquad \gamma^\mu, Z^\mu \qquad q,\ k_+,\ k_-,\ W^{+\alpha},\ W^{-\beta} \tag{A.23}$$

$$\Gamma_{VZZ}^{\mu\nu\alpha} \qquad \gamma^\mu, Z^\mu \qquad p,\ q_1,\ q_2,\ Z^\alpha,\ Z^\beta \tag{A.24}$$

We used the abbreviations:

$$L_f = 2I_3 - 2Q_f s_W^2, \tag{A.25}$$
$$R_f = -2Q_f s_W^2, \tag{A.26}$$
$$g_W = \left(\frac{G_F m_W^2}{\sqrt{2}}\right)^{1/2}, \tag{A.27}$$
$$G_Z = \left(\frac{G_F m_Z^2}{\sqrt{2}}\right)^{1/2}. \tag{A.28}$$

The electric charge Q_f and the third component of the weak isospin I_3 of a fermion f can be taken from table 2.1.

For the three gauge boson vertices we used the vertex functions:

$$\Gamma_\gamma^{\mu\nu\alpha}{}_{\rm SM} = ie\left[g^{\alpha\beta}(k_+-k_-)^\mu + g^{\alpha\mu}(q-k_+)^\beta + g^{\beta\mu}(k_- - q)^\alpha\right], \tag{A.29}$$
$$\Gamma_Z^{\mu\nu\alpha}{}_{\rm SM} = ie\cot\theta_W\left[g^{\alpha\beta}(k_+-k_-)^\mu + g^{\alpha\mu}(q-k_+)^\beta + g^{\beta\mu}(k_- - q)^\alpha\right], \tag{A.30}$$
$$\begin{aligned}\Gamma_\gamma^{\mu\nu\alpha}{}_{\rm ano} = {} & -ie\left\{x_\gamma\left[g^{\mu\beta}q^\alpha - g^{\mu\alpha}q^\beta\right]\right. \\ & + \frac{y_\gamma}{m_W^2}\left[k_+^\beta q^\alpha k_-^\mu - k_+^\mu q^\beta k_-^\alpha + (qk_+)\left(g^{\mu\beta}k_-^\alpha - g^{\alpha\beta}k_-^\mu\right)\right. \\ & \left.\left. + (qk_-)\left(g^{\alpha\beta}k_+^\mu - g^{\mu\alpha}k_+^\beta\right) + (k_-k_+)\left(g^{\mu\alpha}q^\beta - g^{\mu\beta}q^\alpha\right)\right]\right\},\end{aligned} \tag{A.31}$$
$$\begin{aligned}\Gamma_Z^{\mu\nu\alpha}{}_{\rm ano} = {} & -ie\left\{\delta_Z\left[g^{\alpha\beta}(k_- - k_+)^\mu + g^{\mu\alpha}(k_+ - q)^\beta + g^{\mu\beta}(q-k_-)^\alpha\right]\right. \\ & \left. + x_Z\left[g^{\mu\beta}q^\alpha - g^{\mu\alpha}q^\beta\right]\right.\end{aligned}$$

$$
\begin{aligned}
&+\frac{y_Z}{m_W^2}\left[k_+^\beta q^\alpha k_-^\mu - k_+^\mu q^\beta k_-^\alpha + (qk_+)\left(g^{\mu\beta}k_-^\alpha - g^{\alpha\beta}k_-^\mu\right)\right.\\
&\qquad\left.+(qk_-)\left(g^{\alpha\beta}k_+^\mu - g^{\mu\alpha}k_+^\beta\right) + (k_-k_+)\left(g^{\mu\alpha}q^\beta - g^{\mu\beta}q^\alpha\right)\right]\\
&\left.+\frac{iz_Z}{m_W^2}\left[\epsilon^{\mu\beta\kappa\sigma}q^\alpha - \epsilon^{\mu\alpha\kappa\sigma}q^\beta\right]q_\kappa(k_+-k_-)_\sigma\right\}, \qquad \text{(A.32)}
\end{aligned}
$$

$$
\Gamma_{VZZ}^{\mu\nu\alpha} = \frac{p^2-m_V^2}{m_Z^2}\left[if_4^V(p^\alpha g^{\mu\beta}+p^\beta g^{\mu\alpha}) + if_5^V\epsilon^{\mu\alpha\beta\rho}(q_1-q_2)_\rho\right]. \qquad \text{(A.33)}
$$

The Standard Model predictions for these vertices are obtained with the parameter set:

$$
\begin{aligned}
x_\gamma &= 0, & y_\gamma &= 0,\\
\delta_Z &= 0, & x_Z &= 0, \qquad \text{(A.34)}\\
y_Z &= 0, & z_Z &= 0.
\end{aligned}
$$

Appendix B

Phase Space and Momenta

In semi-analytic calculations it is important to find an appropriate notation for the particle momenta. Our choice of the parameterization of the four-particle final state is presented in appendix B.1, the three-particle final state in B.3, and the two-particle final state is given in appendix B.2. As a demonstration how suitable momenta can simplify a calculation we present in B.4 the Born cross-section for muon decay.

B.1 W Pair Production

In the process $e^+e^- \to W^+W^- \to 4f$ four fermions are produced. We have to find a suitable base to construct the particle momenta and the four-particle phase space. The general expression for n final state fermions is:

$$\mathrm{d}\Gamma = \prod_{i=1}^{n} \frac{\mathrm{d}^3 p_i}{(2\pi)^3 (2p_i^0)} \delta^4 \left(\sum_{i=1}^{n} p_i - k_1 - k_2 \right), \tag{B.1}$$

where k_1 and k_2 are the momenta of the incoming particles. The phase space in (B.1) can be parameterized by a subsequent decay which leads to a product of several one particle into two particles phase spaces. This is, for example, worked out in chapter 4.2 of [200]. In the special case of four-particle production the procedure leads to:

$$\mathrm{d}\Gamma = \frac{1}{128} \frac{\sqrt{\lambda(s, s_1, s_2)}}{s} \frac{\sqrt{\lambda(s_1, m_1^2, m_2^2)}}{s_1} \frac{\sqrt{\lambda(s_2, m_3^2, m_4^2)}}{s_2} \mathrm{d}s_1 \mathrm{d}s_2 \mathrm{d}\Omega \mathrm{d}\Omega_1 \mathrm{d}\Omega_2. \tag{B.2}$$

The phase space elements $\mathrm{d}\Omega$, $\mathrm{d}\Omega_1$, $\mathrm{d}\Omega_2$ are the solid angles in the rest system of a decaying compound particle and can be split up in a polar angle θ and an azimuthal angle ϕ:

$$\mathrm{d}\Omega = \mathrm{d}\phi \, \mathrm{d}\cos\theta, \tag{B.3}$$

$$\mathrm{d}\Omega_1 = \mathrm{d}\phi_1 \, \mathrm{d}\cos\theta_1, \tag{B.4}$$

$$\mathrm{d}\Omega_2 = \mathrm{d}\phi_2 \, \mathrm{d}\cos\theta_2, \tag{B.5}$$

while s_1 and s_2 are invariant masses defined by the final state particles:

$$s_1 = (p_1 + p_2)^2, \tag{B.6}$$

$$s_2 = (p_3 + p_4)^2. \tag{B.7}$$

The allowed kinematical regions for the eight integration variables in (B.2) are:

$$\begin{array}{rcccl} (m_1+m_2)^2 & \leq & s_1 & \leq & (\sqrt{s}-m_3-m_4)^2, \\ (m_3+m_4)^2 & \leq & s_2 & \leq & (\sqrt{s}-\sqrt{s_1})^2, \\ -1 & \leq & \cos\theta, \cos\theta_1, \cos\theta_2 & \leq & 1, \\ 0 & \leq & \phi, \phi_1, \phi_2 & \leq & 2\pi. \end{array} \tag{B.8}$$

Note, that none of the particle momenta will depend on the variable ϕ (see below) and the integration over ϕ in (B.2) will just give a factor 2π.

To construct the particle momenta out of the phase space variables, we follow the strategy from [127, 131] and express the momenta by the variables s, s_1, s_2, θ, ϕ, θ_1, ϕ_1, θ_2, and ϕ_2.

The momenta of the initial state fermions are chosen to be:

$$k_1 = (k_0, -k\sin\theta, 0, k\cos\theta), \tag{B.9}$$

$$k_2 = (k_0, k\sin\theta, 0, -k\cos\theta), \tag{B.10}$$

with the energy $k_0 = \sqrt{s}/2$. The three-momentum is:

$$k \equiv |\vec{k}| = \frac{\sqrt{\lambda(s, m_e^2, m_e^2)}}{2\sqrt{s}} \approx k_0. \tag{B.11}$$

The momenta of the W bosons fix the W production angle θ:

$$p_{W^-} = \frac{1}{2\sqrt{s}}\left(s + s_1 - s_2, 0, 0, \sqrt{\lambda}\right), \tag{B.12}$$

$$p_{W^+} = \frac{1}{2\sqrt{s}}\left(s - s_1 + s_2, 0, 0, -\sqrt{\lambda}\right), \tag{B.13}$$

with $\lambda \equiv \lambda(s, s_1, s_2)$. The relations $p_{W^-}^2 = s_1$ and $p_{W^+}^2 = s_2$ follow from (B.12) and (B.13).

The momenta of the final state fermions can be easily constructed in the rest frame R of the W bosons. They are:

$$p_1^R = \left(\frac{s_1 + m_1^2 - m_2^2}{2\sqrt{s_1}}, p_{12}^R \sin\theta_1\cos\phi_1, p_{12}^R \sin\theta_1 \sin\phi_1, p_{12}^R \cos\theta_1\right), \tag{B.14}$$

$$p_2^R = \left(\frac{s_1 - m_1^2 + m_2^2}{2\sqrt{s_1}}, -p_{12}^R \sin\theta_1\cos\phi_1, -p_{12}^R \sin\theta_1 \sin\phi_1, -p_{12}^R \cos\theta_1\right), \tag{B.15}$$

with the abbreviation

$$p_{12}^R = \frac{\sqrt{\lambda(s, m_1^2, m_2^2)}}{2\sqrt{s_1}}. \tag{B.16}$$

Equations similar to (B.14) and (B.15) hold for p_3^R and p_4^R. To get the momenta in the center-of-mass system (B.14) and (B.15) have to be boosted along the z-axis. This leads

to:

$$\begin{aligned}
p_1 &= (\gamma^0_{12} p^R_{1,0} + \gamma_{12} p^R_{12}\cos\theta, p^R_{12}\sin\theta_1\cos\phi_1, p^R_{12}\sin\theta_1\sin\phi_1, \gamma^0_{12} p^R_{12}\cos\theta_1 + \gamma_{12} p^R_{1,0}),\\
p_2 &= (\gamma^0_{12} p^R_{2,0} - \gamma_{12} p^R_{12}\cos\theta, -p^R_{12}\sin\theta_1\cos\phi_1, -p^R_{12}\sin\theta_1\sin\phi_1, -\gamma^0_{12} p^R_{12}\cos\theta_1 + \gamma_{12} p^R_{2,0}),\\
p_3 &= (\gamma^0_{34} p^R_{3,0} - \gamma_{34} p^R_{34}\cos\theta, p^R_{34}\sin\theta_1\cos\phi_1, p^R_{34}\sin\theta_1\sin\phi_1, \gamma^0_{34} p^R_{34}\cos\theta_1 - \gamma_{34} p^R_{3,0}),\\
p_4 &= (\gamma^0_{34} p^R_{4,0} + \gamma_{34} p^R_{34}\cos\theta, -p^R_{34}\sin\theta_1\cos\phi_1, -p^R_{34}\sin\theta_1\sin\phi_1, -\gamma^0_{34} p^R_{34}\cos\theta_1 - \gamma_{34} p^R_{4,0}),
\end{aligned} \tag{B.17}$$

with

$$\gamma^0_{12} = \frac{s + s_1 - s_2}{2\sqrt{s s_1}}, \tag{B.18}$$

$$\gamma_{12} = \frac{\sqrt{\lambda}}{2\sqrt{s s_1}}, \tag{B.19}$$

$$\gamma^0_{34} = \frac{s + s_2 - s_1}{2\sqrt{s s_2}}, \tag{B.20}$$

$$\gamma_{34} = \frac{\sqrt{\lambda}}{2\sqrt{s s_2}}, \tag{B.21}$$

$$p^R_{1,0} = \frac{s_1 + m_1^2 - m_2^2}{2\sqrt{s_1}}, \tag{B.22}$$

$$p^R_{3,0} = \frac{s_1 + m_3^2 - m_4^2}{2\sqrt{s_2}}. \tag{B.23}$$

The expressions for $p^R_{2,0}$ and $p^R_{4,0}$ can be obtained by exchanging the masses in (B.22) and (B.23).

This completes the set of particle momenta and phase space variables.

B.2 ZZ Production

In the process $e^+e^- \to ZZ$ the decay of the gauge bosons is not considered and the final state contains only the two spin-1 bosons. This simplifies the phase space drastically. We just have a two-particle final state leading to the differential cross-section:

$$\frac{\mathrm{d}\sigma}{\mathrm{d}\cos\theta} = \frac{\sqrt{\lambda}}{64\pi s^2}\left|\mathcal{M}\right|^2. \tag{B.24}$$

The 'off-shellness' of the Z bosons in (B.24) can be included into the calculation by making an assumption about the masses $\sqrt{s_1}$ and $\sqrt{s_2}$ for the Z bosons and convoluting them with the Breit-Wigner factors $\rho(s_i)$:

$$\frac{d\sigma}{d\cos\theta} = \int \mathrm{d}s_1 \int \mathrm{d}s_2 \, \frac{\sqrt{\lambda}}{64\pi s^2}\left|\mathcal{M}\right|^2 \rho(s_1)\rho(s_2), \tag{B.25}$$

where $\rho(s_i)$ is:

$$\rho(s_i) = \frac{1}{\pi}\frac{\sqrt{s_i}\Gamma_Z(s_i)}{(s_i - m_Z^2)^2 + s_i\Gamma_Z^2(s_i)} \tag{B.26}$$

The momenta of the incoming e^- and e^+ particles are denoted by:

$$p_1 = \frac{\sqrt{s}}{2}(1, \sin\theta, 0, \cos\theta), \tag{B.27}$$

$$p_2 = \frac{\sqrt{s}}{2}(1, -\sin\theta, 0, -\cos\theta). \tag{B.28}$$

The produced Z bosons have the momenta:

$$k_1 = \frac{1}{2\sqrt{s}}\left(s + s_1 - s_2, 0, 0, \sqrt{\lambda}\right), \tag{B.29}$$

$$k_2 = \frac{1}{2\sqrt{s}}\left(s - s_1 + s_2, 0, 0, -\sqrt{\lambda}\right), \tag{B.30}$$

with the polarizations:

$$\epsilon^*_{1\pm} = \sqrt{\frac{1}{2}}(0, \mp 1, i, 0), \tag{B.31}$$

$$\epsilon^*_{10} = \frac{1}{2\sqrt{s s_1}}\left(\sqrt{\lambda}, 0, 0, (s + s_1 - s_2)\right), \tag{B.32}$$

$$\epsilon^*_{2\pm} = \sqrt{\frac{1}{2}}(0, \pm 1, i, 0), \tag{B.33}$$

$$\epsilon^*_{20} = \frac{1}{2\sqrt{s s_2}}\left(\sqrt{\lambda}, 0, 0, -(s - s_1 + s_2)\right). \tag{B.34}$$

B.3 $e^+e^- \to \tau^+\tau^-\gamma$

The process investigated in chapter 3 implies a phase space for three-fermion production. According to (B.1) it is:

$$\mathrm{d}\Gamma = \frac{\mathrm{d}^3p_1}{(2\pi)^3 2p_1^0}\frac{\mathrm{d}^3p_2}{(2\pi)^3 2p_2^0}\frac{\mathrm{d}^3k}{(2\pi)^3 2k^0}\delta^4(k_1 + k_2 - p_1 - p_2 - k). \tag{B.35}$$

Again, the phase space can be split up in a sequence of decays into two particles:

$$\mathrm{d}\Gamma = \frac{s}{(2\pi)^9}\,\mathrm{d}\Gamma_\tau\,\mathrm{d}\Gamma_c\,\mathrm{d}x', \tag{B.36}$$

with

$$\mathrm{d}\Gamma_\tau = \frac{\sqrt{\lambda(x', m_\tau^2/s, m_\tau^2/s)}}{8x'}\mathrm{d}\varphi_1\mathrm{d}\cos\theta_1 = \frac{\beta'}{8}\mathrm{d}\varphi_1\mathrm{d}\cos\theta_1, \tag{B.37}$$

$$\mathrm{d}\Gamma_c = \frac{\sqrt{\lambda(1, x', 0)}}{8}\mathrm{d}\varphi_\gamma\mathrm{d}\cos\theta_\gamma. \tag{B.38}$$

As abbreviations we used the invariant mass squared x' of the τ pair and the velocity β' of the τ leptons in the rest system of the τ pair. These values are:

$$x' = \frac{(p_1+p_2)^2}{s}, \tag{B.39}$$

$$\beta' = \sqrt{1-\frac{4m_\tau^2}{x's}}. \tag{B.40}$$

In the construction of the moments we follow the same strategy as in section B.1. The momenta of e^- and e^+ are again defined by:

$$k_1 = \frac{\sqrt{s}}{2}\left(1,\sin\theta_\gamma,0,-\cos\theta_\gamma\right), \tag{B.41}$$

$$k_2 = \frac{\sqrt{s}}{2}\left(1,-\sin\theta_\gamma,0,\cos\theta_\gamma\right). \tag{B.42}$$

The masses of the incoming e^- and e^+ are already neglected in (B.41) and (B.42). The photon momentum is set to be:

$$q = \frac{\sqrt{s}}{2}\left(1-x',0,0,1-x'\right). \tag{B.43}$$

That is equivalent to the momentum of the W^- in (B.12) under the assumption that $s_1 = 0$ and $s_2 = x'$. The momentum of the photon fixes already the invariant mass of the τ pair, but leaves still some freedom for the decay angles of the individual τ leptons. Their momenta are then:

$$p_{1/2} = \frac{\sqrt{s}}{4}\left(\mp a(1-x')+1+x', \pm b\cos\varphi_1, \pm b\sin\varphi_1, \pm a(1+x')-1+x'\right), \tag{B.44}$$

with the abbreviations

$$a = \beta'\cos\theta_1, \tag{B.45}$$

$$b = 2\sqrt{x'}\beta'\sin\theta_1. \tag{B.46}$$

Note that all momenta (B.43) – (B.44) are independent of φ_γ so integration over φ_γ results in a trivial factor 2π.

The integrations over the production angles of the particles are carried out in chapter 3. For completeness, we present the integrals over x' which require an infrared cutoff:

$$\int_0^x \frac{\ln(x's/m_\tau^2)}{1-x'}\mathrm{d}x' = \ln\frac{s}{m_\tau^2}\ln\frac{1}{1-x} - \mathrm{Li}_2(1) + \mathrm{Li}_2(1-x), \tag{B.47}$$

$$\int_0^x \frac{1}{1-x'}\mathrm{d}x' = \ln\frac{1}{1-x}. \tag{B.48}$$

In (B.47) and (B.48) the approximations $\beta' \to 1$ and $m_\tau^2/x' \to 0$ are used.

B.4 $\mu^- \to e^- \nu_\mu \bar{\nu}_e$

This simple decay $\mu^- \to e^- \nu_\mu \bar{\nu}_e$, taking into account the masses of muon and electron (as might be reasonable for the decay $\tau \to \mu \nu_\tau \bar{\nu}_\mu$), serves as a nice example how a suitable choice of particle momenta can simplify an analytical calculation. The calculation was inspired by Tord Riemann after he found a discrepancy between his result and the one presented in the literature [201–203]. The literature result disagrees because not all mass terms are considered there correctly. It should be emphasized that the neglected terms are unmeasurably small and can be safely ignored. For a real calculation the radiative corrections are much more important, but here we just want to demonstrate the simplicity of the calculation with an appropriate phase space parameterization. The final result given in (B.78) was checked with an independent calculation by L. Kalinovskaya and T. Riemann [204].

We start with the transition probability for a particle decay:

$$\mathrm{d}\Gamma = \frac{(2\pi)^4}{2m_\mu} |\mathcal{M}|^2 \prod_{i=1}^{3} \frac{\mathrm{d}^3 p_i}{(2\pi)^3 2p_i^0} \delta\left(p_\mu - \sum_{i=1}^{3} p_i\right), \tag{B.49}$$

where m_μ and p_μ are already the mass and the momentum of the muon. The phase space factor

$$\mathrm{dPS} = \frac{\mathrm{d}^3 p_{e^-}}{(2\pi)^3 2p_{e^-}^0} \frac{\mathrm{d}^3 p_{\nu_\mu}}{(2\pi)^3 2p_{\nu_\mu}^0} \frac{\mathrm{d}^3 p_{\bar{\nu}_e}}{(2\pi)^3 2p_{\bar{\nu}_e}^0} \delta\left(p_\mu - \sum_{i=1}^{3} p_i\right), \tag{B.50}$$

can be rewritten as:

$$\mathrm{dPS} = \frac{1}{(2\pi)^9} \mathrm{d}\Gamma_1 \mathrm{d}\Gamma_c \mathrm{d}s, \tag{B.51}$$

with the abbreviations

$$\mathrm{d}\Gamma_1 = \frac{s - m_e^2}{8s} \mathrm{d}\Omega_e \tag{B.52}$$

$$\mathrm{d}\Gamma_c = \frac{m_\mu^2 - s}{8m_\mu^2} \mathrm{d}\Omega_{\nu_\mu}. \tag{B.53}$$

The solid angle Ω_e in equation (B.52) denotes the direction of the electron in the rest system of the $e^- \bar{\nu}_e$ pair. For the ν_μ the direction is given by Ω_μ in the same Lorentz system.

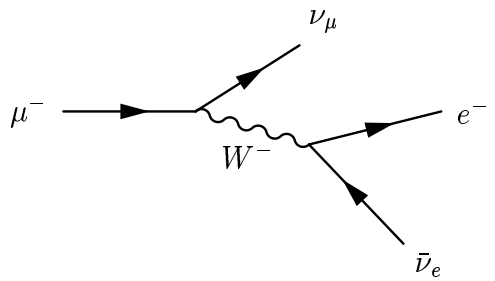

Figure B.1: *The tree-level diagram for muon decay.*

Since the particle momenta and the matrix element (B.73), as we will see, do not depend on all phase space variables, we can perform some integrations immediately. We have:

$$\int \Omega_{\nu_\mu} = 4\pi, \tag{B.54}$$

$$\int \mathrm{d}\Omega_e = 2\pi \int \mathrm{d}\cos\theta. \tag{B.55}$$

This leads to

$$\mathrm{d}\Gamma = \frac{1}{64m_\mu^3}\frac{1}{(2\pi)^3}\left|\mathcal{M}\right|^2 \frac{(m_\mu^2 - s)(s - m_e^2)}{s}\mathrm{d}s\mathrm{d}\cos\theta, \tag{B.56}$$

for the decay width of the muon.

If we are not interested in the electron energy, a suitable frame for the momenta is the W boson rest system.

First, we define the momentum of the W boson:

$$p_{W^-} = (\sqrt{s}, 0, 0, 0). \tag{B.57}$$

This choice fixes the energy of all particles. For the μ^- and ν_μ we get

$$p_{\mu^-} = \left(\frac{s + m_\mu^2}{2\sqrt{s}}, 0, 0, \frac{m_\mu^2 - s}{2\sqrt{s}}\right) \tag{B.58}$$

$$p_{\nu_\mu} = \left(\frac{m_\mu^2 - s}{2\sqrt{s}}, 0, 0, \frac{m_\mu^2 - s}{2\sqrt{s}}\right). \tag{B.59}$$

In (B.58) we made use of the freedom to choose the direction of the momentum of the μ^-. The remaining momenta are:

$$p_{e^-} = \left(\frac{s + m_e^2}{2\sqrt{s}}, \frac{s - m_e^2}{2\sqrt{s}}\sin\theta\cos\phi, \frac{s - m_e^2}{2\sqrt{s}}\sin\theta\sin\phi, \frac{s - m_e^2}{2\sqrt{s}}\cos\theta\right) \tag{B.60}$$

$$p_{\bar{\nu}_e} = \frac{s - m_e^2}{2\sqrt{s}}\left(1, -\sin\theta\cos\phi, -\sin\theta\sin\phi, -\cos\theta\right). \tag{B.61}$$

The matrix element is in unitary gauge:

$$\mathcal{M} = \frac{G_\mu m_W^2}{\sqrt{2}i}\bar{u}(p_{\nu_\mu})\gamma_\mu(1 - \gamma_5)u(p_\mu)\frac{(-g^{\mu\nu} + k^\mu k^\nu/m_W^2)}{p_{W^-}^2 - m_W^2}\bar{u}(p_e)\gamma_\nu(1 - \gamma_5)u(p_{\bar{\nu}_e}) \tag{B.62}$$

We can express the neutrino momenta by the momenta of the other three particles in the decay:

$$p_{\nu_\mu} = p_{\mu^-} - p_{W^-}, \tag{B.63}$$

$$p_{\bar{\nu}_e} = p_{W^-} - p_{e^-}. \tag{B.64}$$

The Lorentz invariant module of the matrix element squared can depend only on Lorentz scalars. These are the masses of the particles and the products:

$$(p_{\mu^-} \cdot p_{W^-}) = \frac{s + m_\mu^2}{2}, \tag{B.65}$$

$$(p_{e^-} \cdot p_{W^-}) = \frac{s + m_e^2}{2}, \tag{B.66}$$

$$(p_{\mu^-} \cdot p_{e^-}) = \frac{m_\mu^2 + m_e^2 - t}{2}, \tag{B.67}$$

with the abbreviations

$$s = \left(p_{\mu^-} - p_{\nu_\mu}\right)^2, \tag{B.68}$$

$$t = \left(p_{\mu^-} - p_{e^-}\right)^2, \tag{B.69}$$

$$u = \left(p_{\mu^-} - p_{\bar{\nu}_e}\right)^2. \tag{B.70}$$

The Feynman diagram to the muon decay is given in fig. B.1. After summing over the final state spins and averaging over the μ^- spin, we get:

$$\begin{aligned} |\mathcal{M}|^2 &= G_\mu m_W^4 \mathrm{Tr}\left\{(1-\gamma_5)/p_{\nu_\mu}\gamma_\mu(/p_\mu + m_\mu)\gamma_\sigma\right\} \mathrm{Tr}\left\{(1-\gamma_5)(/p_{e^-} + m_e)\gamma_\nu/p_{\bar{\nu}_e}\gamma_\rho\right\} \\ &\quad \times \frac{(-g^{\mu\nu} + k^\mu k^\nu/m_W^2)}{p_{W^-}^2 - m_W^2} \frac{(-g^{\rho\sigma} + k^\rho k^\sigma/m_W^2)}{p_{W^-}^2 - m_W^2} \end{aligned} \tag{B.71}$$

Performing the traces leads to:

$$\begin{aligned} |\mathcal{M}|^2 &= \frac{16 G_\mu m_W^4}{(s-m_W^2)^2} \left\{ 2y m_e^2 s - x y^2 s^2 + \frac{8}{m_W^2} (p_{\mu^-}\cdot p_{e^-})(p_{\mu^-}\cdot p_{W^-})(p_{e^-}\cdot p_{W^-}) \right. \\ &\quad + 4\left(1 - \frac{s}{m_W^2}\right)\left[(p_{\mu^-}\cdot p_{e^-})(p_{\mu^-}\cdot p_{W^-}) + (p_{\mu^-}\cdot p_{e^-})(p_{e^-}\cdot p_{W^-})\right] \\ &\quad + \frac{2s^2}{m_W^2}(p_{\mu^-}\cdot p_{e^-}) - 4(p_{\mu^-}\cdot p_{e^-})^2 - \left(4 + \frac{s^2}{m_W^4}\right)(p_{\mu^-}\cdot p_{W^-})(p_{e^-}\cdot p_{W^-}) \\ &\quad + \frac{2s}{m_W^4}(p_{\mu^-}\cdot p_{W^-})(p_{e^-}\cdot p_{W^-})\left[(p_{\mu^-}\cdot p_{W^-}) + (p_{e^-}\cdot p_{W^-})\right] \\ &\quad - \frac{4}{m_W^4}(p_{\mu^-}\cdot p_{W^-})^2(p_{e^-}\cdot p_{W^-})^2 + 2xy\left(\frac{s}{m_W^2} - 4\right)(p_{\mu^-}\cdot p_{W^-})^2 \\ &\quad \left. + y\left(2 - \frac{s}{m_W^2}\right)\left[s(p_{e^-}\cdot p_{W^-}) - 2(p_{e^-}\cdot p_{W^-})^2 + xs(p_{\mu^-}\cdot p_{W^-})\right]\right\} \end{aligned} \tag{B.72}$$

Finally, we get the result:

$$|\mathcal{M}|^2 = \frac{16 G_\mu^2 m_W^4}{(s-m_W^2)^2}\left\{\left(m_\mu^2 - u\right)\left(u - m_e^2\right) - y m_e^2 t + \frac{xy^2}{4}\left[s(u+t) - m_\mu^2 m_e^2\right]\right\} \tag{B.73}$$

After performing the simple phase space integrations over $\cos\theta$ and s we get the exact expression for the muon decay on Born level:

$$\begin{aligned} \Gamma &= \frac{G_\mu^2 m_\mu^5}{192\pi^3}\left[\left(3x - 12\frac{x}{y^3} + 9\frac{x}{y^2} - 3x^3y^2 + 3x^3 + \frac{12}{y^4} - \frac{12}{y^3}\right)\ln\left(\frac{1-y}{1-xy}\right)\right. \\ &\quad + \left(2 + x^3y^3 - 6\frac{x}{y^2} + 9\frac{x}{y} - 3xy + 2x^3 - 3x^3y + \frac{4}{y^3} - \frac{6}{y^2}\right)\frac{(1-x)}{(1-y)(1-xy)} \\ &\quad \left. + 12x^2\ln x + 3x^3y^2\ln x - 8\frac{x}{y^3} - \frac{17}{2}x + 4\frac{x^2}{y^2} + 2x^2y - 2x^3y + \frac{17}{2}x^3 + \frac{8}{y^3} - \frac{4}{y^2}\right], \end{aligned} \tag{B.74}$$

where, we used the abbreviations:

$$x = \frac{m_e^2}{m_\mu^2}, \tag{B.75}$$

$$y = \frac{m_\mu^2}{m_W^2}. \tag{B.76}$$

With a Taylor expansion for $y \ll 1$ and the identity

$$\frac{1}{1-y} = 1 + \frac{y}{1-y} \tag{B.77}$$

we get the tree-level result:

$$\Gamma = \frac{G_\mu^2 m_\mu^5}{192\pi^3} f(x) \left(1 + \frac{3}{5}y + \frac{9}{5}xy\right) \tag{B.78}$$

with the well-known function

$$f(x) = 1 - 8x + 12x^2 \ln x + 8x^3 - x^4. \tag{B.79}$$

In (B.78) we neglect terms of the order $\mathcal{O}(y^2)$ and $\mathcal{O}(yx^2)$.

Appendix C

Electromagnetic Multipole Moments

In this appendix we derive expressions for some electromagnetic multipole moments.

C.1 Magnetic Moments of Leptons

The most general form for the matrix element of the current of a spin 1/2 particle with charge e is:

$$\langle \Psi(p',\sigma')|J^{\mu}(0)|\Psi(p,\sigma)\rangle = \frac{e}{(2\pi)^3}\bar{u}(p',\sigma')\Gamma^{\mu}(p',p)u(p,\sigma), \tag{C.1}$$

where Γ^{μ} is a four-vector 4×4 matrix function depending on the momenta p and p'. The σ and σ' denote the spin of the particle.

After expanding Γ^{μ} in the 16 covariant matrices 1, γ_{ρ}, $[\gamma_{\rho},\gamma_{\sigma}]$, $\gamma_5\gamma_{\rho}$ and γ_5 and using the Dirac equations:

$$\begin{aligned} \bar{u}(p',\sigma')(\not{p}'-m) &= 0, \\ (\not{p}-m)u(p,\sigma) &= 0, \end{aligned} \tag{C.2}$$

it can be shown that the right hand side of equation (C.1) can be rewritten as [11]:

$$\begin{aligned} \bar{u}(p',\sigma')\Gamma^{\mu}(p',p)u(p,\sigma) &= \bar{u}(p',\sigma')\left[\gamma^{\mu}F(q^2)+\frac{1}{2m}(p+p')^{\mu}G(q^2)\right. \\ &\quad \left.+\frac{(p-p')^{\mu}}{2m}H(q^2)\right]u(p,\sigma), \end{aligned} \tag{C.3}$$

with $q=p'-p$. The structure functions F, G, and H can only depend on q^2, the only scalar kinematic variable. Since $J^{\mu}(0)$ is hermitian, $F(q^2)$, $G(q^2)$, and $H(q^2)$ must be real. After multiplying equation (C.3) by q_{μ}, it follows with the current conservation $q_{\mu}J^{\mu}=0$ that $H(q^2)$ must be zero.

For the remaining functions the normalization condition

$$F(0)+G(0)=1 \tag{C.4}$$

can be proved [11, 205]. It is more common to express the functions F and G by two other functions F_1 (the electric form factor) and F_2:

$$\bar{u}(p')\Gamma^{\mu}(p',p)u(p)=\bar{u}(p')\left[\gamma^{\mu}F_1(q^2)+\frac{iF_2(q^2)}{2m}\sigma^{\mu\nu}(p'-p)_{\nu}\right]u(p), \tag{C.5}$$

where the common abbreviation $\sigma^{\mu\nu} = \frac{i}{2}[\gamma^\mu, \gamma^\nu]$ is used. For simplicity we also dropped the spin indices σ and σ'. By commuting p' to the left and p to the right in equation (C.5) and applying the Dirac equations (C.2) one gets the identification:

$$F_1(q^2) = G(q^2) + F(q^2), \tag{C.6}$$
$$F_2(q^2) = -G(q^2), \tag{C.7}$$

which together with equation (C.4) immediately leads to

$$F_1(0) = 1. \tag{C.8}$$

To derive an expression for the magnetic moment of spin 1/2 particles, we rewrite equation (C.3) using the Gordon identity

$$\bar{u}(p')\sigma^{\mu\nu}(p'-p)_\nu u(p) = i\bar{u}(p')\left[(p'^\mu + p^\mu) - 2m\gamma^\mu\right]u(p) \tag{C.9}$$

and dropping the term proportional to H. This leads to

$$\begin{aligned}\bar{u}(p')\Gamma^\mu(p',p)u(p) &= \frac{1}{2m}\bar{u}(p')\Big\{(p+p')^\mu\left[F(q^2)+G(q^2)\right] \\ &\quad + i\sigma^{\mu\nu}(p'-p)_\nu F(q^2)\Big\}u(p).\end{aligned} \tag{C.10}$$

For vanishing momenta p' and p we have:

$$\bar{u}(0,\sigma')[\gamma^i,\gamma^j]u(0,\sigma) = 4i\epsilon_{ijk}\left(\tau_k\right)_{\sigma,\sigma'}, \tag{C.11}$$
$$\bar{u}(0,\sigma')[\gamma^i,\gamma^0]u(0,\sigma) = 0, \tag{C.12}$$

with $\vec{\tau} = \frac{1}{2}\vec{\sigma}$. With these approximations the second term on the right hand side of equation (C.10) leads in first order of the small momenta to

$$\frac{i}{m}\left[(\vec{p}-\vec{p}')\times\vec{\tau}\right]_{\sigma',\sigma}F(0). \tag{C.13}$$

The contribution of this term to the interaction energy with an external vector potential $\vec{A}(\vec{x})$ is

$$\begin{aligned}\langle\Psi_{p',\sigma'}|E|\Psi_{p,\sigma}\rangle &= \frac{-ieF(0)}{m(2\pi)^3}\int \mathrm{d}^3x\, e^{i(\vec{p}-\vec{p}')\cdot\vec{x}}\vec{A}(\vec{x})\cdot\left[(\vec{p}-\vec{p}')\times\vec{\tau}\right]_{\sigma,\sigma'} \\ &= \frac{-eF(0)}{m(2\pi)^3}\int \mathrm{d}^3x\, e^{i(\vec{p}-\vec{p}')\cdot\vec{x}}\left(\vec{\tau}\right)_{\sigma,\sigma'}\cdot\vec{B}(\vec{x}),\end{aligned} \tag{C.14}$$

with the magnetic field $\vec{B} = \vec{\nabla}\times\vec{A} = -i\vec{q}\times\vec{A}$. Here, the definition

$$E = -\int J_\mu(x)A^\mu(x)\mathrm{d}^3x. \tag{C.15}$$

was used.

In a slowly varying magnetic field, we get

$$\langle\Psi_{p,\sigma'}|E|\Psi_{p,\sigma}\rangle = -\frac{eF(0)}{m}\left(\vec{\tau}\right)_{\sigma,\sigma'}\cdot\vec{B}\,\delta(\vec{p}-\vec{p}'), \tag{C.16}$$

which might be related to the definition of the magnetic moment of a particle with spin 1/2:

$$\langle \Psi_{p,\sigma'} | E | \Psi_{p,\sigma} \rangle = -\frac{\mu}{1/2} \left(\vec{\tau}\right)_{\sigma,\sigma'} \cdot \vec{B}\, \delta(\vec{p} - \vec{p}'). \tag{C.17}$$

Comparing the equations (C.16) and (C.17) leads to:

$$\mu = \frac{eF(0)}{2m} = \frac{e}{2m} \left[F_1(0) + F_2(0)\right]. \tag{C.18}$$

In lowest order, $F_2(0) = 0$ and equation (C.18) leads to the famous Dirac result [15]

$$\mu = \frac{e}{2m}. \tag{C.19}$$

The anomalous magnetic moment is the deviation of this value and is defined as:

$$a = F_2(0) = \frac{2m}{e\hbar}\, \mu \; - \; 1. \tag{C.20}$$

C.2 The Magnetic Dipole Moment of the W Boson

Classically, the magnetic dipole moment is defined by the energy of a particle in a magnetic field:

$$E = -\vec{\mu} \cdot \vec{B}. \tag{C.21}$$

In quantum mechanics, we can describe the electromagnetic force by coupling a current to the field $A^\mu(x)$:

$$E = -\int J_\mu(x) A^\mu(x) \mathrm{d}^3x. \tag{C.22}$$

Let us choose a circularly polarized field:

$$A_0 \;=\; 0, \tag{C.23}$$

$$\vec{A} \;=\; \frac{1}{\sqrt{2}} \left(\vec{e}_x - i\vec{e}_y\right) e^{-i\vec{q}\cdot\vec{r}}, \tag{C.24}$$

where $\vec{q} = q\vec{e}_z$. For $\vec{B}$ follows:

$$\vec{B} = -i\vec{q} \times \vec{A}. \tag{C.25}$$

By inserting the expressions for A^μ and $\vec{B}$ into the equations (C.21) and (C.22), we get:

$$\mu_- = \lim_{q\to 0} \frac{1}{q} \int J_-(x) e^{-i\vec{q}\cdot\vec{r}} \mathrm{d}^3x, \tag{C.26}$$

with the abbreviations:

$$J_\pm(x) \;=\; J_x(x) \pm i J_y(x), \tag{C.27}$$

$$\mu_\pm \;=\; \mu_x \pm i\mu_y. \tag{C.28}$$

In quantum mechanics the magnetic dipole moment is defined as the expectation value of the z component of the dipole vector in the state of maximal spin. This is:

$$\mu \equiv \langle ss | \mu_z | ss \rangle. \tag{C.29}$$

Using the Wigner-Eckart theorem the expectation values of the various spin states can be put into the relations [206, 207]:

$$\langle s\, s_z'|\mu_\pm|s\, s_z\rangle = \frac{(-1)}{\sqrt{2s+1}}\langle s\, s_z'|1\, \pm 1\, s\, s_z\rangle\langle s|\mu|s\rangle \tag{C.30}$$

and

$$\langle s\, s|\mu_z|s\, s\rangle = \frac{1}{\sqrt{2s+1}}\langle s\, s|1\, 0\, s\, s\rangle\langle s|\mu|s\rangle. \tag{C.31}$$

Equations (C.30) and (C.31) lead immediately to

$$\mu = \frac{\langle s\, s|1\, 0\, s\, s\rangle}{\langle s\, s_z'|1\, -1\, s\, s_z\rangle}\lim_{q\to 0}\frac{1}{q}\int\langle s s_z'|J_-(x)|s s_z\rangle e^{-i\vec{q}\cdot\vec{r}}\mathrm{d}^3x, \tag{C.32}$$

where equation (C.26) was used to express μ_-.

The calculation of the right hand side of equation (C.32) can be easily performed in the Breit-frame, in which the incoming W and the outgoing W have the same momenta, but in opposite direction. The helicity states in this frame can be written as:

$$\begin{aligned}
\epsilon_\pm &= \mp\frac{1}{\sqrt{2}}(0, 1, \pm i, 0),\\
\epsilon_0 &= (p/m, 0, 0, E/m),\\
\epsilon_\pm' &= \epsilon_\mp,\\
\epsilon_0' &= (p/m, 0, 0, -E/m).
\end{aligned} \tag{C.33}$$

Let us define

$$\frac{e\Gamma^\mu_{h'h}}{2E} \equiv \frac{\langle -\vec{p}h'|J_\mu(0)|\vec{p}h\rangle}{2E}, \tag{C.34}$$

where E is the energy of the W boson. It can be shown that:

$$\frac{e\Gamma^\mu_{h'h}}{2E} = \lim_{q\to 0}(-1)^{s+s_z'}\int\langle s s_z'|J_-(x)|s s_z\rangle e^{-i\vec{q}\cdot\vec{r}}\mathrm{d}^3x. \tag{C.35}$$

With the relation

$$\langle\vec{p}'h'|J_\mu(0)|\vec{p}h\rangle = i\,(\epsilon_{h'}')^*_\beta\,\epsilon_{h\alpha}V_\mu^{\alpha\beta} \tag{C.36}$$

it follows

$$\Gamma^\mu_{h'h} = \epsilon'^*_{h'\beta}\epsilon_{h\alpha}V^{\mu\alpha\beta}. \tag{C.37}$$

Here, we used for the γW^+W^- vertex

$$\begin{aligned}
V^{\mu\alpha\beta} &= ie\left\{(p+p')^\mu\left[g^{\alpha\beta}\left(1-2\lambda\frac{p^2}{m^2}\right)-\lambda\frac{q^\alpha q^\beta}{m^2}\right]\right.\\
&\quad\left.+(1+\kappa+\lambda)\left(g^{\alpha\mu}q^\beta - g^{\beta\mu}q^\alpha\right)\right\},
\end{aligned} \tag{C.38}$$

where both W bosons are considered to be on-shell. The first term in equation (C.38) disappears in the Breit-frame.

With equations (C.32) and (C.35) we get for the magnetic dipole moment:

$$\mu = \frac{\langle 1\,1|1\,0\,1\,1\rangle}{\langle 1\,0|1\,-1\;\;1\,1\rangle}\frac{1}{q}(-1)\frac{e}{2E}\Gamma^{-}_{0+}, \tag{C.39}$$

where Γ^{-}_{0+} can be determined with equation (C.37) to

$$\Gamma^{-}_{0+} = -\frac{2Ep(1+\kappa+\lambda)}{m}. \tag{C.40}$$

This leads to the final expression for the anomalous magnetic moment:

$$\mu = \frac{e}{2m}(1+\kappa+\lambda). \tag{C.41}$$

C.3 The Electric Quadrupole Moment of the W Boson

The non-relativistic electrical quadrupole moment is defined by:

$$\begin{aligned} Q &= \int\langle s\,s|(3z^3 - r^2)\rho(\vec{x})|s\,s\rangle \mathrm{d}^3x \\ &= 2\int\langle s\,s|r^2\rho(\vec{x})P_2(\cos\Theta)|s\,s\rangle \mathrm{d}^3x, \end{aligned} \tag{C.42}$$

with $\rho(\vec{x})$ being the charge density J^0. P_2 is the Legendre polynom. Equation (C.42) must be compared with a relativistic expression for the quadrupole moment.

To achieve this, we split up the vertex function (C.34) in tensors Q_J:

$$\Gamma^0_{s'\lambda';s\lambda} = (-1)^{2s'}\sum_{J=0}^{\infty}\begin{pmatrix} s' & J & s \\ \lambda' & 0 & \lambda \end{pmatrix} Q_J(s',s). \tag{C.43}$$

The introduced tensors Q_J can be compared with the multipole moments of the W boson. The tensors Q_J differ from each other by their behavior under rotations. They transform like the spheric harmonics $Y_{J,0}$ and form a complete base, so that the decomposition (C.43) is unique. The Wigner $3j$-symbols can be calculated with the Clebsch-Gordan coefficients by the relation:

$$\begin{pmatrix} j_1 & j_2 & j_3 \\ m_1 & m_2 & m_3 \end{pmatrix} = \frac{(-1)^{j_1-j_2-m_3}}{\sqrt{2j_3+1}}\langle j_1 m_1 j_2 m_2|j_3 - m_3\rangle. \tag{C.44}$$

After applying (C.43) on equation (C.34), we get:

$$\Gamma^0_{h'h} = \begin{pmatrix} 1 & 0 & 1 \\ h' & 0 & h \end{pmatrix} Q_0 + \begin{pmatrix} 1 & 2 & 1 \\ h' & 0 & h \end{pmatrix} Q_2. \tag{C.45}$$

Higher multipole moments do not contribute to $\Gamma^0_{h'h}$, since the Wigner $3j$ symbols vanish for $J > 2$.

With

$$\Gamma^0_{0\,0} = -2E\left[G_1 + \frac{2p^2}{m^2}\left(G_1 - g + \frac{2\lambda E^2}{m^2}\right)\right] \tag{C.46}$$

and

$$\Gamma^0_{-+} = 2EG_1, \tag{C.47}$$

from (C.38), equation (C.45) can be solved for Q_0 and Q_2.

With the abbreviations

$$G_1 = 1 - 2\lambda\frac{p^2}{m^2} \tag{C.48}$$

and

$$g = 1 + \kappa + \lambda, \tag{C.49}$$

it follows that

$$\begin{aligned} Q_2 &= -\sqrt{\frac{10}{3}}4E\frac{p^2}{m^2}\left(G_1 - g + 2\lambda\frac{e^2}{m^2}\right) \\ &= -\sqrt{\frac{10}{3}}E\frac{q^2}{m^2}(\lambda - \kappa). \end{aligned} \tag{C.50}$$

With the expansion of the exponential factor in (C.34)

$$e^{-i\vec{q}\cdot\vec{r}} = e^{-qr\cos\Theta} = \sum_{J=0}^{\infty}(-i)^J(2J+1)j_J(qr)P_J(\cos\Theta) \tag{C.51}$$

the right hand side of (C.34) is

$$(-1)^{1+s'_z}\int\langle 1s'_z|J_0(x)|1s_z\rangle e^{-i\vec{q}\cdot\vec{x}}\mathrm{d}^3x = \begin{pmatrix} 1 & 0 & 1 \\ h' & 0 & h \end{pmatrix} Q_0^{\mathrm{NR}} + \begin{pmatrix} 1 & 2 & 1 \\ h' & 0 & h \end{pmatrix} Q_2^{\mathrm{NR}}. \tag{C.52}$$

This leads to the expressions

$$Q_J^{\mathrm{NR}}(q^2) = \frac{(2J+1)(-i)^J}{\begin{pmatrix} s & J & s \\ -s & 0 & s \end{pmatrix}}\int\langle ss|\rho(\vec{x})P_J(\cos\Theta)|ss\rangle j_J(qr)\mathrm{d}^3x \tag{C.53}$$

for the non-relativistic moments Q_0^{NR} and Q_2^{NR}. The comparison of (C.43) and Q_2^{NR} leads to

$$\frac{e}{2E}Q_2 = Q_2^{\mathrm{NR}}. \tag{C.54}$$

The expansion of the Bessel function j_2

$$j_2(qr) = \frac{q^2r^2}{15} \tag{C.55}$$

allows a direct comparison of Q and Q_2^{NR}

$$Q = -\sqrt{\frac{6}{5}}\frac{1}{q^2}Q_2^{\mathrm{NR}}. \tag{C.56}$$

With (C.50) and (C.54) it follows immediately

$$Q = -\frac{e}{m^2}(\kappa - \lambda). \tag{C.57}$$

Appendix D

GENTLE v. 2.02

For the calculations in chapter 4, the version 2.02 of the Fortran program GENTLE was used. This appendix gives a brief introduction into the program. A more detailed description can be found in reference [124], where GENTLE v. 2.0 is described. New features in version 2.02, added after version 2.0, are illustrated in section D.2. GENTLE v. 2.02 has now about 9100 lines of code.

D.1 Description of the Program

The Fortran program GENTLE allows to calculate the total and differential cross-sections for four-fermion production processes in e^+e^- annihilation. This is achieved by a semi-analytic calculation, where analytical expressions for the Muta cross-sections $\mathrm{d}\sigma/\mathrm{d}s_1\mathrm{d}s_2$, respective $\mathrm{d}\sigma/\mathrm{d}s_1\mathrm{d}s_2\mathrm{d}\cos\theta$ are numerically integrated using an adaptive one-dimensional Simpson integration routine.

As shown in table D.1 GENTLE consists of two main branches (the CC and the NC-branch). The last column shows the publications on which the corresponding GENTLE parts are mainly based. These branches are shortly introduced in the following sections. For more details see http://www.ifh.de/~riemann/doc/Gentle/gentle.html.

CC	QED ISR total cross-section	[208]
	Background total cross-section	[131]
	Anomalous couplings	[127]
	Differential cross-section	[127]
NC	QED ISR total cross-section	[189]
	Background total cross-section	[135]
	Anomalous couplings	[191]

Table D.1: *Overview over the different branches and subbranches of* GENTLE. *Corresponding publications are given in the last column. Note, the anomalous couplings calculation in the* NC*-branch is only available in the stand-alone program ZAC [190] and is not a part of* GENTLE v. 2.02.

D.1.1 The CC-branch and Anomalous Triple Gauge Boson Couplings

The CC-branch of GENTLE allows to calculate total and differential cross-sections for the CC03 and CC11 classes, see table D.2. This branch is switched on by setting the flag IPROC = 1. The flag ICDS determines whether the total cross-section or the angular differential cross-section is supposed to be calculated. The latter option is chosen by IDCS = 1. For the CC03 class a bin-wise analytical integrated differential cross-section can be calculated with IBIN = 1. This feature does not exist for the CC11 class background. Here, only fixed points of the differential cross-section can be determined.

Electroweak radiative corrections can be controlled by the flags: IBORNF, ICOLMB, ICONVL, IQEDHS, ITNONU, IZERO, and IZETTA. Inclusive QCD corrections to the W width can be taken into account with the flag IIQCD = 1. The exact meaning of these flags is described in detail in [124].

Anomalous triple gauge boson couplings are available in the CC-branch of GENTLE. They can be switched on by the flag setting IANO = 1.

	$\bar{d}u$	$\bar{s}c$	$\bar{e}\nu_e$	$\bar{\mu}\nu_\mu$	$\bar{\tau}\nu_\tau$
$d\bar{u}$	*43*	**11**	20	**10**	**10**
$e\bar{\nu}_e$	20	20	*56*	18	18
$\mu\bar{\nu}_\mu$	**10**	**10**	18	*19*	**9**

Table D.2: *Number of diagrams in the* CC*-branch. The boldfaced entries can be calculated with* GENTLE.

D.1.2 The NC-branch

The NC-branch contains the cross-sections for classes containing the production of two Z bosons. The total cross-sections of the classes NC32, NC24, NC10, and NC06 can be

	$\bar{d}d$	$\bar{u}u$	$\bar{e}e$	$\bar{\mu}\mu$	$\bar{\nu}_e\nu_e$	$\bar{\nu}_\mu\nu_\mu$
$\bar{d}d$	4·16	*43*	48	**24**	21	**10**
$\bar{s}s, \bar{b}b$	**32**	*43*	48	**24**	21	**10**
$\bar{u}u$	*43*	4·16	48	**24**	21	**10**
$\bar{e}e$	48	48	4·36	48	*56*	20
$\bar{\mu}\mu$	**24**	**24**	48	4·12	19	*19*
$\bar{\tau}\tau$	**24**	**24**	48	**24**	19	**10**
$\bar{\nu}_e\nu_e$	21	21	*56*	19	4·9	12
$\bar{\nu}_\mu\nu_\mu$	**10**	**10**	20	*19*	12	4·3
$\bar{\nu}_\tau\nu_\tau$	**10**	**10**	20	**10**	12	**6**

Table D.3: *Number of diagrams in the* NC*-branch. The boldfaced entries can be calculated with* GENTLE.

calculated [135], see table D.3.

Although the Fortran program `ZAC` belongs in principle into the `NC`-branch it is only available as a stand-alone version due to historical reasons.

D.2 New Features

The most complex change after version 2.0 was the inclusion of the differential cross-section to the complete `CC11` class. Also anomalous couplings are considered in this part in an analogous way as they were applied for the `CC03` part of `GENTLE`.

Another new feature is the possibility to use a constant, s-independent W boson width in the calculations. Especially for higher energies this should give better results, since gauge invariance is not destroyed by this choice. For a more detailed discussion of this problem, see [116, 166, 167].

Appendix E

A Sample FORM File

FORM is a program by J. Vermaseren [6] to perform analytical calculations. The full FORM file used for the calculation of the CC11 cross-section has about 500 lines of text and is too long to be shown completely. To illustrate the calculation, extracts are presented and explained.

The file begins with the declaration of some variables:

```
*  Calculation of CC11 with anomalous couplings
S a,tmp,GZ,XZ,YZ,ZZ,GZ2,XZ2,YZ2,ZZ2,ssa,sta,sua,sda;

⋮

S g012,g034,g12,g34,pr10,pr20,pr12,pr30,pr40,pr34;
i al,be,ga,ka,si,mu,nu,rho;
S MW2;
```

The three vertical dots indicate that lines were omitted. After the declaration of the symbols, matrix elements and their charged conjugates are defined:

```
g schnl = vc(1,k2)*V1(al)*u(1,k1)*V3(k,ss2,ss1,al,be,ga)*
          uc(2,p3)*V2p(be)*v(2,p4)*uc(3,p1)*V2(ga)*v(3,p2);
*
g tchnl = vc(1,k2)*V2pp(be)*pe*V2pp(ga)*u(1,k1)*
          uc(2,p3)*V2p(be)*v(2,p4)*uc(3,p1)*V2(ga)*v(3,p2);
*
g udeer1 = vc(1,k2)*V1(al)*u(1,k1)*uc(3,p1)*V2(ga)*pu1*V1pp(al)*
           v(3,p2)*uc(2,p3)*V2p(ga)*v(2,p4);

⋮

g schnlc = uc(1,k1)*V1c(mu)*v(1,k2)*V3c(k,ss2,ss1,mu,nu,rho)*
vc(2,p4)*V2pc(nu)*u(2,p3)*vc(3,p2)*V2c(rho)*u(3,p1);

⋮
```

```
g ddeer2c = uc(1,k1)*V1c(mu)*v(1,k2)*vc(2,p4)*V1pc(mu)*
pd2*V2pc(rho)*u(2,p3)*vc(3,p2)*V2c(rho)*u(3,p1);
```

Altogether six amplitudes and their charge conjugates must be defined. The particle momenta are denoted in the same way as in chapter 4. The vertices are introduced as functions and given below:

```
* all momenta are outgoing
id V3(p1?,p2?,p3?,al?,be?,ga?)=GZ*(d_(ga,be)*(p3(al)-p2(al))
        +d_(al,be)*(p2(ga)-p1(ga))+d_(al,ga)*(p1(be)-p3(be)))
        +XZ*(d_(al,ga)*p1(be)-d_(al,be)*p1(ga))
        +YZ/MW2*(p2(ga)*p1(be)*p3(al)-p2(al)*p1(ga)*p3(be)
           + p1.p2*(d_(al,ga)*p3(be)-d_(ga,be)*p3(al))
           + p1.p3*(d_(ga,be)*p2(al)-d_(al,be)*p2(ga))
           + p2.p3*(d_(al,be)*p1(ga)-d_(al,ga)*p1(be)))
        +ZZ/MW2*(e_(al,ga,ka,si)*p1(be)-e_(al,be,ka,si)*p1(ga))*
          p1(ka)*(p2(si)-p3(si));
*
id V3c(p1?,p2?,p3?,al?,be?,ga?)=GZ*(d_(ga,be)*(p3(al)-p2(al))
        +d_(al,be)*(p2(ga)-p1(ga))+d_(al,ga)*(p1(be)-p3(be)))
        +XZ*(d_(al,ga)*p1(be)-d_(al,be)*p1(ga))
        +YZ/MW2*(p2(ga)*p1(be)*p3(al)-p2(al)*p1(ga)*p3(be)
           + p1.p2*(d_(al,ga)*p3(be)-d_(ga,be)*p3(al))
           + p1.p3*(d_(ga,be)*p2(al)-d_(al,be)*p2(ga))
           + p2.p3*(d_(al,be)*p1(ga)-d_(al,ga)*p1(be)))
        -ZZ/MW2*(e_(al,ga,ka,si)*p1(be)-e_(al,be,ka,si)*p1(ga))*
          p1(ka)*(p2(si)-p3(si));
*
* couplings of the Z boson:
id V1(al?)=g_(1,al)*(RZe*g7_(1)+LZe*g6_(1));
al V1c(al?)=g_(1,al)*(RZce*g7_(1)+LZce*g6_(1));
al V1p(al?)=g_(2,al)*(RZ2*g7_(2)+LZ2*g6_(2));
al V1pc(al?)=g_(2,al)*(RZc2*g7_(2)+LZc2*g6_(2));
al V1pp(al?)=g_(3,al)*(RZ1*g7_(3)+LZ1*g6_(3));
al V1ppc(al?)=g_(3,al)*(RZ1*g7_(3)+LZ1*g6_(3));
*
* couplings of the W boson:
*
al V2(al?)=g_(3,al)*g6_(3);
al V2c(al?)=g_(3,al)*g6_(3);
al V2p(al?)=g_(2,al)*g6_(2);
al V2pc(al?)=g_(2,al)*g6_(2);
al V2pp(al?)=g_(1,al)*g6_(1);
al V2ppc(al?)=g_(1,al)*g6_(1);
```

The next step is to include the fermion propagators and define the squared amplitudes. Twenty-one functions are needed to describe all squared amplitudes.

```
id pe=1/pes*g_(1,tp);
al pu1=1/pus1*g_(3,up1);
al pu2=1/pus2*g_(2,up2);
al pd1=1/pds1*g_(3,dp1);
al pd2=1/pds2*g_(2,dp2);
.sort
g ssg   =  9/16384*schnl*schnlc;
g stg   =  9/8192*(tchnl*schnlc+schnl*tchnlc);

⋮

g d2d2g =  9/16384*ddeer2*ddeer2c;
.sort
```

The normalization in `ssg` and the other functions is chosen in such a way that the G-functions in chapter 4 are produced.

After the construction of the squared matrix elements we can start with the phase space integration. First, the number of terms is reduced by renaming the couplings.

```
s CPe,CMe;
id LZc2=LZ2;
al RZce=RZe;
al LZce=LZe;
id LZe^2=(CPe/2+CMe/2);
id RZe^2=(CPe/2-CMe/2);
.sort
```

Then the spinors are expressed by γ-matrices and the traces are calculated.

```
id u(1,p1?)=1;
al uc(1,p1?)=g_(1,p1);

⋮

al v(3,p1?)=1;
al vc(3,p1?)=g_(3,p1);
.sort
trace4,3;
trace4,2;
trace4,1;
```

The phase space integrations are prepared by successively substituting the components of the momenta with the expressions derived in appendix B.1 and using relations between the momenta.

```
id tp=(k1-p1-p2);
al up1=k1+k2-p2;
al up2=p3-k1-k2;
```

```
al dp1=p1-k1-k2;
al dp2=k1+k2-p4;
contract 0 ;
id k1.k1=0;
al k2.k2=0;
al p1.p1=0;
al p2.p2=0;
al p3.p3=0;
al p4.p4=0;
.sort
id p1.p3=p10*p30-p13*p33-p1t*p3t*sth1*sth2*(cphi1*cphi2+sphi1*sphi2);
```

⋮

Now, the integration over ϕ_2 can be carried out: ⋮

```
id sphi2^2=1-cphi2^2;
id sphi2=0;
al cphi2^5=0;
id cphi2^4=3/8;
id cphi2^3=0;
al cphi2^2=1/2;
id cphi2=0;
```

The integration over ϕ_1 is performed in the same way:

```
id k1.p1=k10*p10-k13*p13-k11*p1t*sth1*cphi1;
al k1.p2=k10*p20-k13*p23+k11*p1t*sth1*cphi1;
al k2.p1=k10*p10+k13*p13+k11*p1t*sth1*cphi1;
al k2.p2=k10*p20+k13*p23-k11*p1t*sth1*cphi1;
.sort
id sphi1^2=1-cphi1^2;
b sphi1,cphi1;
id sphi1=0;
al cphi1^5=0;
id cphi1^4=3/8;
id cphi1^3=0;
id cphi1^2=1/2;
id cphi1=0;
```

The integration over θ_1 and θ_2 require a little bit more preparation, because of the fermion propagators in the background diagrams. The various propagator terms have to be separated from each other.

```
id p10=g012*pr10+g12*pr12*cth1;
al p13=g012*pr12*cth1+g12*pr10;
al p20=g012*pr20-g12*pr12*cth1;
al p23=-g012*pr12*cth1+g12*pr20;
```

```
.sort
id pus1^-1*pds1^-1=1/sca1*(pus1^-1+pds1^-1);
id sth1^2=1-cth1^2;
Repeat;
id cth1*pds1^-1=-1*(s12-s-s34+2*pds1)/slam/pds1;
al cth1*pus1^-1=(s12-s-s34+2*pus1)/slam/pus1;
Endrepeat;
.sort
id sth1=0;
id pus1^-2=1/s/s34;
al pds1^-2=1/s/s34;
id pus1^-1=-1*Log1;
id pds1^-1=-1*Log1;
id cth1^5=0;
id cth1^4=1/5;
id cth1^3=0;
id cth1^2=1/3;
id cth1=0;
.sort
id p30=g034*pr30-g34*pr34*cth2;
al p33=g034*pr34*cth2-g34*pr30;
al p40=g034*pr40+g34*pr34*cth2;
al p43=-g034*pr34*cth2-g34*pr40;
.sort
id pus2^-1*pds2^-1=1/sca2*(pus2^-1+pds2^-1);
id sth2^2=1-cth2^2;
Repeat;
id cth2*pus2^-1=+1*(s34-s-s12+2*pus2)/slam/pus2;
al cth2*pds2^-1=-1*(s34-s-s12+2*pds2)/slam/pds2;
Endrepeat;
id pus2^-2=1/s/s12;
al pds2^-2=1/s/s12;
id pus2^-1=-1*Log2;
al pds2^-1=-1*Log2;
id cth2^5=0;
id cth2^4=1/5;
id cth2^3=0;
id cth2^2=1/3;
id cth2=0;
```

After the four integrations we have to simplify the result. First we replace all auxiliary variables by invariant expressions like s_1 and s_2 and by the scattering angle θ. This process is simple, so we do not reproduce it here. Our result can be further simplified by extracting factors of λ:

```
multiply slam^6*[ALAM-3];
```

```
id slam^2=s^2+s12^2+s34^2-2*s*s12-2*s*s34-2*s12*s34;
.sort
id   s^8=  s^6*(slam^2-s12^2-s34^2+2*s*s12+2*s*s34+2*s12*s34);
id s12^8=s12^6*(slam^2-s^2-s34^2+2*s*s12+2*s*s34+2*s12*s34);

⋮

id   s^4=  s^2*(slam^2-s12^2-s34^2+2*s*s12+2*s*s34+2*s12*s34);
id s12^4=s12^2*(slam^2-s^2-s34^2+2*s*s12+2*s*s34+2*s12*s34);
id s34^4=s34^2*(slam^2-s^2-s12^2+2*s*s12+2*s*s34+2*s12*s34);
.sort
id s^4=s^2*(slam^2-s12^2-s34^2+2*s*s12+2*s*s34+2*s12*s34);
b [ALAM-3],[ALAM-2],[ALAM-1],[3-costh^2],slam,sinth,costh,pes,pus1,pus2,
pds1,pds2,CPe,CMe,RZe,LZe,Log1,LZ1,Log2,LZ2,XZ,GZ,YZ,ZZ;
print;
.end
```

The now produced output can be used for further simplifications by hand, as was done to get the results on the differential cross-section presented in chapter 4. For the calculation of the total cross-section and for explicit cross-checks with the results in reference [135] the integration over θ is performed and a comparison with the function in [135] is made[1]:

```
id pes^-2=1/s12/s34;
id pes^-1=Log;
id costh^9=0;
id costh^8=1/9;
id costh^7=0;
id costh^6=1/7;
id costh^5=0;
id costh^4=1/5;
id costh^3=0;
id costh^2=1/3;
id costh=0;
.sort
s scas;
f gff,g3f,gud,guu,gnc2,gnc24,gdu,g33;
.global
* comparison with published data:
*
g sd1c= slam^4*(sd1g-g3f(s12,s,s34,Log1));
*
* this is function (2.3) of the Bardin/Riemann article
*
id g3f(s?,s12?,s34?,Log?)=1/48*((s-s12-s34)*(slam^2+12*
```

[1]The comparison is only demonstrated for one interference. Of course also the other functions were checked successfully.

```
        (s*s12+s12*s34+s*s34))-24*(s*s12+s12*s34+s*s34)*
s12*s34*Log);
*
id Log1/scas=1/sca1*Log1;
al Log2/scas=1/sca2*Log2;
id sca1=(s12-s-s34);
al sca2=s34-s-s12;
id slam^2=s^2+s12^2+s34^2-2*s*s12-2*s*s34-2*s12*s34;
id CPe=2;
id LZ1=1;
id GZ=1;
id XZ=0;
id YZ=0;
id ZZ=0;
b slam,Log,Log1,Log2,sca1,sca2;
print sd1c;
.end
```

Bibliography

[1] S. Weinberg, *Phys. Rev. Lett.* **19** (1967) 1264.

[2] A. Salam, "Weak and Electromagnetic Interactions", in *Proc. of the Nobel Symposium, 1968, Lerum, Sweden* (N. Svartholm, ed.), p. 367, Almqvist and Wiksell, Stockholm, 1968.

[3] S. L. Glashow, *Nucl. Phys.* **22** (1961) 579.

[4] D. E. Groom *et al.*, *Eur. Phys. J.* **C15** (2000) 1.

[5] Super-Kamiokande Collaboration, Y. Fukuda *et al.*, *Phys. Rev. Lett.* **81** (1998) 1562–1567.

[6] J. A. M. Vermaseren, "Symbolic Manipulation with `FORM`" (Computer Algebra Nederland, Amsterdam, 1991).

[7] C. Itzykson and J. B. Zuber, *"Quantum Field Theory"*. McGraw-Hill, 1980.

[8] Becher, Böhm, and Joos, *"Eichtheorien der starken und elektroschwachen Wechselwirkung"*. Teubner Studienbücher, 1981.

[9] D. Ebert, *"Eichtheorien: Grundlage der Elementarteilchenphysik"*. VCH Verlagsgesellschaft, Weinheim, Germany, 1989.

[10] O. Nachtmann, *"Elementary Particle Physics: Concepts and Phenomena"*. Springer, Berlin, Germany, 1990.

[11] S. Weinberg, *"The Quantum Theory of Fields"*, vol. I. University of Cambridge, Cambridge, USA, 1995.

[12] S. Weinberg, *"The Quantum Theory of Fields"*, vol. II. University of Cambridge, Cambridge, USA, 1996.

[13] J. C. Maxwell, *"Treatise on Electricity and Magnetism"*, 3$^{\rm rd}$ edition (1891), 2 vols., reprint by Dover, New York (1964).

[14] P. A. M. Dirac, *Proc. Roy. Soc.* **A114** (1927) 243.

[15] P. A. M. Dirac, *Proc. Roy. Soc.* **A117** (1928) 610.

[16] J. Schwinger, *Phys. Rev.* **73** (1947) 416.

[17] H. Becquerel, *C.R. Acad. Sci. (Paris)* **122** (1896) 501.

[18] E. Fermi, *Z. Phys.* **88** (1934) 161.

[19] H. Yukawa, *Proc. Phys. Math. Soc. Jap.* **17** (1935) 48.

[20] R. L. Mößbauer, "History of Neutrino Physics: Pauli's Letters", in *Proc. of Ringberg Workshop on Neutrino Astrophysics, 20–24 Oct. 1997, Tegernsee, Germany* (M. Altmann, W. Hillebrandt, H.-T. Janka, and G. Raffelt, eds.), p. 3, München, 1998.

[21] F. Reines and C. L. Cowan, *Phys. Rev.* **92** (1953) 830.

[22] C. L. Cowan, F. Reines, F. B. Harrison, H. W. Kruse, and A. D. McGuire. In W. Kropp (ed.) et al.: "Neutrinos and other matters", 57.

[23] F. Reines and C. L. Cowan, *Phys. Rev.* **113** (1959) 273.

[24] S. H. Neddermeyer and C. D. Anderson, *Phys. Rev.* **51** (1937) 884.

[25] J. C. Street and E. C. Stevenson, *Phys. Rev.* **52** (1937) 1003.

[26] C. M. G. Lattes, H. Muirhead, G. P. S. Occhialini, and C. F. Powell, *Nature* **159** (1947) 694.

[27] G. D. Rochester and C. C. Butler, *Nature* **160** (1947) 855.

[28] C. S. Wu, E. Ambler, R. W. Hayward, D. D. Hoppes, and R. P. Hudson, *Phys. Rev.* **105** (1957) 1413.

[29] L. Landau, *JETP* **32** (1956) 405.

[30] A. Salam, *Nuovo Cim.* **5** (1957) 299.

[31] C. N. Yang and R. L. Mills, *Phys. Rev.* **96** (1954) 191.

[32] Y. Nambu and G. Jona-Lasinio, *Phys. Rev.* **122** (1961) 345.

[33] Y. Nambu and G. Jona-Lasinio, *Phys. Rev.* **124** (1961) 246.

[34] J. Goldstone, *Nuovo Cim.* **19** (1961) 154.

[35] P. W. Higgs, *Phys. Lett.* **12** (1964) 132.

[36] P. W. Higgs, *Phys. Rev. Lett.* **13** (1964) 508.

[37] F. Englert and R. Brout, *Phys. Rev. Lett.* **13** (1964) 321.

[38] M. Veltman, *Nucl. Phys.* **B7** (1968) 637–650.

[39] G. 't Hooft, *Nucl. Phys.* **B33** (1971) 173.

[40] G. 't Hooft, *Nucl. Phys.* **B35** (1971) 167.

[41] G. 't Hooft and M. Veltman, *Nucl. Phys.* **B44** (1972) 189–213.

[42] G. 't Hooft and M. Veltman, *Nucl. Phys.* **B50** (1972) 318–353.

[43] M. Gell-Mann, *Phys. Lett.* **8** (1964) 214.

[44] M. Gell-Mann, *Phys. Rev. Lett.* **12** (1964) 155.

[45] G. Zweig, "An SU(3) Model for strong interaction symmetry and its breaking. 2", CERN preprint CERN-TH-412 (1964).

[46] S. L. Glashow, J. Iliopoulos, and L. Maiani, *Phys. Rev.* **D2** (1970) 1285.

[47] J. J. Aubert *et al.*, *Phys. Rev. Lett.* **33** (1974) 1404.

[48] J. E. Augustin *et al.*, *Phys. Rev. Lett.* **33** (1974) 1406.

[49] E. G. Cazzoli *et al.*, *Phys. Rev. Lett.* **34** (1975) 1125.

[50] G. Goldhaber *et al.*, *Phys. Rev. Lett.* **37** (1976) 255.

[51] Gargamelle Neutrino Collaboration, F. J. Hasert *et al.*, *Phys. Lett.* **B46** (1973) 138.

[52] Gargamelle Neutrino Collaboration, F. J. Hasert *et al.*, *Nucl. Phys.* **B73** (1974) 1.

[53] M. Kobayashi and T. Maskawa, *Prog. Theor. Phys.* **49** (1973) 652.

[54] J. H. Christenson, J. W. Cronin, V. L. Fitch, and R. Turlay, *Phys. Rev. Lett.* **13** (1964) 138.

[55] M. L. Perl *et al.*, *Phys. Rev. Lett.* **35** (1975) 1489.

[56] M. L. Perl *et al.*, *Phys. Lett.* **63B** (1976) 466.

[57] S. W. Herb *et al.*, *Phys. Rev. Lett.* **39** (1977) 252.

[58] CDF Collaboration, F. Abe *et al.*, *Phys. Rev.* **D50** (1994) 2966.

[59] Fermilab Press Release: "Physicists Find First Direct Evidence for Tau Neutrino at Fermilab", `http://www.fnal.gov/directorate/public_affairs/press_releases/donut.html`.

[60] G. Arnison *et al.*, *Phys. Lett.* **122 B** (1983) 103.

[61] P. Bagnaia *et al.*, *Phys. Lett.* **129 B** (1983) 130.

[62] K. Nishijima, *Prog. Theor. Phys.* **13** (1955) 285.

[63] K. Fujikawa, B. W. Lee, and A. I. Sanda, *Phys. Rev.* **D6** (1972) 2923.

[64] L. D. Faddeev and V. N. Popov, *Phys. Lett.* **25B** (1967) 29.

[65] D. V. Volkov and V. P. Akulov, *Phys. Lett.* **B46** (1973) 109.

[66] J. Wess and B. Zumino, *Nucl. Phys.* **B70** (1974) 39.

[67] M. B. Green, J. H. Schwarz, and E. Witten, *Superstring theory, vol. 1 and vol. 2.* Univ. Pr., Cambridge, Uk, 1987.

[68] D. Lüst and S. Theisen, Berlin, Germany: Springer (1989) 346 p. (Lecture notes in physics, 346).

[69] S. L. Adler, *Phys. Rev.* **177** (1969) 2426–2438.

[70] J. S. Bell and R. Jackiw, *Nuovo Cim.* **A60** (1969) 47–61.

[71] C. Bouchiat, J. Iliopoulos, and P. Meyer, *Phys. Lett.* **B38** (1972) 519.

[72] H. Georgi and S. L. Glashow, *Phys. Rev. Lett.* **32** (1974) 438.

[73] G. G. Ross, *Grand Unified Theories.* Benjamin/Cummings, Reading, USA, 1984.

[74] F. Jegerlehner, "The 'Ether world' and elementary particles", talk at *31st International Ahrenshoop Symposium On The Theory Of Elementary Particles, 2–6 Sep 1997, Buckow, Germany* (H. Dorn, D. Lüst, G. Weigt, eds.), p. 386, Berlin, 1998.

[75] L. Susskind, *Phys. Rev.* **D20** (1979) 2619.

[76] S. Weinberg, *Phys. Rev.* **D19** (1979) 1277.

[77] S. Dimopoulos and L. Susskind, *Nucl. Phys.* **B155** (1979) 237.

[78] B. Holdom, *Phys. Lett.* **150B** (1985) 301.

[79] K. Yamawaki, M. Bando, and K. Matumoto, *Phys. Rev. Lett.* **56** (1986) 1335.

[80] T. W. Appelquist, D. Karabali, and L. C. R. Wijewardhana, *Phys. Rev. Lett.* **57** (1986) 957.

[81] T. Appelquist and L. C. R. Wijewardhana, *Phys. Rev.* **D35** (1987) 774.

[82] I. D'Souza and C. Kalman, *"Preons: Models of leptons, quarks and gauge bosons as composite objects"*. World Scientific, Singapore, Singapore, 1992.

[83] T. Appelquist, J. Terning, and L. C. R. Wijewardhana, *Phys. Rev. Lett.* **79** (1997) 2767.

[84] K. J. F. Gaemers and G. J. Gounaris, *Z. Phys.* **C1** (1979) 259.

[85] K. Hagiwara, R. D. Peccei, D. Zeppenfeld, and K. Hikasa, *Nucl. Phys.* **B282** (1987) 253.

[86] G. Gounaris *et al.*, "Triple gauge boson couplings", in *Physics at LEP2,* CERN 96–01 (1996) (G. Altarelli, T. Sjöstrand, and F. Zwirner, eds.), p. 525.

[87] M. Kuroda, F. M. Renard, and D. Schildknecht, *Phys. Lett.* **B183** (1987) 366.

[88] A. D. Rujula, M. B. Gavela, P. Hernandez, and E. Massó, *Nucl. Phys.* **B384** (1992) 3.

[89] K. Hagiwara, S. Ishihara, R. Szalapski, and D. Zeppenfeld, *Phys. Lett.* **B283** (1992) 353.

[90] K. Hagiwara, S. Ishihara, R. Szalapski, and D. Zeppenfeld, *Phys. Rev.* **D48** (1993) 2182.

[91] G. J. Gounaris and F. M. Renard, *Z. Phys.* **C59** (1993) 133.

[92] W. Buchmüller and D. Wyler, *Nucl. Phys.* **B268** (1986) 621.

[93] W. Buchmüller, B. Lampe, and N. Vlachos, *Phys. Lett.* **197B** (1987) 379.

[94] C. N. Leung, S. T. Love, and S. Rao, *Z. Phys.* **C31** (1986) 433.

[95] C. J. C. Burges and H. J. Schnitzer, *Nucl. Phys.* **B228** (1983) 464.

[96] A. Manohar and H. Georgi, *Nucl. Phys.* **B234** (1984) 189.

[97] C. Caso *et al.*, *Eur. Phys. J.* **C3** (1998) 1.

[98] M. L. Perl, *Rept. Prog. Phys.* **55** (1992) 653.

[99] S. Gentile and M. Pohl, *Phys. Rept.* **274** (1996) 287.

[100] CDF Collaboration, M. Gallinaro, *Nucl. Phys. Proc. Suppl.* **65** (1998) 147.

[101] G. Rahal-Callot, *Int. J. Mod. Phys.* **A13** (1998) 695.

[102] M. A. Samuel, G. Li, and R. Mendel, *Phys. Rev. Lett.* **67** (1991) 668.

[103] D. J. Silverman and G. L. Shaw, *Phys. Rev.* **D27** (1983) 1196.

[104] R. Escribano and E. Masso, *Phys. Lett.* **B395** (1997) 369.

[105] J. A. Grifols and A. Mendez, *Phys. Lett.* **B255** (1991) 611.

[106] OPAL Collaboration, K. Ackerstaff *et al.*, *Phys. Lett.* **B431** (1998) 188.

[107] L3 Collaboration, M. Acciarri *et al.*, *Phys. Lett.* **B434** (1998) 169.

[108] P. A. Baikov *et al.*, "Physical results by means of CompHEP", in Proc. of X Workshop on High Energy Physics and Quantum Field Theory (QFTHEP-95), 1996, Moscow, Russia (B. Levtchenk and V. Savrin, eds.), p. 101, `hep-ph/9701412`.

[109] E. E. Boos, M. N. Dubinin, V. A. Ilin, A. E. Pukhov, and V. I. Savrin, "Comphep: Specialized package for automatic calculations of elementary particle decays and collisions", preprint INP MSU - 94 - 36/358 (1994), `hep-ph/9503280`.

[110] D. Bardin *et al.*, *Nucl. Phys.* **B351** (1991) 1.

[111] R. Escribano and E. Masso, *Phys. Lett.* **B301** (1993) 419.

[112] J. Biebel and T. Riemann, *Z. Phys.* **C76** (1997) 53.

[113] `Anotau` is available at `http://www.ifh.de/~riemann/Anotau/anotau.html`.

[114] S. S. Gau, T. Paul, J. Swain, and L. Taylor, *Nucl. Phys.* **B523** (1998) 439.

[115] T. Paul and Z. Was, "Inclusion of τ anomalous magnetic and electric dipole moments in the KORALZ Monte Carlo", CERN preprint L3-Note-2184 (1998), `hep-ph/9801301`.

[116] W. Beenakker *et al.*, "WW cross-sections and distributions", in *Physics at LEP2,* CERN 96–01 (1996) (G. Altarelli, T. Sjöstrand, and F. Zwirner, eds.), p. 79.

[117] Z. Kunszt *et al.*, "Determination of the mass of the W boson", in *Physics at LEP2,* CERN 96–01 (1996) (G. Altarelli, T. Sjöstrand, and F. Zwirner, eds.), p. 141, `hep-ph/9602352`.

[118] F. Boudjema *et al.*, "Standard model processes", in *Physics at LEP2,* CERN 96–01 (1996) (G. Altarelli, T. Sjöstrand, and F. Zwirner, eds.), p. 79, `hep-ph/9601224`.

[119] V. Flambaum, I. Khriplovich, and O. Sushkov, *Sov. J. Nucl. Phys.* **20** (1975) 537.

[120] W. Alles, C. Boyer, and A. J. Buras, *Nucl. Phys.* **B119** (1977) 125.

[121] Y.-S. Tsai and A. C. Hearn, *Phys. Rev.* **140** (1965) B721.

[122] T. Muta, R. Najima, and S. Wakaizumi, *Mod. Phys. Lett.* **A1** (1986) 203.

[123] D. Bardin, M. Bilenky, D. Lehner, A. Olchevski, and T. Riemann, *Nucl. Phys. (Proc. Suppl.) 37B* (1994) 148.

[124] D. Bardin, J. Biebel, D. Lehner, A. Leike, A. Olchevski, and T. Riemann, *Comput. Phys. Commun.* **104** (1997) 161.
`GENTLE` is available at `http://www.ifh.de/~riemann/doc/Gentle/gentle.html`.

[125] J. Biebel, "Four fermion production with anomalous couplings at LEP-2 and NLC", in Proc. of the *XIIth International Workshop on High Energy Physics and Quantum Field Theory, 4–10 Sept 1997, Samara, Russia*, (B. Levtchenko, ed.) p. 220, `hep-ph/9711439`.

[126] J. Biebel and T. Riemann, "Semianalytic predictions for W pair production at 500 GeV", in Proc. of *ECFA/DESY Study on Physics and Detectors for the Linear Collider*, DESY 97-123E, (R. Settles, ed.), p. 139, `hep-ph/9709207`.

[127] J. Biebel and T. Riemann, *Eur. Phys. J.* **C8** (1999) 655.

[128] J. Biebel, *Acta Phys. Polon.* **B29** (1998) 2839.

[129] L3 Collaboration, M. Acciarri *et al.*, *Phys. Lett.* **B407** (1997) 419.

[130] L3 Collaboration, M. Acciarri *et al.*, *Phys. Lett.* **B398** (1997) 223.

[131] D. Bardin and T. Riemann, *Nucl. Phys.* **B462** (1996) 3.

[132] A. Leike, "Semianalytic distributions in four fermion neutral current processes", in *Proc. of Int. Workshop on Perspectives for Electroweak Interactions in e^+e^- Collisions, 5–8 Feb. 1995, Tegernsee, Germany* (B. Kniehl, ed.), p. 121, World Scientific, Singapore, 1995.

[133] V. Baĭer, V. Fadin, and V. Khoze, *Sov. J. Nucl. Phys.* **23** (1966) 104.

[134] M. Cvetič and P. Langacker, *Phys. Rev.* **D46** (1992) 4943. E:ibid. **D48** (1993) 4484.

[135] D. Bardin, A. Leike, and T. Riemann, *Phys. Lett.* **B344** (1995) 383.

[136] C. L. Bilchak and J. D. Stroughair, *Phys. Rev.* **D30** (1984) 1881.

[137] F. Jegerlehner, *Nucl. Phys. (Proc. Suppl.) 37B* (1994) 129.

[138] A. M. H. ar Rashid and K. S. Islam, *Int. J. Mod. Phys.* **A9** (1994) 2783.

[139] M. Diehl and O. Nachtmann, *Z. Phys.* **C62** (1994) 397.

[140] H. Aronson, *Phys. Rev.* **186** (1969) 1434.

[141] T. Yasuda, "Tevatron results on gauge boson couplings", talk at *12th Workshop on Hadron Collider Physics (HCP 97), 5–11 June 1997, Stony Brook, NY*, FNAL preprint FERMILAB-Conf-97/206-E, `hep-ex/9706015`.

[142] R. Clare, *Acta Phys. Polon.* **B29** (1998) 2667.

[143] D. Bardin, S. Riemann, and T. Riemann, *Z. Phys.* **C32** (1986) 121.

[144] F. Jegerlehner, *Z. Phys.* **C32** (1986) 425; E: ibid., **C38** (1988) 519.

[145] W. Beenakker, F. Berends, M. Böhm, A. Denner, H. Kuijf, and T. Sack, *Nucl. Phys.* **B304** (1988) 463.

[146] J. Fleischer, F. Jegerlehner, and M. Zralek, *Z. Phys.* **C42** (1989) 409.

[147] A. Denner and T. Sack, *Z. Phys.* **C46** (1990) 653.

[148] W. Beenakker, K. Kolodziej, and T. Sack, *Phys. Lett.* **B258** (1991) 469.

[149] S. Dittmaier, M. Böhm, and A. Denner, *Nucl. Phys.* **B376** (1992) 29.

[150] J. Fleischer, K. Kolodziej, and F. Jegerlehner, *Phys. Rev.* **D47** (1993) 830.

[151] D. Bardin, W. Beenakker, and A. Denner, *Phys. Lett.* **B317** (1993) 213.

[152] W. Beenakker, A. P. Chapovsky, and F. A. Berends, *Phys. Lett.* **B411** (1997) 203.

[153] W. Beenakker, A. P. Chapovsky, and F. A. Berends, *Nucl. Phys.* **B508** (1997) 17.

[154] A. Denner, S. Dittmaier, and M. Roth, *Nucl. Phys.* **B519** (1998) 39.

[155] A. Denner, S. Dittmaier, and M. Roth, *Phys. Lett.* **B429** (1998) 145.

[156] G. Passarino, *Comp. Phys. Commun.* **97** (1996) 261–303.

[157] E. Accomando and A. Ballestrero, *Comput. Phys. Commun.* **99** (1997) 270–296.

[158] A. Vicini, *Acta Phys. Polon.* **B29** (1998) 2847.

[159] F. Jegerlehner and K. Kolodziej, *Eur. Phys. J.* **C12** (2000) 77.

[160] A. Denner, S. Dittmaier, M. Roth, and D. Wackeroth, *Nucl. Phys.* **B587** (2000) 67.

[161] A. Denner, S. Dittmaier, M. Roth, and D. Wackeroth, *Nucl. Phys. Proc. Suppl.* **89** (2000) 100.

[162] E. A. Kuraev and V. S. Fadin, *Sov. J. Nucl. Phys.* **41** (1985) 466.

[163] D. Bardin *et al.*, "Event generators for WW physics", in *Physics at LEP2,* CERN 96–01 (1996) (G. Altarelli, T. Sjöstrand, and F. Zwirner, eds.), vol. 2, p. 3.

[164] T. Ohl, *Acta Phys. Polon.* **B28** (1997) 847.

[165] W. Beenakker, F. A. Berends, and W. L. van Neerven, "Applications of renormalization group methods to radiative corrections", in *Proc. of Workshop on Electroweak Radiative Corrections for e^+e^- Collisions, 3–7 April 1989, Tegernsee, Germany* (J. H. Kühn, ed.), p. 3, Springer-Verlag, Berlin, 1989.

[166] E. N. Argyres *et al.*, *Phys. Lett.* **B358** (1995) 339.

[167] W. Beenakker *et al.*, *Nucl. Phys.* **B500** (1997) 255.

[168] F. A. Berends and A. I. van Sighem, *Nucl. Phys.* **B454** (1995) 467.

[169] H. Anlauf, J. Biebel, H. Dahmen, A. Himmler, P. Manakos, T. Mannel, and W. Schönau, *Comput. Phys. Commun.* **79** (1994) 487.

[170] H. Anlauf, P. Manakos, T. Ohl, and H. Dahmen, "`WOPPER`, version 1.5: A Monte Carlo event generator for $e^+e^- \to (W^+W^-) \to 4f + n\gamma$ at LEP-2 and beyond", Darmstadt preprint IKDA 96–15 (1996), `hep-ph/9605457`.

[171] F. M. Renard, *Phys. Lett.* **126B** (1983) 59.

[172] M. Claudson, E. Farhi, and R. L. Jaffe, *Phys. Rev.* **D34** (1986) 873.

[173] A. Barroso, F. Boudjema, J. Cole, and N. Dombey, *Z. Phys.* **C28** (1985) 149.

[174] G. J. Gounaris, J. Layssac, and F. M. Renard, "Off-shell structure of the anomalous Z and γ self-couplings", preprint (2000), `hep-ph/0005269`.

[175] R. W. Brown and K. O. Mikaelian, *Phys. Rev.* **D19** (1979) 922.

[176] P. Mery, M. Perrottet, and F. M. Renard, *Z. Phys.* **C38** (1988) 579.

[177] F. M. Renard, *Nucl. Phys.* **B196** (1982) 93.

[178] U. Baur and E. L. Berger, *Phys. Rev.* **D41** (1990) 1476.

[179] U. Baur and E. L. Berger, *Phys. Rev.* **D47** (1993) 4889.

[180] F. Cornet, R. Graciani, and J. I. Illana, "Bounds on the $Z\gamma\gamma$ couplings from HERA", in *Proc. of the Workshop on Future Physics at HERA, 25–26 Sep 1995, Hamburg, Germany*, (G. Ingelman, A. De Roeck, R. Klanner, eds.), vol. 1, pp. 208, DESY, Hamburg, 1996.

[181] CDF Collaboration, F. Abe *et al.*, *Phys. Rev. Lett.* **74** (1995) 1941.

[182] D0 Collaboration, S. Abachi *et al.*, *Phys. Rev. Lett.* **78** (1997) 3640.

[183] D0 Collaboration, B. Abbott *et al.*, *Phys. Rev.* **D57** (1998) 3817.

[184] L3 Collaboration, M. Acciarri *et al.*, *Phys. Lett.* **B412** (1997) 201.

[185] DELPHI Collaboration, P. Abreu *et al.*, *Phys. Lett.* **B423** (1998) 194.

[186] L3 Collaboration, M. Acciarri *et al.*, *Phys. Lett.* **B436** (1998) 187.

[187] L3 Collaboration, M. Acciarri *et al.*, *Phys. Lett.* **B450** (1999) 281.

[188] D. Bardin, A. Leike, and T. Riemann, *Phys. Lett.* **B353** (1995) 513.

[189] D. Bardin, D. Lehner, and T. Riemann, *Nucl. Phys.* **B477** (1996) 27.

[190] `ZAC` is available at `http://www.ifh.de/~riemann/doc/ZAC/zac.html`.

[191] J. Biebel, *Phys. Lett.* **B448** (1999) 125.

[192] ECFA/DESY LC Physics Working Group Collaboration, E. Accomando *et al.*, *Phys. Rept.* **299** (1998) 1.

[193] T. Kinoshita, *"Quantum Electrodynamics"*. World Scientific, Singapore, 1990.

[194] C. Heisey et al. "A new precision measurement of the muon $(g-2)$ value at the level of 0.35 ppm", Brockhaven AGS Proposal 821, Sept. 1985, revised Sept. 1986. (See also Design Report for AGS 821, March 1989.).

[195] C. Quick, *"Gauge Theories of the Strong, Weak, and Electromagnetic Interactions"*. Benjamin/Cummings, Menlo Park, Canada, 1983.

[196] F. Mandl and G. Shaw, *"Quantum Field Theory"*. John Wiley & Sons, New York, 1984.

[197] M. Böhm, H. Spiesberger, and W. Hollik, *Fortsch. Phys.* **34** (1986) 687.

[198] J.D. Bjorken and S.D. Drell,
"*Relativistic Quantum Mechanics*", McGraw-Hill, New York, 1964;
"*Relativistic Quantum Fields*", McGraw-Hill, New York, 1965.

[199] R. Field, *Applications of Perturbative QCD*. Addison-Wesley, 1989.

[200] Z. Was, "Radiative Corrections", in *1993 European School of High-Energy Physics*, CERN 94-04 (1994) (N. Ellis and M.B. Gavela, eds.), 307.

[201] W. J. Marciano and A. Sirlin, *Phys. Rev. Lett.* **61** (1988) 1815.

[202] W. J. Marciano, *Nucl. Phys. Proc. Suppl.* **40** (1995) 3.

[203] A. Pich, "Tau physics", in *Heavy flavours II* (A. Buras, M. Lindner, eds.), p. 453, World Scientific, Singapore, 1998.

[204] L. Kalinovskaya and T. Riemann, private communication.

[205] G. Köpp and F. Krüger, *"Einführung in die Quanten-Elektrodynamik"*. Teubner, Stuttgart, Germany, 1997.

[206] L. Durand, P. DeCelles, and R. Marr, *Phys. Rev.* **126** (1962) 1882.

[207] K. J. Kim and Y.-S. Tsai, *Phys. Rev.* **D7** (1973) 3710.

[208] D. Bardin, A. Olshevsky, M. Bilenky, and T. Riemann, *Phys. Lett.* **B308** (1993) 403. E: ibid., B357 (1995) 725, hep-ph/9507277.

Acknowledgement

I like to thank my thesis advisor Dr. Tord Riemann. Without T. Riemann this thesis would probably not exist at all. He was pushing and inspiring me and a good friend during the last five years. His influence on my work was essential.

I am very much indebted to Prof. Dr. Dieter Lüst for kindly acting as my official thesis supervisor.

I am also grateful to DESY for paying my salary for more than three years and supporting this thesis due to travel money, computers, books and paper.

In addition, I like to thank my co-authors of the `GENTLE` project D. Bardin, A. Leike, D. Lehner, A. Olchevski, T. Riemann for their support and collaboration. Further, I gratefully acknowledge many useful discussions with F. Jegerlehner, S. Riemann, M. Jack, A. Leike, D. Bardin and T. Ohl.

I am grateful to J. Swain, L. Taylor, T. Paul, S. Gau, W. Lohmann from the L3 collaboration to point out the interesting problem of the anomalous magnetic moment of the τ-lepton to T. Riemann and me. Chapter 3 of this thesis and the Fortran program `Anotau` are the results of the investigations on that subject.

Also, my studies in chapter 5 were initiated by questions of the L3 collaboration. Here, it was T. Hebbeker and P. Molnár who pointed out the experimental interest in the examination of anomalous ZZZ and $ZZ\gamma$ couplings. I am grateful for their input and for communications with them and J. Alcaraz and W. Lohmann.

Thanks for discussions and events between live and physics for Johannes Blümlein, Penka Christova, Christopher Ford, Marco Guagnelli, Stefan Herrlich, Axel Höfer, José Illana, Mark Jack, Fred Jegerlehner, Hans Kaiser, Lida Kalinovskaya, Francesco Knechtli, Martin Kurth, Stefan Kurth, Andre Krüger, Dietrich Lehner, Uwe Müller, Andreas Nyffeler, Ravindran, Kurt Riesselmann, Sabine Riemann, Tord Riemann, Steve Riemersma, Rainer Sommer, Oleg Veretin, Alessandro Vicini, Gerhard Weigt, and all the others for the nice time in Zeuthen.

At last, I would like to thank my parents and Jenny for believing in me and supporting me in all possible ways. They had to suffer most under this thesis and they should not be forgotten.

Curriculum Vitae

Name	Jochen Biebel
4.9.1966	geboren in Groß-Gerau
1973–1977	Besuch der Grundschule in Nauheim
1977–1979	Besuch der Förderstufe in Königstädten, Rüsselsheim
1978–1986	Besuch der Immanuel-Kant-Schule in Rüsselsheim
Juni 1986	Abitur, Durchschnittsnote 1.8
1986–1987	Wehrdienst
Okt. 1987	Aufnahme des Physikstudiums an der Technischen Hochschule Darmstadt
1989	Vordiplom
1993 – 1995	Diplomarbeit "Off-Shell-W-Produktion in $e^-\gamma$-Streuung unter Berücksichtigung anomaler Kopplungen" bei Prof. Dr. P. Manakos, TH Darmstadt.
Juli 1995	Diplom, Gesamturteil "sehr gut"
Seit 15.11.1995	Doktorand bei Prof. Dr. D. Lüst, Humboldt-Universität zu Berlin und Dr. T. Riemann, DESY Zeuthen
Juni 1999 - Mai 2000	Projektleiter bei Institut Eurospec im Bereich Beratung

List of Publications and Talks

Publications

[1] H. Anlauf, J. Biebel, H.D. Dahmen, A. Himmler, P. Manakos, T. Mannel and W. Schonau: WOPPER: A Monte Carlo Event Generator for W Off Shell Pair Production including Higher Order Electromagnetic Radiative Corrections.
Comput. Phys. Commun. **79** (1994) 487-502.

[2] J. Biebel, T. Riemann:
Predictions for Anomalous $\tau^+\tau^-\gamma$ Production at LEP 1.
Z. Phys. **C76** (1997) 53-58.

[3] D. Bardin, J. Biebel, D. Lehner, A. Leike, A. Olchevski, T. Riemann:
GENTLE/4fan v.2.0 — A Program for the Semi-Analytic Calculation of Predictions for the Process $e^+e^- \to 4f$.
Comput. Phys. Commun. **104** (1997) 161-187.

[4] ECFA/DESY LC Physics Working Group (E. Accomando et al.):
Physics with e^+e^- Linear Colliders.
Phys. Rept. **299** (1998) 1-78.

[5] J. Biebel, T. Riemann:
Semi-analytic predictions for W pair production at 500 GeV.
in Proc. of *ECFA/DESY Study on Physics and Detectors for the Linear Collider*, DESY 97-123E, (R. Settles, ed.), p 139, `hep-ph/9709207`.

[6] J. Biebel:
Four-Fermion Production with Anomalous Couplings at LEP2 and NLC.
in Proc. of the XIIth International Workshop on *"High Energy Physics and Quantum Field Theory"*, Samara, Russia, 4-10 Sept 1997 (B. Levtchenko, ed.) p. 220, `hep-ph/9711439`.

[7] J. Biebel, T. Riemann:
Off-Shell W Pair Production with Anomalous Couplings: The `CC11` Process.
Eur. Phys. J. **C8** (1999) 655.

[8] J. Biebel:
Anomalous Couplings in W Pair Production.
Acta. Phys. Polon. **B29** (1998) 2839.

[9] J. Biebel:
Seeking CP Violating Couplings in ZZ Production at LEP2.
Phys. Lett. **B448** (1999) 125.

Talks

[1] DPG Frühjahrstagung Teilchenphysik, Hamburg, Germany (1996)
"Untersuchung von anomalen Kopplungen bei $e^+e^- \to 4f$ mit semi-analytischem Zugang"

[2] Linear Collider Workshop, DESY Hamburg, Germany (1996)
"Studying Anomalous W Couplings with `GENTLE`"

[3] Herbstschule für Hochenergiephysik, Maria Laach, Germany (1996)
"Untersuchung von anomalen Kopplungen bei $e^+e^- \to 4f$ mit semi-analytischem Zugang"

[4] Linear Collider Workshop, DESY Hamburg, Germany (1996)
"Studying several anomalous W couplings simultaneously"

[5] L3 W group meeting, CERN, Switzerland (1997)
"GENTLE/4fan v. 2.0"

[6] DPG Frühjahrstagung Teilchenphysik, München, Germany (1997)
"Vorhersagen für die anomale Erzeugung von $\tau\tau\gamma$ bei LEP 1"

[7] XIIth Int. Workshop on High Energy Physics and Quantum Field Theory, Samara, Russia (1997)
"Four-Fermion production with anomalous couplings at LEP2 and NLC"

[8] DESY Theory Workshop, Hamburg, Germany (1997)
"Four-Fermion production with anomalous couplings at LEP2 and NLC"

[9] DPG Frühjahrstagung Teilchenphysik, Freiburg, Germany (1998)
"W-Paarerzeugung mit anomalen Kopplungen bei LEP2 und LC"

[10] Zeuthen Workshop on Elementary Particle Theory 'Loops and Legs in Gauge Theories', Rheinsberg, Germany (1998)
"Anomalous Couplings in W Pair Production"

[11] Physics Working Group Meeting of the ECFA/DESY Linear Collider Study, Frascati, Italy (1998)
"Anomalous Couplings in ZZ Production"

Selbständigkeitserklärung

Hiermit erkläre ich, die vorliegende Arbeit selbständig ohne fremde Hilfe verfaßt zu haben und nur die angegebene Literatur und Hilfsmittel verwendet zu haben.

Jochen Biebel
12. Dezember 2000